SPECTRUM HANDOFF STRATEGY FOR COGNITIVE RADIO-BASED MAC IN INDUSTRIAL WIRELESS SENSOR AND ACTUATOR NETWORKS

Pedro M. Rodríguez Torija

Supervisors:

Dr. Mikel Mendicute (Mondragon Unibertsitatea)

Dr. Iñaki Val (IK4-Ikerlan)

Submitted for the degree of DOCTOR

MONDRAGON UNIBERTSITATEA

May 2016

ACKNOWLEDGEMENTS

First and foremost, I would like to express my most sincere gratitude to my thesis supervisors, Mikel Mendicute and Iñaki Val. I am thankful for their guidance, support and all I have learned from them. This would not be possible without them.

I wish to thank my thesis committee members, Dr. Marion Berbineau, Dr. Wilfried Steiner, Dr. M. Elena de Cos, Dr. Iker Sobrón and Dr. Eñaut Muxika for their helpful participation in my thesis examination.

Furthermore, I would like to thank the working group composed of researchers from IK4-Ikerlan and Mondragon Unibertsitatea who have helped me with the cognitive platform.

Additionally, I am grateful to the Communications Systems group at IK4-IKERLAN. Without their help and interest this thesis would have not been possible.

My time in Mondra was enjoyable in large part due to my friends. I thank Gustavo Pérez, Damián Gómez, Gabriel García and Ugai Unalde for all the fun moments.

And finally, I thank to my family and my girlfriend for the support during this journey.

Thank you Muchas gracias Eskerrik asko

ABSTRACT

Abstract

In this thesis, a Cognitive Radio(CR)-based MAC for Industrial Wireless Sensor and Actuator Network (IWSAN) applications is proposed. IWSANs are typically used for closed-loop control applications, and they demand strict requirements in terms of time and robustness. Low latency and low error rates are required in order not to endanger persons or machinery. Moreover, these applications operate in industrial environments such as factories or transport scenarios (as aeronautics or railway) where multipath fading and shadowing are present due to metal surfaces. Furthermore, interference from other communication systems or industrial machinery is also common in these environments. The proposed MAC, based on the CR paradigm, is capable of ensuring time and robustness requirements in industrial channels.

In the process of designing the CR-based MAC for IWSAN applications, a comparison between several non-CR-based MACs and CR-based MACs has been carried out. This comparison, which allows stating the benefits of CR for these applications, is presented in this thesis. The performance of every MAC is determined theoretically using Network Calculus, and it is validated through OPNET simulations. CR solutions, due to their adaptability characteristics, are capable of avoiding interference and ensuring robustness in industrial environments. However, none of the selected MACs are capable of ensuring robustness without comprising time requirements, since interference is avoided but not in a bounded time. On the other hand, the MAC proposed in this thesis is capable of avoiding interference ensuring time and robustness requirements at the same time. This MAC is therefore suitable for IWSAN applications.

To ensure a deterministic behavior against interference, a novel handoff algorithm, which detects interference and hops to another channel, has been proposed. This algorithm has been designed to be used jointly with one of the evaluated MACs. The detection of the interference and the hop to another channel is done in a bounded time, because the proposed algorithm detects interference while the system is transmitting. The performance of this proposal is evaluated using Network Calculus and OPNET simulations, and the results are compared with the system without the proposed handoff algorithm. The comparison of the results shows how the evaluated MAC is only capable of ensuring both time and robustness requirements when the proposed handoff strategy is used.

Moreover, the spectrum sensing algorithm used to obtain information about the environment is delved and its performance is measured through MATLAB simulations. An energy detector has been chosen due to its simplicity. Also, a cyclostationary Modulation Classifier is presented and a simplification has been carried out allowing its implementation on real hardware. The Modulation Classifier is capable of distinguishing between OFDM, QPSK and GFSK signals. The performance of the algorithm is presented in this thesis for different signals and for different receiver impairments such as frequency offset, DC offset and I/Q imbalance.

Finally, a cognitive platform to validate the spectrum sensing algorithms is presented. This platform has been designed using a Xilinx Virtex 6 FPGA by a working group composed of researchers from IK4-Ikerlan and Mondragon Unibertsitatea. The platform, which uses both spectrum sensing algorithms, is an Ethernet-to-RF bridge. It has been designed to replace an Ethernet wired link by a wireless one for IWSAN applications. The proposed platform ensures a reliable communication link against interference. In the proposed implementation, the energy detector is used by the transmitter in order to find a free channel to transmit data, whereas the modulation classifier is used by the receiver in order to distinguish between the signal transmitted by the RF-Ethernet bridge and other signals. In this way the receiver can find the channel where the transmitter is carrying out the communication.

Resumen

En esta tesis se propone una MAC basada en el paradigma de la Radio Cognitiva (RC) para redes de sensores y actuadores inalámbricos industriales. Estas redes se suelen utilizar para aplicaciones de control en lazo cerrado, que exigen requisitos estrictos de tiempo y robustez. Para no poner en peligro la salud de las personas o la maquinaria es necesario que la red asegure una baja latencia y una tasa baja de errores. Además, al trabajar en ambientes industriales como fábricas o transportes (trenes, aviones, etc.), estas redes tienen que hacer frente a canales con mucho desvanecimiento por multitrayecto y efecto sombra debido a las superficies metálicas. También es común en estos entornos que haya interferencias de otros sistemas de comunicaciones o de la propia maquinaria industrial. La MAC propuesta en esta tesis es capaz de asegurar los requisitos temporales y de robustez demandados trabajando en este tipo de entornos.

En el proceso de diseño de la MAC basada en RC para redes de sensores y actuadores inalámbricos industriales, se ha llevado a cabo una comparación de diferentes MACs diseñadas para estas redes. Se han evaluado tanto MACs basadas en RC como no basadas en ella, estableciendo las ventajas de la RC para estas aplicaciones. La evaluación se ha llevado a cabo haciendo un estudio teórico mediante *Network Calculus*, cuyos resultados se han validado mediante simulaciones en OPNET. Los resultados muestran como la RC es capaz de evitar interferencias y asegurar robustez en ambientes industriales. Sin embargo, ninguna de las MACs seleccionadas ha conseguido asegurar ambos requisitos, temporales y de robustez, al mismo tiempo; se puede evitar las interferencias pero no sin comprometer los requisitos temporales de la aplicación. Sin embargo, la MAC propuesta es capaz de evitar interferencias asegurando al mismo tiempo los requisitos temporales y de robustez. Por lo tanto, la MAC propuesta es apropiada para este tipo de redes.

Para asegurar el comportamiento determinista del sistema, se ha propuesto un novedoso algoritmo de *handoff* que es capaz de detectar una interferencia y saltar a otro canal. Este algoritmo se ha diseñado para ser utilizado conjuntamente con una de las MACs previamente evaluadas. La detección de la interferencia y el salto a otro canal se hace en un tiempo determinado de tiempo, ya que es posible detectar interferencias mientras el sistema está transmitiendo. Su rendimiento se ha evaluado mediante *Network Calculus* y simulaciones en OPNET, y se ha comparado con los resultados obtenidos con la MAC cuando no se utiliza el esquema propuesto. De la comparación se deduce que el esquema de *handoff* añade a la MAC la capacidad de asegurar a la vez los requisitos temporales y de robustez.

Además, en la tesis se explica el algoritmo de *spectrum sensing* que la MAC utiliza para obtener información del entorno, y su rendimiento se ha estudiado mediante simulaciones en MATLAB. Debido a su simplicidad, se ha optado por un detector de energía para este propósito. También se presenta un clasificador de modulaciones cicloestacionario. Este clasificador ha sido simplificado todo lo posible para posibilitar su implementación en hardware real. El clasificador de modulaciones es capaz de distinguir entre señales OFDM, QPSK y GFSK. Su rendimiento se detalla para diferentes señales y para diferentes deficiencias presentes en el receptor, como son *offset* de frecuencia, *offset* de continua o desequilibrios I/Q.

Por último, se presenta una plataforma cognitiva que se ha utilizado para validar los algoritmos de spectrum sensing. Un grupo de trabajo compuesto por investigadores de IK4-Ikerlan y Mondragon Unibertsitatea ha diseñado esta plataforma sobre una FPGA Virtex 6 de Xilinx. La plataforma, que utiliza los dos algoritmos de *spectrum sensing*, es un puente Ethernet-RF. Su objetivo es reemplazar un enlace cableado de Ethernet por uno inalámbrico para aplicaciones de redes de sensores y actuadores industriales. Gracias a los algoritmos de *spectrum sensing*, la plataforma es capaz de asegurar un enlace robusto ante interferencias. El detector de energía se utiliza en el transmisor para encontrar los posibles canales libres donde transmitir la información. Mientras que el clasificador de modulaciones se utiliza en el receptor para distinguir entre la señal del transmisor y otras posibles señales. Esto permite al receptor saber en qué canal de todos los posibles está el transmisor.

Laburpena

Tesi honetan proposatzen da Irrati Kognitiboaren (IK) paradigman oinarritutako MAC bat industriako haririk gabeko sentsore eta eragingailuen sareetarako. Sare horiek begizta itxiko kontrol aplikazioetarako erabili ohi dira, denbora eta sendotasunaren aldetik baldintza ugari eskatzen dute eta. Pertsonen osasuna eta makinak arriskuan ez jartzeko, beharrezkoa da sareak latentzia eta hutsegite tasa txikiak bermatzea. Gainera, industri giroetan lan egiteko direnez, esaterako, lantegietan edo garraioetan (trenak, hegazkinak, etab.), sare horiek gai izan behar dira gainazal metalikoek eragiten dituzten ibilbide aniztunaren eta itzal efektuaren ondorioz asko barreiatzen diren kanalei aurre egiteko. Ingurune horien ohiko ezaugarria da, baita ere, beste komunikazio sistema batzuen edo industriako makinen beraien interferentziak egotea. Tesi honetan proposatzen den MACa gai da honelako inguruetan lan egiteko denborari eta sendotasunari dagokienez eskatzen dituen baldintzak ziurtatzeko.

IKan oinarrituta haririk gabeko sentsore eta eragingailu industrialen sareetarako MACa diseinatzeko prozesuan, horrelako sareetarako aurkeztu diren hainbat MAC alderatu dira. IKan oinarritutako MACak zein bestelakoak ebaluatu dira, eta IKak aplikazio hauetarako dituen abantailak ezarri dira. Ebaluaziorako Network Calculus erabili da, zeinaren bidez azterketa teoriko bat egin baita, eta azterketaren emaitzak OPNETen simulazioak eginda baliozkotu dira. Emaitzek erakusten dutenez, IKa gai da industriako inguruneetan interferentziak ekidin eta sendotasuna ziurtatzeko. Halere, aukeratu diren MACetatik batek ere ez du lortu baldintza biak, denborari buruzkoa zein sendotasunari buruzkoa, aldi berean ziurtatzea; interferentziak ekidin daitezke, baina ez aplikazioaren denborari buruzko baldintzak arriskuan jarri gabe. Dena dela, proposatu den MACak portaera determinista bat ziurtatzen du interferentziekiko, eta aldi berean denborari eta sendotasunari buruzko baldintzak ere ziurtatzen ditu. Hortaz, MAC hau egokia da sare mota honetarako.

Sistemaren portaera determinista ziurtatzeko, *handoff* algoritmo berritzailea proposatu da, zeina interferentzia bat antzeman eta beste kanal bat igarotzeko gai den. Algoritmo hori aurretik ebaluatutakoa MACetako batekin batera erabiltzeko diseinatu da. Interferentzia antzeman eta beste kanal batera salto egitea denbora jakin batean egiten da, izan ere, sistema transmititzen ari dela antzeman baitaitezke interferentziak. *Network Calculusen* bitartez eta OPNETeko simulazioen bitartez ebaluatu da sistemaren errendimendua, eta proposatutako eskema erabiltzen ez denean MACak ematen dituen emaitzekin alderatu da. Alderaketa horretatik ondorioztatzen denez, *handoff* eskemak denborari eta sendotasunari buruzko baldintzak batera ziurtatzeko ahalmena ematen dio MACari.

Gainera, tesiak azaltzen du inguruneari buruzko informazioa eskuratzeko MACak erabiltzen duen *spectrum sensing* algoritmoa, eta bere errendimendua MATLABen simulazioak eginez aztertu da. Bere sinpletasuna dela eta, energia detektore bat aukeratu da asmo honetarako. Modulazio sailkatzaile zikloegonkor bat ere aurkezten da. Sailkapen hori ahalik eta gehien sinplifikatu da benetako hardwarean inplementatu ahal izateko. Modulazioen sailkatzaileak OFDM, QPSK eta GFSK seinaleak bereizi ditzake. Bere errendimendua hargailuan dauden seinale eta akats desberdinetarako zehazten da, esaterako maiztasunaren *offset*-a,zuzenaren *offset*-a edo I/Q desorekak.

Bukatzeko, *spectrum sensing*-eko algoritmoak baliozkotzeko erabili den plataforma kognitibo bat aurkezten da. IK4-Ikerlaneko eta Mondragon Unibertsitateko ikertzailez osatutako lantalde batek diseinatu du plataforma hori Xilinxen Virtex 6 FPGA baten oinarrutz. Plataformak *spectrum sensing*-eko bi algoritmo erabiltzen ditu eta Ethernet-RF zubi bat da. Bere helburua da Etherneteko kable bidezko lotura bat haririk gabeko batekin ordeztea industriako sentsore eta eragingailuen sareetan aplikatzeko. *Spectrum sensing*-eko algoritmoei esker, plataformak lotura sendoa bermatu dezake interferentziak gertatzen direnean. Energia detektorea transmisorean erabiltzen da informazioa transmititzeko erabilgarri egon daitezkeen kanalak aurkitzeko. Modulazioen sailkatzailea, berriz, hargailuan erabiltzen da transmisorearen seinalea eta egon daitezkeen beste seinale batzuk bereizteko. Horri esker, hargailuak badaki posible diren kanal guztietatik non dagoen transmisorea.

GLOSSARY

ALRT	Average Likelihood Ratio Test
AMD	Arithmetic Mean Detector
BE	Best Effort
CCC	Common Control Channel
CD	Cyclostationary Detector
CDF	Cumulative Distribution Functions
CE	Cognitive Engine
CFAR	Constant False Alarm Rate
CORDIC	COordinate Rotation DIgital Computer
CP	Contention Phase
CR	Cognitive Radio
CSMA/CA	Carrier Sense Medium Access / Collision Avoidance
DCF	Distributed Coordination Function
DFT	Discrete Fourier Transform
DSA	Dynamic Spectrum Access
DSP	Digital Signal Processor
ED	Energy Detector

EDB	Eigenvalue-based Detector
EDCA	Enhanced Distributed Channel Access
EDF	Early Deadline First
EMED	Energy with Minimum Eigenvalue Detector
FDD	Frequency Division Duplex
FDMA	Frequency Division Multiple Access
FH	Frequency Hopping
FPGA	Field Programmable Gate Array
flexWARE	Flexible Wireless Automation in Real-Time Environments
GLRT	Generalized Likelihood Ratio Test
GFSK	Gaussian Frequency Shift Keying
GMD	Geometric Mean Detector
HLRT	Hybrid Likelihood Ratio Test
IF	Intermediate Frequency
ISA	International Society of Automation
ISI	Inter Symbol Interference
ISM	Industrial Scientific and Medical
IsoMAC	Isochronous MAC
IWSAN	Industrial Wireless and Actuator Networks
LOS	Line of Sight
LUT	Look-Up-Tables
MAC	Medium Access Control
MC	Modulation Classifier
MD	Matched-filter Detector
MED	Maximum Eigenvalue Detector
MMED	Maximum-Minimum Eigenvalue Detector
MTTR	Maximum Time To Rendezvous
NC	Network Calculus
NLOS	Non Line of Sight
OFDM	Orthogonal Frequency Division Multiplexing
OSA	Opportunistic Spectrum Access
PDP	Power Delay Profile
PDF	Probability Density Function
PER	Packet Error Rate

PU	Primary User
QAM	Quadrature Amplitude Modulation
QPSK	Quadrature Phase Shift Keying
RMS	Root Mean Square
RF	Radio Frequency
ROC	Receiver Operating Characteristics
SDR	Software Defined Radio
SNR	Signal to Noise Ratio
SRL	Shift Register Lut
SP	Scheduled Phase
TDMA	Time Division Multiple Access
WIA-PA	Wireless Networks for Industrial Automation/Process Automation
WISA	Wireless Interface for Sensor and Actuator
WLAN	Wireless Local Area Network
WPAN	Wireless Personal Area Network
WSAN	Wireless Sensor and Actuator Networks

INDEX OF CONTENTS

LIST OF FIGURES

LIST OF TABLES

Chapter 1

INTRODUCTION

1.1 Industrial Wireless Sensor and Actuator Networks

A Wireless Sensor and Actuator Network (WSAN) is composed of a set of sensors and actuators connected wirelessly. The goal of these networks is to gather physical information in order to carry out actions which depend on the gathered information. The information is collected by a number of sensors and sent through the wireless network to a controller, which analyses it and makes decisions accordingly. Finally, the decisions are transmitted to the actuators. All the transmissions in an Industrial WSAN (IWSAN) are carried out through an industrial channel, which are considered a highly dispersive due to large metal surfaces. Furthermore, other communication systems or industrial equipments may lead to interference which disturb the desired transmission. Therefore, the communication system must ensure several requirements to ensure a correct connectivity in these channels. An important industrial application of this kind of networks may be closed-loop control applications [1], used in factories or critical transport scenarios as aeronautics or railway. An illustrative example of closed-loop control applications is shown in Figure 1. These kinds of applications, known as mission-critical and time-critical applications, demand certain requirements to ensure safety. A communication system for IWSAN must be capable of guarantee the requirements demanded by this applications in an industrial channel[2]:

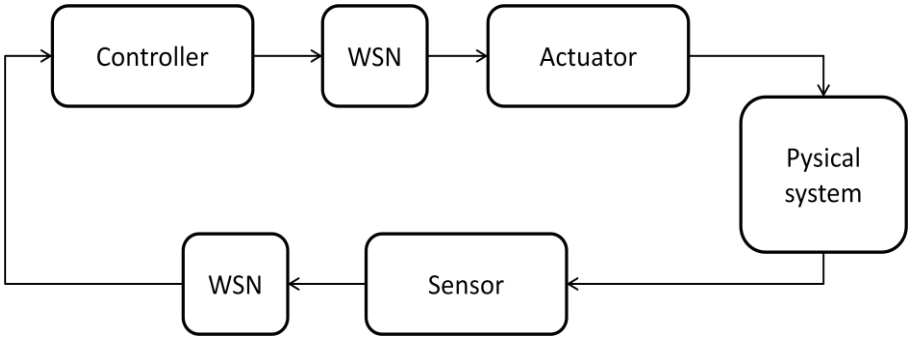

Figure 1. WSAN-based scheme for closed-loop control [1].

- Latency: in closed-loop applications the time between the observation and the start of a reaction, known as dead time, is limited and depends on the kind of applications. The communication system must ensure a latency lower than the dead time. In these applications the information with latency greater than the dead time is considered erroneous, and it may cause from process or service disruption to injuries or machinery losses.
- Reliability: as it has been told before, errors can carry serious consequences, so mechanism to ensure a correct transmission must be used. Most communication systems use time redundancy to achieve reliability; however, in time-critical systems, retransmissions of lost packets increase jitter and compromise determinism. Furthermore, as the network size increases, retransmissions carry collisions which may collapse the system.
- Error detection: in order to ensure safety, the system must detect a possible error. In case of any error, such as a lost packet or a higher latency than the expected, the detection of the error allows the system to enter a safe state.
- Security: authenticity and integrity of the data must be established in order to avoid attacks to the system. If no authenticity and integrity is ensured in a wireless communication, an external node can sabotage the system and cause any kind of damage.
- WSN requirements: WSAN inherit some of their requirements from WSN. Low cost and low energy solutions are required by these networks in order to make their implementation possible.

Typically, these applications are connected by wired communications such as Ethernet/IP, Powerlink; Profinet-IRT, ModBus/TCP or EtherCAT; due to the lower reliability and robustness in wireless systems. However, there is an increasing interest in the use of wireless solution because they provide some advantages [3, 4]:

- Cost: in wired systems, wires between nodes imply big costs in material and deployment, which wireless networks save. Furthermore, maintenance supposes higher costs and the disruption in the operations.
- Flexibility: wireless networks have more flexibility than their wired counterparts. When there are new nodes to add to the network no wires must be added like in wired systems, making any update easier.

- Accessibility: wireless technology allows nodes to be located in places where it is impossible to route a wire, such as moving or rotating elements. This possibility may result in new industrial applications.

The wireless communication system must ensure the time-critical and mission-critical requirements demanded by closed-loop applications. In addition, the network must deal with industrial channels; shadowing, fading and multipath are common in factories or critical transport scenarios as avionics or trains, as well as interference from other communication systems or industrial machinery. Therefore, the interest in robust and reliable wireless networks to be used in industrial environments is increasing. In order to address the problems of the aforementioned industrial environments, Cognitive Radio (CR) can be a good approach.

1.2 Cognitive Radio

CR is a technique which allows a wireless system to monitor the environment and adapt to it. A CR system can take decisions in function of environment information, and reconfigure the parameters of a Software Defined Radio (SDR). Defined by Mitola [5], SDR is a radio communication system where components are implemented by means of software or programmable logic devices. The interest on CR systems has emerged because of the low use of some licensed bands. For example, TV bands are occupied less than 6% [6]. As a result, the IEEE 802.22 [7] standard has been proposed to be used for wireless regional area network using white frequency bands (or spectrum holes) in television bands. CR networks have been proposed in order to use the available channels in the licensed bands without disturbing licensed users. This is known as Opportunistic Spectrum Access (OSA) or Dynamic Spectrum Access (DSA). Thus, a CR user can transmit in any spectrum hole, but if the Primary User (PU) appears, it must vacate the channel, as shown in Figure 2. Also, it is possible to transmit simultaneously with the PU if the interference level is below a maximum.

A CR user should carry out many tasks to monitor the environment and adapt to it. These tasks are summarized in Figure 3. The cognitive cycle provide awareness and intelligence to the system through these tasks:

- Spectrum sensing. In this stage the system gets information about the environment. The spectrum sensing algorithm finds spectrum holes where the CR node can operate, and gathers information about these spectrum holes.
- Analysis and decision. This block represents the intelligence of the system, the Cognitive Engine (CE). The CE analyses the information supplied by the spectrum sensing block and evaluates the options to take a decision. It decides how to interact with the environment. The appropriate band, bandwidth of the transmission, data rate, etc. are determined in this step. Depending on the system's state it is necessary to carry out different tasks such as rendezvous, hand-off or optimization. In the rendezvous problem several nodes try to find a common channel to initiate the communications, while the hand-off is the process of vacating the channel when a PU appears.

- Configuration. The SDR, commanded by the CE, reconfigures the system parameters to start the transmission. However, since the environment changes over time and space, the CR should stop the transmission and start the cycle again.
- Learning. The learning task improves both the spectrum sensing and analysis tasks. The CE can develop models to predict the presence of a spectrum hole or modify the analysis and decision techniques. Therefore, decisions do not depend only in the environment information, but also in previous decisions and statistics.

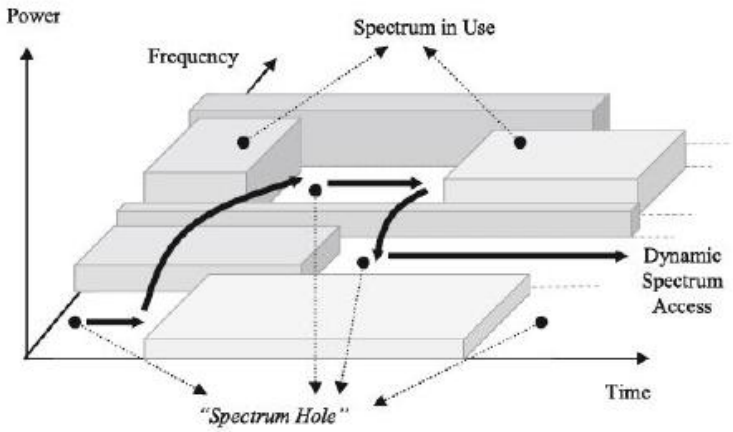

Figure 2. Opportunistic Spectrum Access operation [8].

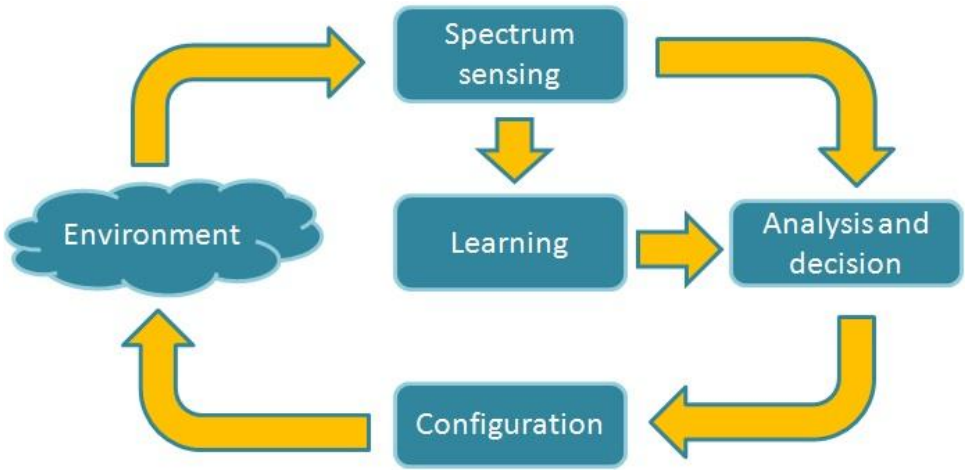

Figure 3. Cognitive cycle.

Although CR was first thought to be use the licensed bands accessing the medium in OSA way, CR may be used in Industrial Scientific and Medical (ISM) bands [9]. CR provide adaptability to the system which can be used for ensuring reliability in noise and interference channels, such as channels found in industrial environments. Therefore, it can be used in order to achieve the mission-critical and time-critical requirements demanded by IWSAN applications.

1.3 Objective

The main objective of this thesis is to evaluate the potential use of CR for IWSAN applications and to propose a CR-based communication system to be used in these applications. It must be capable of ensuring the requirements of mission-critical and time-critical WSAN in an environment under interference. In order to achieve this objective, several particular objectives have been established:

- To evaluate different CR-based and non CR-based Medium Access Control (MAC) layers for mission-critical and time-critical WSAN in industrial environment. To evaluate these MACs by means of a theoretical analysis using Network Calculus (NC), which is validated through simulations in OPNET. This evaluation allows knowing the advantages and disadvantages of CR for WSAN in industrial environments.
- To evaluate spectrum sensing algorithms. These algorithms are used by the CR-based MACs to obtain information about the environment, allowing them to avoid interference. The algorithms are evaluated through MATLAB simulations.
- To propose and to evaluate a handoff algorithm for CR-based MACs for mission-critical and time-critical IWSAN. The evaluation is carried out using NC, and validated through simulations in OPNET. A CR-based MAC from the evaluation is chosen and the handoff process is added to it. This MAC is evaluated with and without handoff, and the results show how the proposed scheme allows the system to achieve the requirements of IWSAN applications.
- Finally, to evaluated the spectrum sensing algorithms in a cognitive platform in order to validate the simulation results.

1.4 Thesis contributions

1.4.1 Proposal of a handoff algorithm for IWSAN

The main contribution of this thesis is the proposition of a novel handoff algorithm for CR. It is capable of detecting interference while the system is transmitting. Thus, the algorithm has been designed to detect and avoid interference in a bounded time. Therefore, the requirements of mission-critical and time-critical IWSANs can be satisfied. This contribution has been submitted to a Journal for publication:

- P. M. Rodriguez, A. Lizeaga, M. Mendicute and I. Val. “Spectrum handoff strategy for cognitive radio-based MAC for time-critical and mission-critical industrial wireless sensor and actuator networks”. *IEEE/ACM Transactions on Networking*. (Submitted).

1.4.2 Comparison between MACs for IWSAN

Other contributions have been achieved in the process of designing the handoff algorithm. An evaluation of several MACs for mission-critical a time-critical IWSAN

applications has been done. The most relevant MACs, both CR-based and non-CR-based, have been chosen for evaluation in industrial environments such as shadowing and Rayleigh channels or under interference. This contribution has been published in an International Conference:

- P. M. Rodriguez, I. Val, A. Lizeaga and M Mendicute. "Evaluation of cognitive radio for mission-critical and time-critical WSAN in industrial environments under interference". *Factory Communication Systems (WFCS), 2015 IEEE World Conference on (pp. 1-4).*

1.4.3 Proposal of a modulation classifier

Furthermore, this thesis contributes with a spectrum sensing algorithm which is capable of distinguish between three different modulations. The algorithm uses some of the cyclostationary characteristics of the received signal to determine whether the modulation is Orthogonal Frequency Division Multiplexing (OFDM), Quadrature Phase Shift Keying (QPSK) or Gaussian Frequency Shift Keying (GFSK). The evaluation and the implementation on a Field Programmable Gate Array (FPGA) have been submitted for publication to a Journal:

- P. M. Rodriguez, Z. Fernandez, R. Torrego, A. Lizeaga, M. Mendicute and I. Val. "A sub-optimal implementation on FPGA of cyclostationary modulation classifier for cognitive radios". *AEÜ - International Journal of Electronics and Communications.* (Submitted).

1.4.4 Validation of the spectrum sensing algorithms in a cognitive platform

Finally, the spectrum sensing algorithms have been implemented and validated in a cognitive platform. This platform has been built in collaboration with a working group which is composed of researchers from IK4-IKERLAN and Mondragon Unibertsitatea. The cognitive platform is implemented on an FPGA, and some articles regarding the spectrum sensing algorithms have been published in Journals, in International Conferences and in a Book Chapter:

- P. M. Rodriguez, Z. Fernandez, R. Torrego, A. Lizeaga, M. Mendicute and I. Val. "A sub-optimal implementation on FPGA of cyclostationary modulation classifier for cognitive radios". *AEÜ - International Journal of Electronics and Communications.* (Submitted).
- A. Arriola, P. M. Rodríguez, R. Torrego, F. Casado, Z. Fernandez, M. Mendicute, E. Muxika, J. I. Sancho, and I. Val, "FPGA-based Cognitive Radio Platform with Reconfigurable Front-End and Antenna," in *Computing Platforms for Software-Defined Radio*, ed: Springer, 2016.
- P.M. Rodriguez, R. Torrego, F. Casado, Z. Fernandez, M. Mendicute, A. Arriola and I. Val "Dynamic spectrum access integrated in a wideband cognitive RF-Ethernet bridge for industrial control applications". *Journal of Signal Processing Systems, 83(1), 19-28 (2016).*

- F. Casado, R. Torrego, P. Rodríguez, A. Arriola and I. Val. "Reconfigurable Antenna and Dynamic Spectrum Access Algorithm: Integration in a Cognitive Radio Platform for Reliable Communications". *Journal of Signal Processing Systems, 78(3), 267-274 (2015).*
- P. Rodriguez, R. Torrego, F. Casado, Z. Fernandez, M. Mendikute, A. Arriola and I. Val. "Wideband cognitive wireless communication system: implementation of an RF-Ethernet bridge for control applications". *SDR-WInnComm-Europe 2014 Conference.*

1.5 Outline of the Thesis

The thesis is organized in the following manner:

- Chapter 2. It summarized the background and related work on mission-critical and time-critical IWSAN and CR. Requirements in IWSAN applications are delved, as well as current solutions. The CR paradigm is also explained, and some CR-based solutions for IWSAN are detailed.
- Chapter 3. A comparison of several MACs for mission-critical and time-critical communications for IWSAN is shown in this chapter. Different existing approaches have been chosen and are evaluated in industrial environments.
- Chapter 4. In this chapter a CR-based handoff algorithm for mission-critical and time-critical IWSANs is proposed. A MAC evaluated in Chapter 3 is used as a basis, and a novel handoff algorithm is proposed. This algorithm is capable of detecting and avoiding interference in a bounded time. The energy detector which the MAC uses to obtain information about the environment is also delved. Furthermore, a cyclostationary modulation classifier is proposed. This classifier has been simplified as much as possible in order to allow implementing in real hardware.
- Chapter 5. In Chapter 5, a cognitive platform is explained, this platform has been designed a working group from IK4-Ikerlan and Mondragon Unibertsitatea. Some of the algorithms proposed in Chapter 4 have been implemented and validated in this platform.
- Chapter 6. Finally, this chapter summarizes the conclusions of this thesis and presents the most interesting future work lines.

Chapter 2

BACKGROUND AND RELATED WORK

2.1 Industrial Wireless Sensor and Actuator Networks

WSANs must satisfy several requirements in terms of costs, energy efficiency or reliability, as it has been described in Section 1.1. Below, the requirements of WSANs regarding the application and the industrial channel are explained. Furthermore, some approaches to be used in WSANs are detailed.

2.1.1 Mission-critical and time-critical Wireless Sensor and Actuator Networks

The reliability and time requirements of WSAN vary depending on the kind of applications. Industrial applications are classified into six classes [10]: safety systems, closed-loop regulatory systems, closed-loop supervisory systems, open-loop systems, alerting systems and information gathering systems. In safety systems, data must arrive at destination as soon as possible to avoid damages. Fire alarms are an example of this class. Closed-loop control systems are used to regulate a system; periodic measurements are needed in order to get a smooth working of the system. These systems may have stricter time requirements than safety systems. Closed-loop supervisory systems are similar to regulatory systems, but no periodical measurements are expected. Information in these systems is usually considered non-critical. In open-loop control systems a human operator analyzes the data gathered by the system and makes decisions accordingly. The system is in charge of gathering data and sends it to the central

database. Alerting systems monitor the environment in order to notify users if an important event occurs. Finally, information gathering systems are used to gather and save information which can be analyzed in the future.

Regarding reliability and time bounds, these formerly detailed applications can be classified into four types, which are shown in Figure 4 [11]:

- Delay-tolerant and loss-tolerant applications: the least restrictive requirements, since these applications accept data losses and delays. The applications can still continue working even if some losses or high delays happen. Monitoring applications, both alerting systems and information gathering systems, are examples of this kind of applications.
- Delay-tolerant and loss-intolerant applications: data is only bounded in reliability domain. Therefore, the communication system must ensure a correct transmission, although long delays are tolerated.
- Delay-intolerant and loss-tolerant applications: in contrast to the previous case, some losses are tolerated, but no delays in data transmission are allowed. A packet whose delay is higher than a threshold is considered as a loss. Closed-loop supervisory systems and open-loop control systems may be classified in this category or in the previous one.
- Delay-intolerant and loss-intolerant applications: time and reliability bounds for the data are demanded by these applications. Information must arrive on time, otherwise, if data do not arrive or arrive late, losses on machinery or human injuries may happen. Closed-loop regulatory systems are delay-intolerant and loss-intolerant. These applications are the most restrictive ones, and they are the focus of this research work.

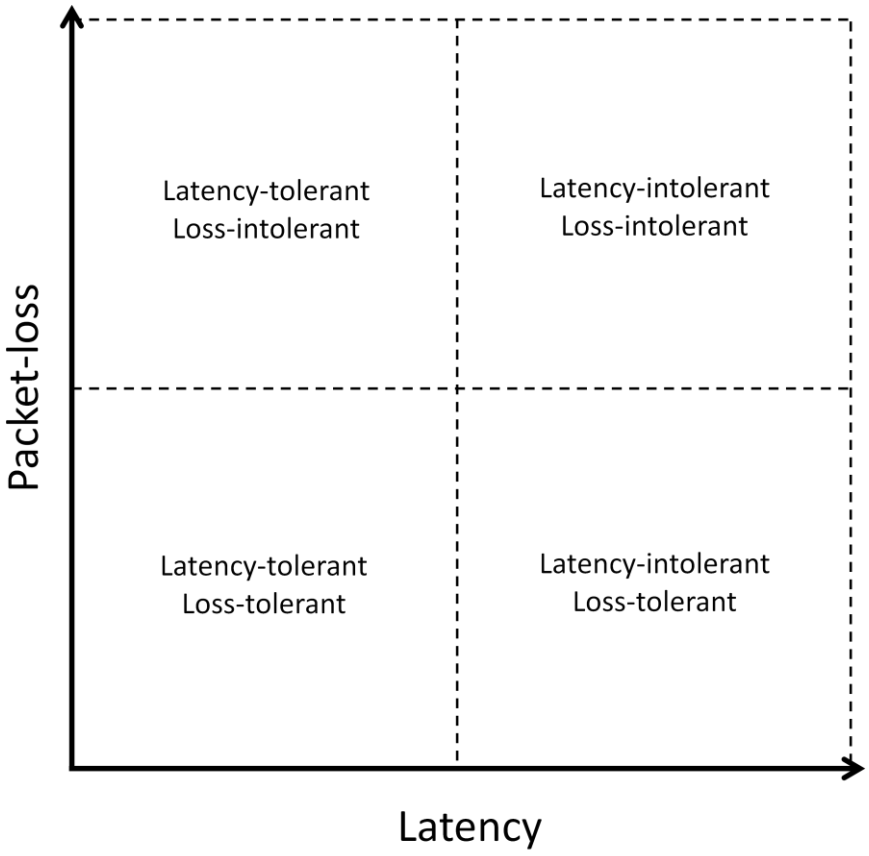

Figure 4. WSANs classes based on requirements [11].

2.1.2 Industrial environments

The environment where the WSAN operates may compromise its performance. Industrial channels affect the transmitted signal and so may cause errors in the transmissions. These errors may lead to a lack of reliability or large delay due to retransmissions. Different effects can modify the signal: path loss, multipath, fading and interference are usually present in industrial channels.

2.1.2.1 Path loss

As an electromagnetic field propagates through space, its power is attenuated. The attenuation depends on the environment where the transmission is carried out. Path losses can be expressed in dB as follows:

$$PL(d) = PL(d_0) + 10nlog_{10}\left(\frac{d}{d_0}\right), \quad (1)$$

where $PL(d_0)$ are the losses at d_0, defined in Equation (2), and n is the path loss exponent which depends on the environment.

$$PL(d_0) = 20\log_{10}\left(\frac{\lambda}{d_0 \cdot 4\pi}\right), \quad (2)$$

where λ is the wavelength. Therefore, the received power is:

$$P_{rx}(dBm) = P_{tx}(dBm) - PL(dB). \quad (3)$$

The value of n in free space is 2, and it has been measured for different industrial environments. Typical values of n for industrial channels in the 2.4 GHz ISM band are 1.6 and 3.3 [12]. In [13, 14] line-of-sight (LOS) and non-line-of-sight (NLOS) scenarios have been measured. Values of n from 1.4 to 1.89 are proposed for LOS environments and values between 2 and 4.31 for NLOS scenarios. Path loss levels for different values of n are shown in Figure 5.

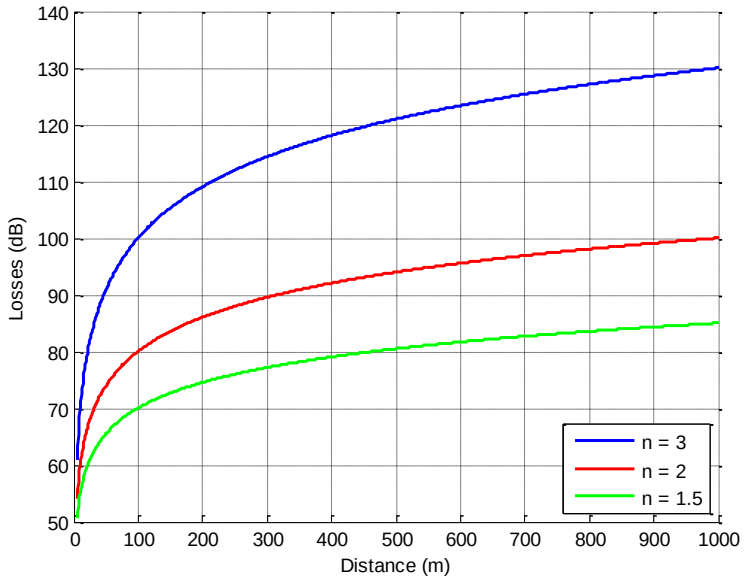

Figure 5. Path loss for different values of n.

2.1.2.2 Multipath

In industrial environments, metallic surfaces belonging to the buildings or equipment are common. These surfaces provoke reflection, refraction and scattering on electromagnetic signals; thus, the received signal is a combination of different paths of the original signal. The Power Delay Profile (PDP) shows the intensity of the received signal which allows distinguishing the spread provoked by the channel.

The fact that different replicas of the same signal are received with different delays may provoke Inter Symbol Interference (ISI). The channel provokes ISI if the symbol time is less than 5 times [15] the Root Mean Square (RMS) Delay, which is defined as [16]:

$$\sigma_t = \sqrt{\overline{\tau^2} - \overline{\tau}^2}, \quad (4)$$

where $\overline{\tau^2}$ and $\overline{\tau}$ are defined as follows:

$$\overline{\tau^2} = \frac{\sum_k a_k^2 \tau_k^2}{\sum_k a_k^2}, \quad (5)$$

$$\overline{\tau} = \frac{\sum_k a_k^2 \tau_k}{\sum_k a_k^2}, \tag{6}$$

where τ_k are the delays of the impulse response taps at the receiver and a_k represent the magnitudes of the signal at each tap.

PDPs for different environments are shown in Figure 6 [15]. As it can be seen, industrial processes lead to higher RMS delay than other scenarios, such as the main tunnel or the paper warehouse mill. The RMS delay for industrial environments varies between 250 and 300 ns. Thus, industrial channels present higher levels of ISI than the environments where it is common use WSN.

The coherence bandwidth, related to the inverse of the delay spread, represents the maximum bandwidth which can be considered flat. If the coherence bandwidth is bigger than the data signal bandwidth the channel is considered flat and hence, ISI free.

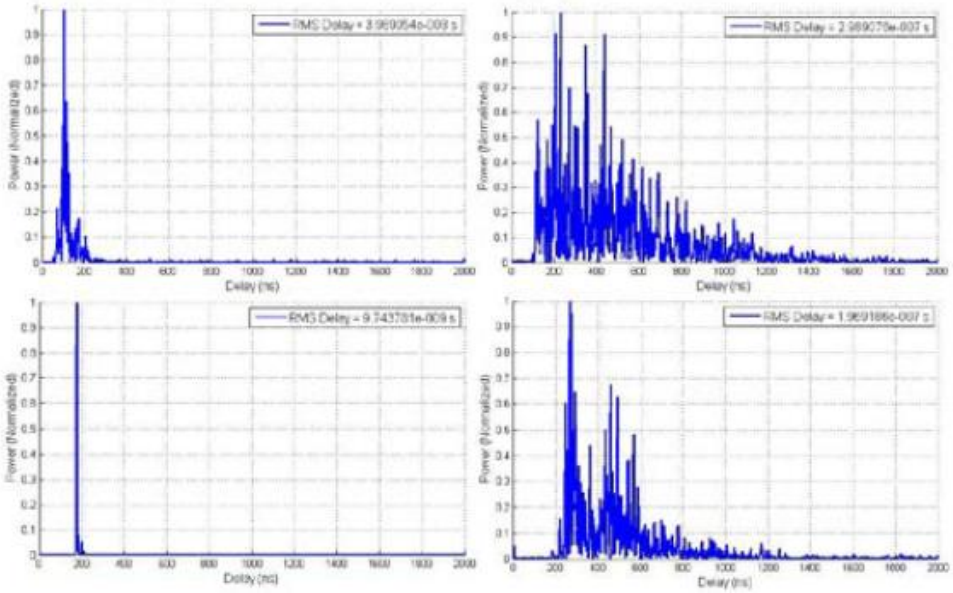

Figure 6. PDP of different environments. From left to rigth: mine tunnel trail, industrial proccess 1, paper warehouse mill, industiral proccess 2 [15].

2.1.2.3 Fading

Fading is the variation of the attenuation in a wireless channel, which may vary with time, frequency or geographical position. It can be divided in slow and fast fading, and it is often modeled by a random process. In Figure 7, the strength of a received signal is shown for a fading channel.

Slow fading, also called shadowing, is caused when something obstructs the main path between the transmitter and the receiver. Shadowing is modeled as a log-normal random process and the mean path loss in dB is:

$$PL(d) = PL(d_0) + 10nlog_{10}\left(\frac{d}{d_0}\right) + X_\sigma, \quad (7)$$

where X_σ is a zero mean random normal variable with a standard deviation σ. The value of σ has been measured for different industrial channels in the 2.4 GHz ISM band. In [14] the standard deviation has been measured for LOS and NLOS industrial environments, obtaining values of 1.82 for LOS and values between 1.22 and 2.17 for NLOS.

Fast fading is due to small changes in the distance between the transmitter and the receiver, and it is due to the multipath effect. Each path experiences a different attenuation, delay and phase shift, so the sum of all reflections can be seen as constructive or destructive interference. Fast fading can be modeled as Rayleigh, Rice, Nakagami or Weibull distributions. Some measurements have been carried out in an indoor environment [17, 18], obtaining an excellent fit of the fading with the Rice distribution.

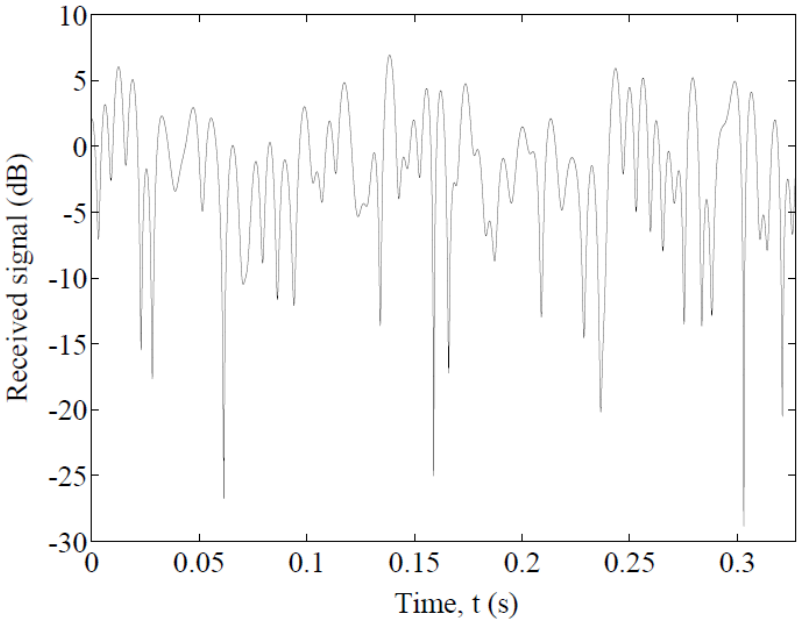

Figure 7. Typical behaviour of a received signal in a fading channel [19].

2.1.2.4 Interference and noise

WSANs operate in the non-commercial ISM bands. However, the number of devices which use these bands is growing more and more nowadays. Therefore, interference is common when these frequency bands are used. This is more critical in industrial environments because, in addition to other communications systems, factory machinery also provokes interference. Motors, inverters, induction heaters or arc welding are some of the processes or devices which may cause interference in industry. In Figure 8, it is shown the frequencies interfered by some industrial processes and devices, and it can be seen how the 2.4 GHz ISM band may be interfered by most of the systems.

Some studies have been carried out to know how other communication systems affect WSAN performance. In [20] the performance of an IEEE 802.15.4 network is studied under different interference sources, such as other networks (IEEE 802.11 or Bluetooth) and microwave ovens. The study published in [21] established that the Packet Error Rate (PER) increases from a typical 2% for an IEEE 802.15.4 to 25% when the network coexists with microwave oven interference. However, robustness against interference is a crucial requirement in IWSAN [10].

In addition to the interference problem, it must taken into account that high levels of noise can be found in industrial environments. In [22] a background noise power of -90 dBm has been measured, a significantly higher value than the noise in outdoor environments, -105 dBm.

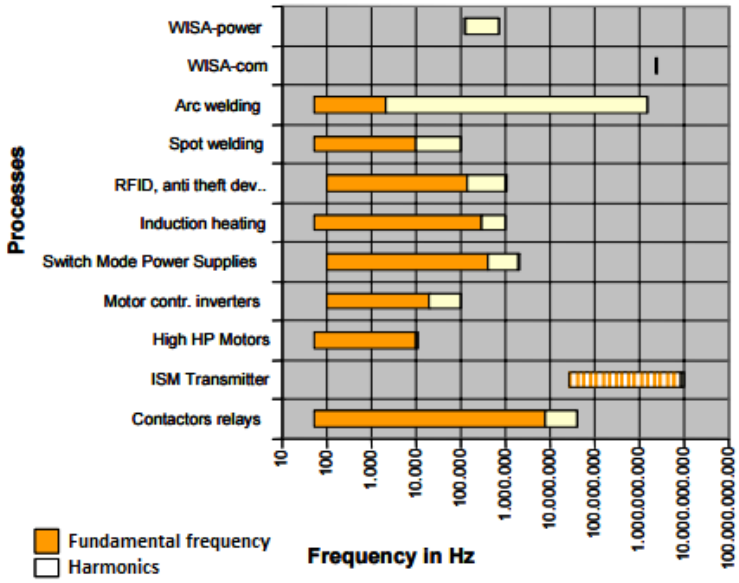

Figure 8. Frequency of different processes and devices in industry [23].

2.1.3 Standards for mission-critical and time-critical WSAN

Wireless communications in WSAN are mainly based on two standards, IEEE 802.11 (Wireless Local Area Network, WLAN) and IEEE 802.15.4 (Wireless Personal Area Network, WPAN). However, neither of them was designed to be used in industrial environments. Thus, other standards have been proposed. IEEE 802.11 offers higher data rate and higher range than IEEE 802.15.4, as it can be seen in Table 1 (different variations of IEEE 802.11 are shown). However, despite the higher data rate and range, all standards for IWSAN are based on IEEE 802.15.4. This is because IEEE 802.15.4 is more energy efficient, which is an important factor in WSAN because sensors and actuators are battery powered. Furthermore, constraints on data rate are less restrictive because closed-loop applications do not require a high data rate. The main standards for WSAN are delved in the following sections.

Standard	Frequency	Data rate	Range
IEEE 802.11a	5 GHz	54 Mbps	120 m
IEEE 802.11b	2.4 GHz	11 Mbps	140 m
IEEE 802.11g	2.4 GHz	54 Mbps	140 m
IEEE 802.11n	2.4/5 GHz	248 Mbps	250 m
IEEE 802.15.4	868/915 Hz 2.4 GHz	40 kbps 250 kbps	75 m

Table 1. Comparison of different standards.

2.1.3.1 Wireless Interface for Sensor and Actuator (WISA)

Developed by ABB and based on the standard IEEE 802.15.1 (Bluetooth), WISA [23] was designed to be used in time-critical WSAN applications. The network is deployed following a cellular topology; each cell is composed of a base station and a number of sensor and actuator nodes (up to 120). End devices are equipped with an 802.15.1 transceiver to communicate with the base station, while the latter is equipped with a special transceiver which is able to receive four channels at the same time. In addition, the base station communicates with the network manager through a wired network. A scheme of a possible WISA network is shown in Figure 9.

Sensors and actuators use the physical layer of IEEE 802.15.1, which operates in the 2.4 GHz ISM band at 1Mb/s. Furthermore, frequency hopping is applied to avoid interference and increase reliability. The WISA specification uses both Time Division Multiple Access (TDMA) and Frequency Division Duplex (FDD). FDD is used in order to define different frequencies to the communication from base station to end devices, known as downlink, and the communication from end devices to base station, known as uplink. Sensors and actuator use TDMA access to transmit data to the base station. The TDMA frame is configured by the base station, which retransmits to every node through the downlink channel. The downlink channel is also used in order to transmit acknowledgments once the base station receives data from sensors.

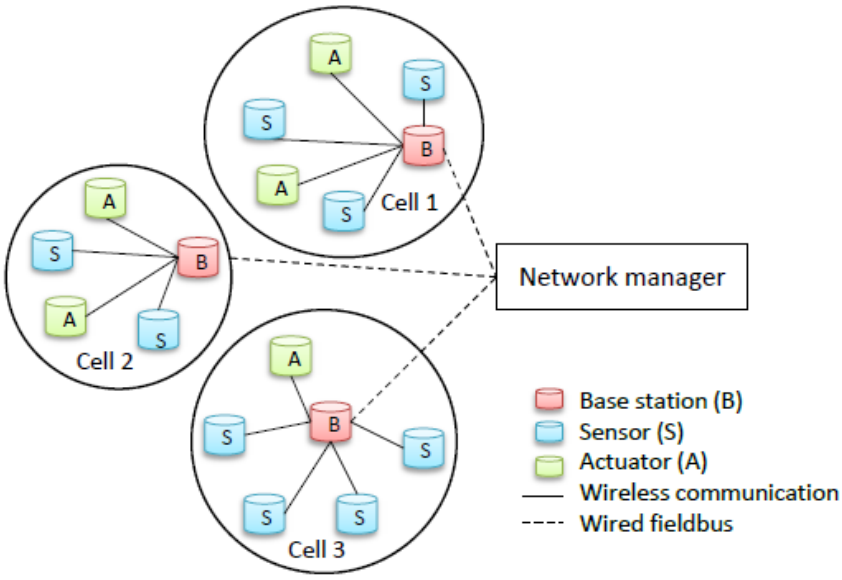

Figure 9. WISA network [24].

2.1.3.2 WirelessHART

This standard has been developed by the HART Communication Foundation [25]; they define the standard as a simple, reliable and secure solution for WSAN. The network is formed by a number of field devices, gateways, a network manager and a security manager; as shown in Figure 10. The field devices are connected to process or plant equipment, and it can be connected in either star or mesh topology. Handheld devices and adapters to connect HART devices to WirelessHART networks are also allowed. The gateway connects the field device network with host applications. It buffers large sensor data, event notifications, and diagnostics and command responses. The network manager configures the networks, scheduling, communications between devices, managing message routes and monitoring network health. The network manager may be integrated into the gateway or host application. Finally, the security manager collaborates with the network manager in order to avoid intrusions or attacks against the network.

Field devices use an IEEE 802.15.4 transceiver, which transmits in the 2.4 GHz ISM band. Direct-Sequence Spread Spectrum and channel hopping are employed in order to ensure a secure and reliable communication. Latency is ensured through a TDMA with a timeslot of 10ms. Each slot may be reserved to be used by a specific node or shared by several nodes which use Carrier Sense Medium Access / Collision Avoidance (CSMA/CA). The slot allocation is carried out by the network manager.

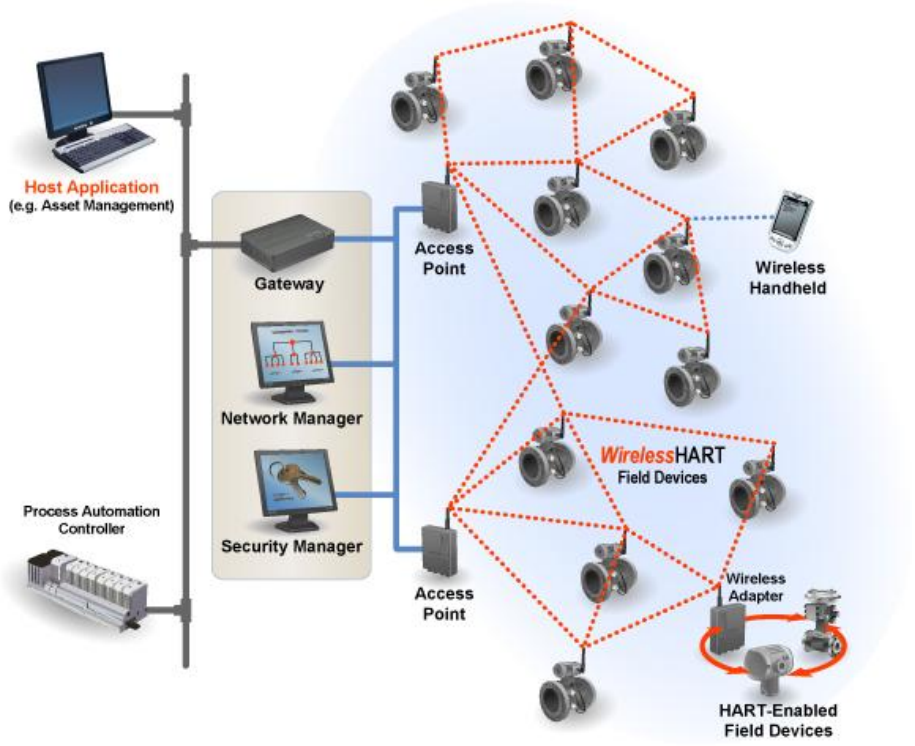

Figure 10. WirelessHART network [25].

2.1.3.3 ISA100.11a

The ISA100 standards committee, which is part of the non-profit International Society of Automation (ISA) organization, has developed the ISA.11a standard [26]. It enables wireless industrial applications, such as process automation and factory automation. An ISA100.11a network is composed of end devices and gateways. An ISA100.11a network is shown in Figure 11. Some of the end devices, which can be both sensor and actuator, are also in charge of routing functionalities. One or several gateways are in charge of providing connection between the WSAN and the user application, and it may provide security and network managers. Furthermore, the gateways also support connection with other standards.

The physical layer is based on the IEEE 802.15.4 standard, but some additional features have been included. The ISA100.11a supports frequency hopping and also blacklisting to increase robustness against interference, being TDMA the access method used by the nodes. Some flexibility in the configuration of the TDMA mechanism is allowed: since timeslot size is configurable. As a result, it is possible that two ISA100.11a devices may not be able to communicate. Every link in the network is associated to one or more slots in the TDMA frame. ISA100.11a also defines network and transport layers, based on 6LoWPAN, IPv6 and UDP.

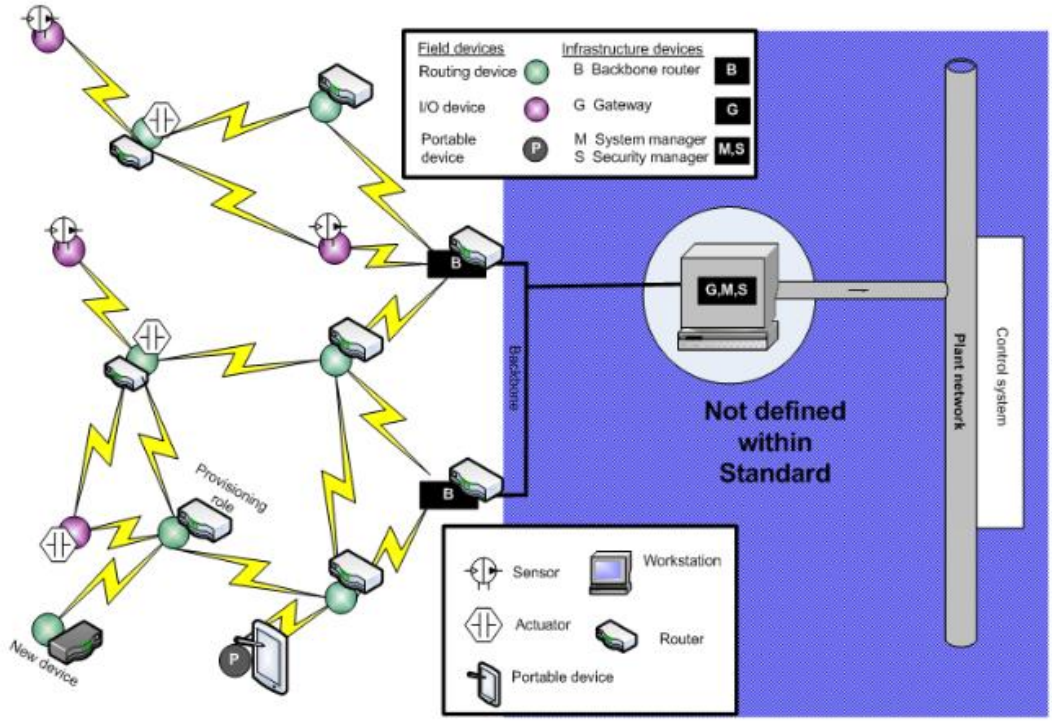

Figure 11. ISA100.11a network [27].

2.1.3.4 ZigBee and ZigBee PRO

ZigBee standard [28] was developed by the ZigBee Alliance to be used for home automation applications. Then, ZigBee PRO was proposed to fulfill the industrial requirements. Hundreds of devices; ZigBee coordinators, ZigBee routers and ZigBee end devices; are supported; and star, mesh and cluster tree topologies are allowed. A ZigBee coordinator controls the formation and security of networks, while also stores information. The ZigBee router is in charge of extending the range of networks, thus making multi-hop communications possible. Manufacturers often create devices which perform several functions, such as end devices which route messages to the rest of the network. In Figure 12, an example of a ZigBee network is shown which also includes a gateway to connect the WSAN to internet.

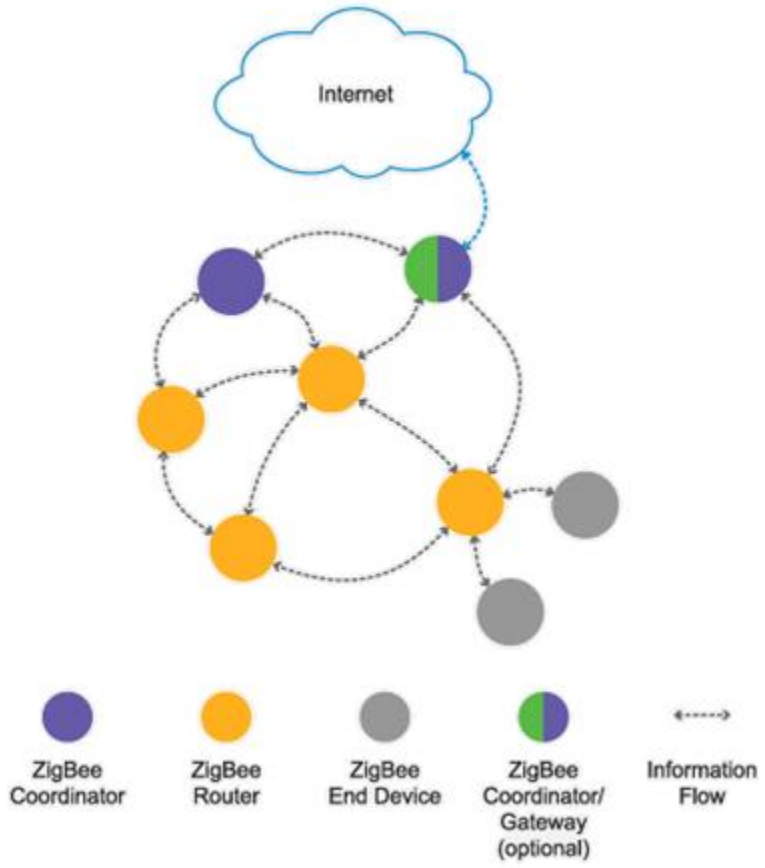

Figure 12. ZigBee PRO network [28].

As well as WirelessHART and ISA100.11a, ZigBee and ZigBee PRO are based on the IEEE 802.15.4 standard. The ZigBee PRO standard improves the IEEE 802.15.4 standard network and application layers with enhanced security features. Frequency agility is added, since all channels are scanning in order to decide the best channel in terms of interference. Then, the channel with the least interference is used by all ZigBee devices.

The channel access is based on a contention access method: unslotted CSMA/CA. However, IEEE 802.15.4 MAC also allows defining a superframe which incorporates a contention-free period. This superframe, shown in Figure 13, starts with a beacon sent by the coordinator in order to provide synchronization. The first part of the superframe is slotted and accessed through CSMA/CA access. After that, the contention-free period is located, where a number of slots are defined. Each slot is reserved for a particular node by the coordinator. Finally, the superframe incorporates an inactive period in which nodes can sleep to save energy.

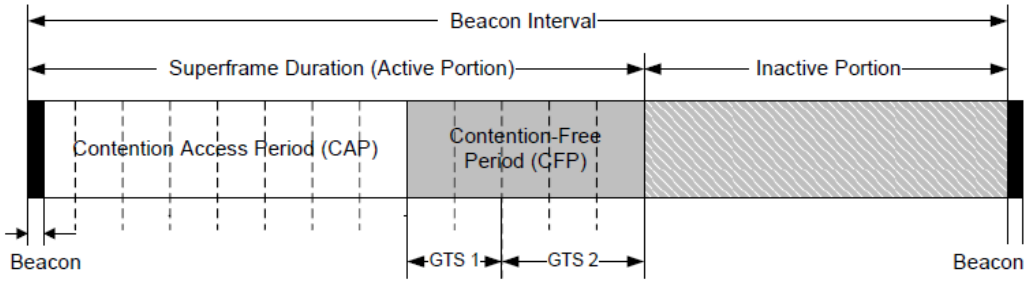

Figure 13. IEEE 802.15.4 superframe structure [29].

2.1.3.5 Wireless Networks for Industrial Automation/Process Automation (WIA-PA)

WIA-PA is the Chinese standard for measuring, monitoring and open loop control of production processes [30]. WIA-PA adopts a hybrid mesh and star network and supports end devices, routers and gateways. Routers and gateways form a mesh network, and end devices construct a star network. Each star network is a cluster managed by a router. An example of a WIA-PA network is shown in Figure 14.

Physical layer in WIA-PA is based on IEEE 802.15.4 and MAC layer is compatible with it. Some extensions to the MAC layer have been done to satisfy the industrial requirements. The contention-free period of the IEEE 802.15.4 MAC shown in Figure 13 is used to carry out the communication between devices and cluster heads, while the nodes used the contention period to join the network. The inactive period can be used to sleep or for inter-cluster and intra-cluster communications.

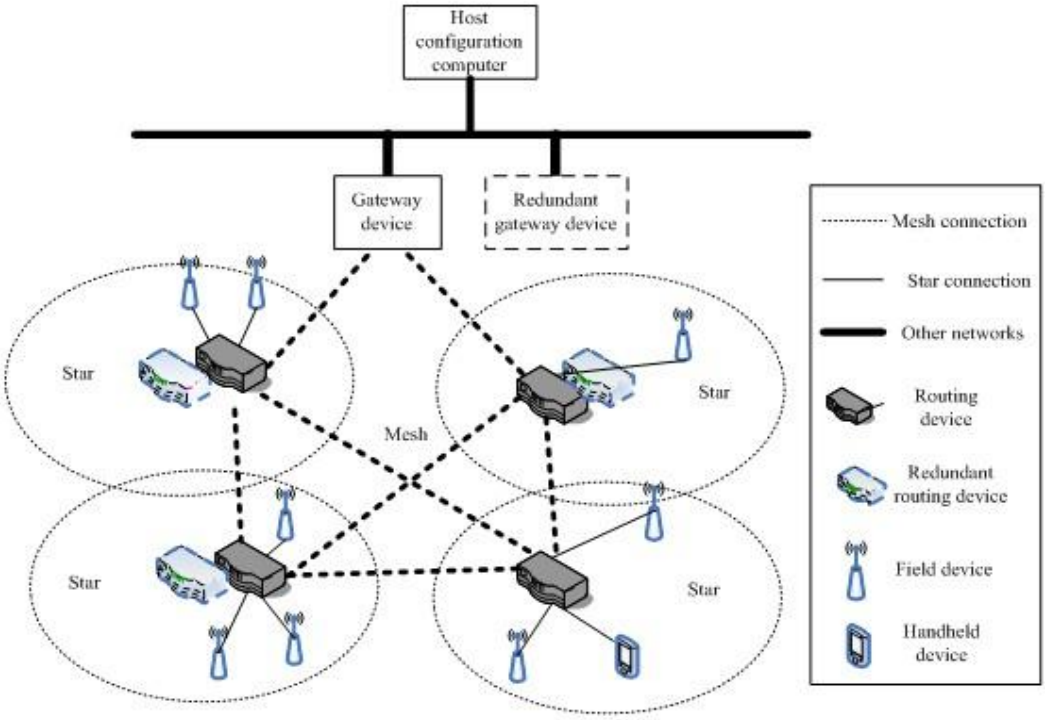

Figure 14. WIA-PA network (hybrid mesh and star) [31].

2.1.4 MACs for mission-critical and time-critical WSAN

Despite some standards have been proposed to be used for IWSAN applications, most of them are not capable of ensuring reliability and latency requirements. ZigBee, as it is based on CSMA/CA, is not effective for time-critical applications due to the increasing number of collisions as the network grows [32]. On the other hand, WirelessHART is based on TDMA and it provides 99.9% end-to-end reliability. However, packet losses due to link burst are not addressed [33]. Furthermore, the standard does not provide proper schedules for deterministic downlink transmission to the field devices [34]. WISA, ISA 100.11a and WIA-PA are only used in non-critical applications, because they lack the mechanism to support time-criticality and reliability [30, 32, 35].

The most important part of a communication system to ensure reliability and short delays is the MAC layer. It addresses how nodes access the medium and decides the schedule for communication among them. Several MACs have been proposed in the literature in order to be used in IWSAN instead of the existing standards.

2.1.4.1 QoS-MAC

QoS-MAC [36] has been proposed to ensure reliability and delay at the node-to-node level. It is based on a TDMA MAC and it assumes a tree topology network. Time is divided into units called epochs, and each epoch is divided into $k \cdot n$ slots. A node can transmit on packet per epoch, but it has k opportunities to correctly transmit this packet. Therefore, the value of k is fixed in function of the channel characteristics and the reliability requirements. The value of n is determined by the number of nodes in the network. In Figure 15 an example for $k = 2$ and $n = 17$ is shown. QoS-MAC is

capable of ensuring node-to-node requirements, but it may not guarantee end-to-end requirements.

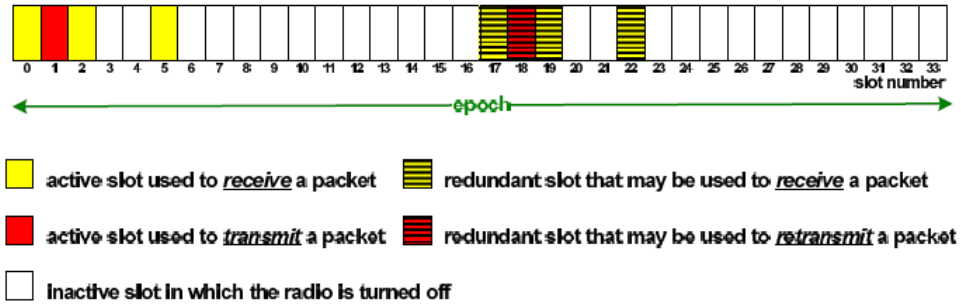

Figure 15. Epoch for QoS-MAC with $k = 2$ and $n = 17$ [11].

2.1.4.2 GinMAC

The GINSENG project tries to offer a solution which ensures the requirements while optimizing the energy consumption, proposing a MAC layer called GinMAC [37]. This MAC is based on a TDMA scheme, and it includes some mechanisms to obtain the required reliability and delay bounds. Several additional slots may be reserved for the same packet in order to achieve reliability, after which the packet is not retransmitted anymore. Slots are assigned to allow a packet to arrive at its destination during the duration of a frame. GinMAC was designed to be implemented in a tree topology network, and it also includes a routing mechanism. In Figure 16 an example of a network is shown, being composed of four sensors, one actuator and one coordinator. The GinMAC with one additional slot is shown in Figure 17, where every node has two dedicated slots in a frame. The number of additional slots is fixed in function of the channel characteristics, being the objective to ensure the correct transmission of a packet in one frame duration. After this time, the packet is discarded. GinMAC is similar to QoS-MAC, but it is oriented to guarantee end-to-end requirements.

The proposed solution has been tested in an industrial environment in Portugal, and some problems have been found because of interference [37]. However, robustness against interference is a crucial matter in IWSAN, as it has been stated in 2.1.2.4.

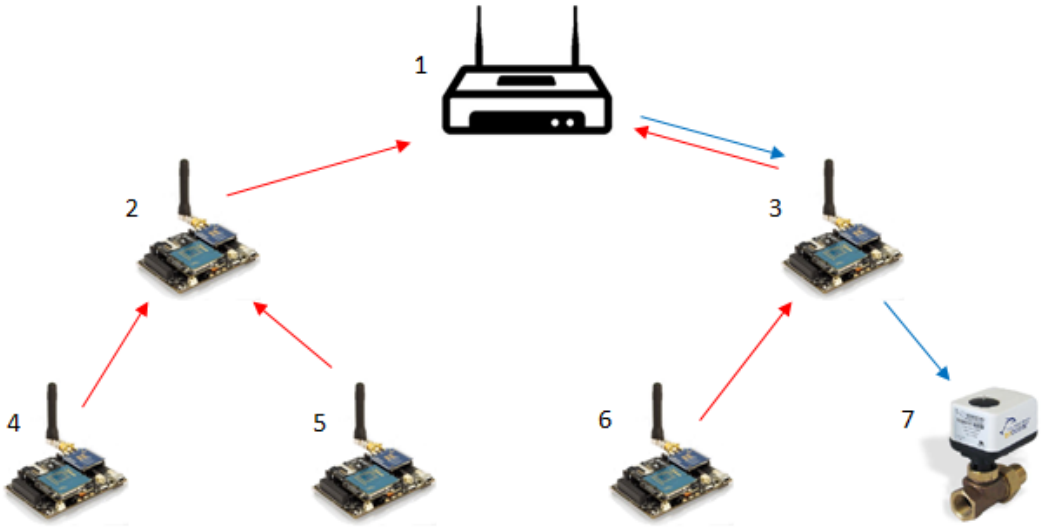

Figure 16. GinMAC topology example.

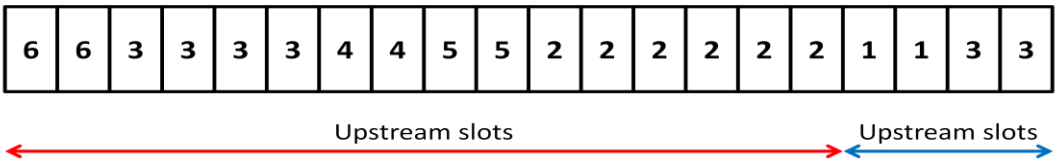

Figure 17. GinMAC frame example.

2.1.4.3 PriorityMAC

Four priorities can be handled in PriorityMAC [32]: data for emergency safety actions, extremely critical control, critical control and periodic monitoring. It is based on a TDMA access in which every priority uses a different medium access method. The MAC adds to a classic TDMA frame two subslots at the beginning of a slot, as shown in Figure 18. Each slot is dedicated to a different node, and priorities 3 and 4 are transmitted in these dedicated slots if there is no transmission of higher priorities. In order to know if a higher priority is using the channel, priorities 3 and 4 look for activity in the subslots at the beginning of a slot. If subslots are free, the node can transmit, otherwise, it has to wait for the next dedicated slot. Priority 2 messages can be transmitted in any slot and the only restriction is that no priority 1 message is being transmitted. The first subslot is checked to detect the presence of a primary transmission. Furthermore, priority 2 transmissions adopt an exponential backoff in order not to interfere among them. Finally, highest priority transmissions defer the other transmission by sending an indication in the boundary of a slot. However, no time bound is ensured using this MAC, especially for priority 2 packets whose access method is based on a contention method. Furthermore, as in GinMAC and QoS-MAC, PriorityMAC has no mechanism to overcome the interference problem.

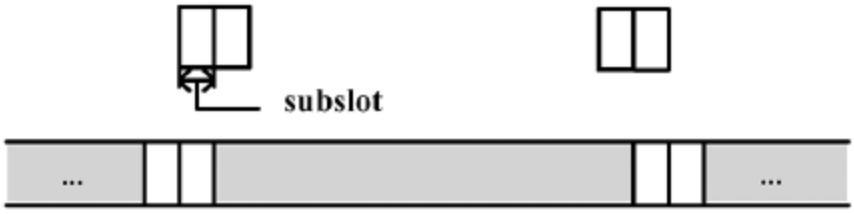

Figure 18. TDMA frame in PriorityMAC [32].

2.1.4.4 Burst

Burstiness and interference are addressed in [33]. It proposed a MAC which is designed in function of a determined bursty channel. The scheduling algorithm is defined to ensure a latency bound for this channel. Measurements must be carried out along 21 days in order to characterize each link of the network by the maximum burst length (B_{MAX}). Then, for each link, the algorithm allocates enough slots to overcome the link burstiness and ensure the transmission in a certain time. However, if any change in the bursty conditions happens, the measurements have no value and time bounds may not be ensured anymore. Therefore, the designed MAC is only useful in static environments. Also, it ensures a delay bound which is imposed by the channel, but it does not cope with the problem of avoiding interference.

2.1.4.5 IsoMAC

The IsoMAC approach (Isochronous MAC) [38] has been proposed for the EU project ^{flex}WARE (Flexible Wireless Automation in Real-Time Environments). It is based on a TDMA scheme, and provides mechanism to dynamically allocate bandwidth, reschedule the communications in the planned phase and to distribute the new schedule to all involved nodes. The TDMA frame is divided into two different phases, a Scheduled Phase (SP) and a Contention Phase (CP), as shown in Figure 19. These two phases allow transmitting two kinds of traffic, real-time traffic during the SP and Best Effort (BE) traffic during the CP. While the access to the CP is based on Distributed Coordination Function (DCF) or Enhanced Distributed Channel Access (EDCA) methods included in 802.11, real-time traffic is allocated during the SP using the scheduler proposed in [39]. This scheduler has been designed for a single-hop network composed by an access point, a controller and several nodes. The slots are assigned by the controller taking into account the requirements of the traffic flow (latency, jitter, update time, etc.) which the node establishes. The transmission scheduler assigns timeslots only to periodic flows. However, non-periodic flows can be transmitted encapsulated into a periodic flow. The generated superframe is repeated over and over again, thus, periodic traffic flows can be handled. For non-periodic traffic, a reservation request is made every time a transmission must be done.

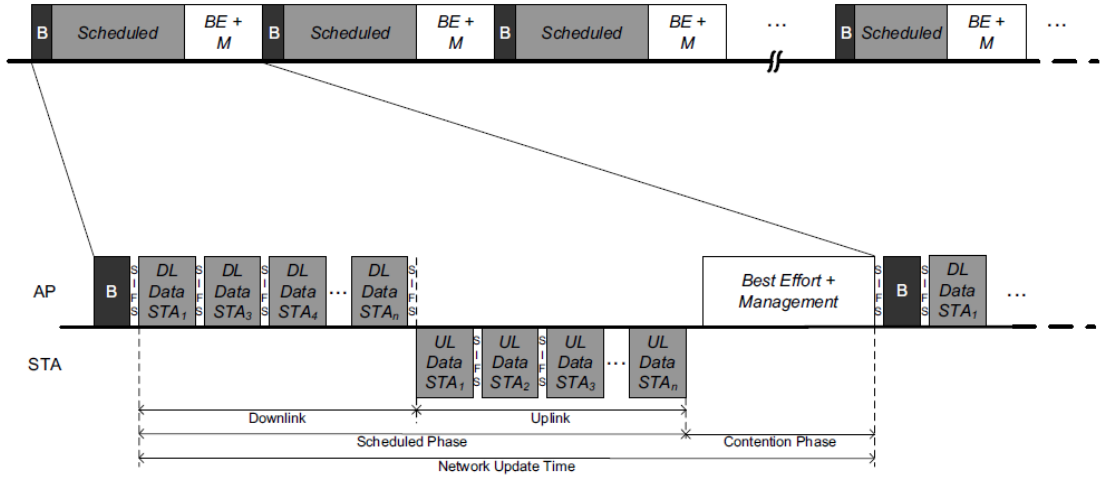

Figure 19. TDMA frame for IsoMAC [38].

2.2 Cognitive radio

CR may be the solution to cope with industrial channels in WSAN due to its ability to adapt to changes in the environment. In order to avoid interference, different tasks must be carried out by a CR system, as described in 1.2. Spectrum sensing algorithms must be added to the physical layer in order to obtain knowledge about the environment; while in the MAC layer some functionalities must be added to analyze information obtained by the spectrum sensing algorithms, to take decisions according to this information and to coordinate the network.

2.2.1 Spectrum sensing

Spectrum sensing algorithms provide knowledge about the environment to the system. Through this algorithms it is possible to know whether a channel is taken by other communication systems or not, avoiding a possible interference.

2.2.1.1 Problem definition

The goal of a spectrum sensing algorithm is to find spectrum holes, i.e., to find a channel which is not occupied. This task will try to distinguish between two hypotheses:

$$y(t) = \begin{cases} w(t), & H_0 \\ h(t) * s(t) + w(t), & H_1, \end{cases} \tag{8}$$

where $y(t)$ is the received signal, $w(t)$ is white Gaussian noise, $s(t)$ is signal to detect, $h(t)$ is the channel impulse response and $*$ represents the convolution operation. H_0 and H_1 are the hypotheses, corresponding to the absence or the presence of the signal respectively. Under H_0, $y(t)$ contains white Gaussian noise $y(t) \sim N(0, \sigma_0^2)$; while under H_1, $y(t)$ is $s(t)$ corrupted by additive white Gaussian noise.

Note that a discrete observation of the continuous signals (Equation (8)) will be used to perform spectrum sensing:

$$y[n] = \begin{cases} w[n], & H_0 \\ h[n] * s[n] + w[n], & H_1, \end{cases} \tag{9}$$

to decide whether $y[n]$ was generated under H_1 or H_0, a test statistic $\phi(y)$ (Equation (10)) from the data $y[n]$ is analyzed, and it is compared with a threshold λ.

$$\phi(y) \underset{H_2}{\overset{H_1}{\gtrless}} \lambda. \tag{10}$$

Probability of detection (P_D) and probability of false alarm (P_{FA}) are the main indicators of the performance of spectrum sensing. P_D, in Equation (11), is the probability of correctly deciding H_1, i.e. decide H_1 when H_1 happened. P_{FA}, in Equation (12), is the probability of deciding H_1 when there is no signal, when H_0 happened. Performance may also be measured by the probability of missed detection P_{MD} and the probability of correct rejection (P_{CR}), in Equations (13) and (14) respectively. However, as P_D and P_{MD} (also P_{FA} and P_{CR}) are complementary events; performance is only measured in terms of P_D and P_{FA}.

$$P_D = P(H_1|H_1) = P(\phi(y) > \lambda|H_1). \tag{11}$$

$$P_{FA} = P(H_1|H_0) = P(\phi(y) > \lambda|H_0). \tag{12}$$

$$P_{MD} = P(H_0|H_1) = P(\phi(y) > \lambda|H_1). \tag{13}$$

$$P_{CR} = P(H_0|H_0) = P(\phi(y) > \lambda|H_0). \tag{14}$$

In a spectrum sensing algorithm, the performance is represented graphically by means of the Receiver Operating Characteristics (ROC) curve, which represents the relationship between P_D and P_{FA}. An example for a matched filter detector is shown in Figure 20, the working point of the detector is defined when the threshold λ is settled. Typically, Constant False Alarm Rate (CFAR) detector are used, which means that the P_{DA} is fixed and determines λ.

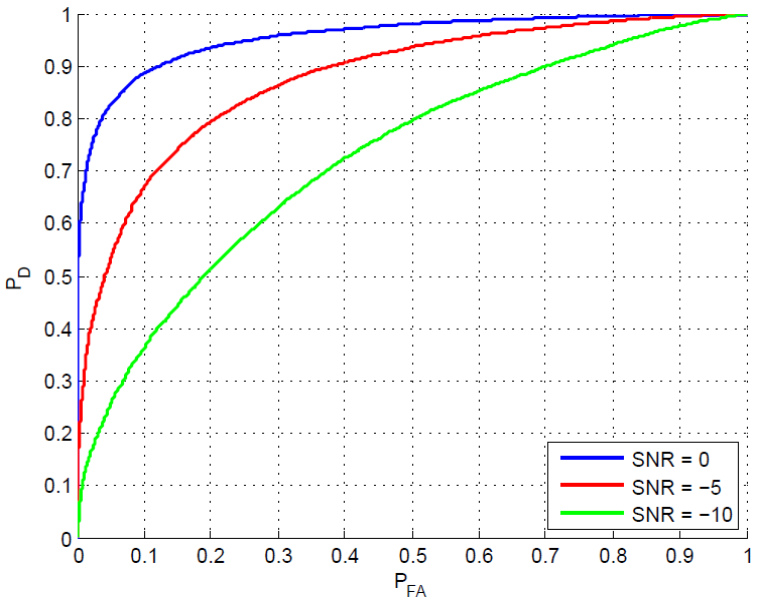

Figure 20. ROC for a matched filter detector.

Different test statistics have been proposed to detect the present or absence of a signal. The most important techniques are shown in Figure 21. Some of them need information about the signal to be detected, whereas others do not need any information (blind detection).

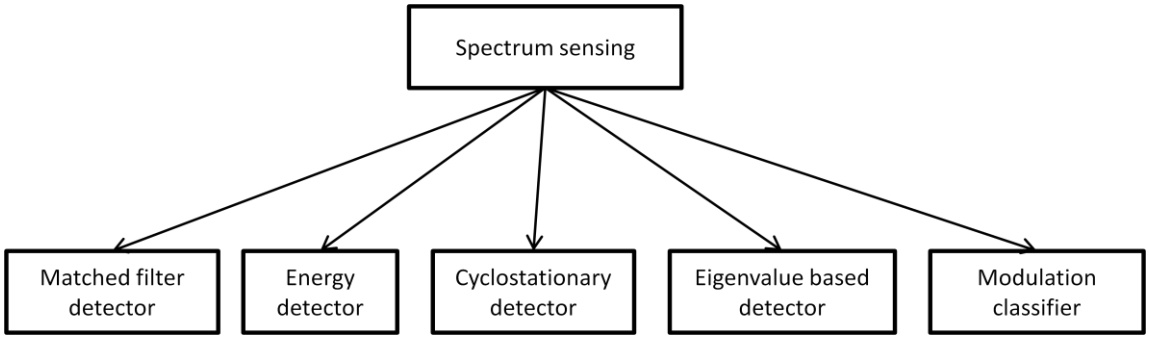

Figure 21. Spectrum sensing techniques.

2.2.1.2 Matched filter detector (MD)

This detector correlates a known reference with the unknown signal (the received signal), to find the presence of the reference in the received signal. The test statistic evaluated is shown in Equation (15).

$$\phi(y) = |\sum_{n=0}^{N-1} y[n] * x_p^*[n]|, \tag{15}$$

where $y[n]$ is the discrete received signal, $x_p^*[n]$ is the reference and $\phi(y)$ is the test statistic. Some information about the signal to detect and synchronization are needed to use a MD. These requirements are the main problem of this kind of detectors; however,

it achieves the optimum performance if these requirements are accomplished. Therefore, some MD have been proposed to be used in CR with OFDM [40] or GSM signals [41].

2.2.1.3 Energy detector (ED)

The test statistic in this detector is the energy of the received signal, as shown in Equation (16).

$$\phi(y) = \sum_{n=0}^{N-1} |y[n]|^2. \tag{16}$$

The ED is the most common spectrum sensing algorithm due to its simplicity. However, the main problem of this kind of detector is to calculate the threshold value. This value depends on P_{FA}, the length of the signal (N) and the noise power. The equation to calculate the threshold is [42]:

$$\lambda = \sigma^2\left[Q^{-1}(P_{FA})\sqrt{2N} + N\right], \tag{17}$$

where σ^2 is the noise power, Q^{-1} is the inverse Q function, P_{FA} is the probability of false alarm of the detector and N is the length of the signal. The problem lies in the necessity of knowing the noise power to fix the threshold. A predetermined threshold can be used [43], or it can be computed using an initial set of samples which are assumed to be noise [44, 45]. However, noise power may change and the initial calculated threshold can no longer be valid. To adapt the threshold to changes in noise power, a near band may be used in order to estimate the noise power [46] [47]. This method relies in the availability of a free band. Another method for estimating the noise power is recursive averaging [48], which estimates the power of signal and noise.

2.2.1.4 Cyclostationary detector (CD)

Generally, modulated signals are cyclostationary, which means their autocorrelation is periodic. This is due to cyclic prefix, synchronization, preambles, modulations, etc. [49]. Therefore, the autocorrelation of a cyclostationary signal x can be expressed as a function of its Discrete Fourier Transform (DFT):

$$R_{x(t,t+\tau)} = \sum_{\alpha=0}^{\infty} R_x^{\alpha}(\tau) e^{j2\pi\alpha t}, \tag{18}$$

where α is the cyclic frequency, τ is the lag, and R_x^{α} is the cyclic autocorrelation, and correspond to the coefficients of the DFT, defined as:

$$R_x^{\alpha}(\tau) = \lim_{T\to\infty} \int_{-T/2}^{T/2} x(t)x^*(t-\tau)e^{j2\pi\alpha t}dt, \tag{19}$$

which, for discrete-time signals, could be approximated by:

$$R_x^{\alpha}[d] = \frac{1}{N}\sum_{n=0}^{N-1} x[n]x^*[n-d]e^{-j\frac{2\pi\alpha n}{N}}. \quad (20)$$

With non-cyclostationary signals the cyclic autocorrelation is zero for all α except zero. On the other hand, when cyclostationary signals are considered, there are some values of α which make the cyclic autocorrelation different from zero. Thus, if the signal to be detected is cyclostationary, there are some values of α which allow detecting it [50]. The cyclic autocorrelation in these values of α is the test statistic in this detector:

$$\phi(y) = R_x^{\alpha}. \quad (21)$$

2.2.1.5 Eigenvalue-based detector (EBD)

EBD was designed for multiple antennas systems or for cooperative spectrum sensing. This detector analyzes the covariance matrix of samples of the received signal. In a multiple antenna system, the matrix of samples are $\boldsymbol{X}[n], n = 1, \dots, N$, where the $i-th$ component of $\boldsymbol{X}[n]; x_i[n], i = 1, \dots, M$; is the output of the $i-th$ antenna and M is the number of antennas. Therefore, the matrix $\boldsymbol{X}[n]$, whose size is $N \times M$, is composed by the N samples from the M antennas. This scheme can also be uses in a cooperative spectrum sensing algorithm, where the multiple antennas correspond to multiple nodes. The covariance matrix is defined in Equation (22), where $\boldsymbol{X}^H[n]$ represents the conjugate transpose of $\boldsymbol{X}[n]$.

$$\hat{R}_x = \frac{1}{N}\sum_{n=0}^{N-1} \boldsymbol{X}[n]\boldsymbol{X}^H[n]. \quad (22)$$

The value of the covariance matrix is different if there is a modulated signal present or there is only noise. Under noise, $\hat{R}_x$ tends to $\sigma_w^2 I$, with I denoting an identity matrix, i.e. $\hat{R}_x$ is a full-rank matrix with equal eigenvalues [51]. On the other hand, if there is any signal present $\hat{R}_x$ complies with one of the following conditions:

1. The covariance matrix of the signal, R_s, is rank-deficient ($rank(R_s) = N_s < M$).). The smallest $M - N_s$ eigenvalues are equal to σ_w^2, while the N_s remaining eigenvalues are approximately equal to an eigenvalue of R_s plus σ_w^2.
2. The covariance matrix of the signal, R_s, is a full-rank matrix (($rank(R_s) = M$). Each eigenvalue of $\hat{R}_x$ will be an eigenvalue of R_s plus σ_w^2. All the eigenvalues of R_S are unequal, hence so are the eigenvalues of $\hat{R}_x$.

Therefore, the properties of the eigenvalues can be used to accomplish the spectrum sensing. To distinguish noise from signal, different test statistics may be used [52, 53]:

- Maximum Eigenvalue Detector (MED).

$$\phi(y) = \frac{\lambda_{max}}{\sigma_w^2}. \tag{23}$$

- Maximum-Minimum Eigenvalue Detector (MMED).

$$\phi(y) = \frac{\lambda_{max}}{\lambda_{min}}. \tag{24}$$

- Energy with Minimum Eigenvalue Detector (EMED).

$$\phi(y) = \frac{\epsilon}{\lambda_{min}}.$$

$$\epsilon = \frac{1}{M \cdot N_s} \sum_{i=1}^{M} \sum_{n=0}^{N_s-1} |x_i[n]|^2. \tag{25}$$

- Arithmetic Mean Detector (AMD).

$$\phi(y) = \frac{\lambda_{max}}{\frac{1}{M}\sum_{i=1}^{M} \lambda_i}. \tag{26}$$

- Geometric Mean Detector (GMD).

$$\phi(y) = \frac{\lambda_{max}}{\sqrt[n]{\prod_{i=1}^{n} \lambda_i}}. \tag{27}$$

Only one option of the aforementioned test statistics requires knowledge of environment information to be calculated, MED. It needs the noise power to get a correct performance; but, if this is fulfilled, MED stands out from the rest [54].

2.2.1.6 Modulation classifiers

All the algorithms described above try to distinguish between the presence of a signal in the channel, H_1, and the absence of any signal, H_0. In addition to finding free channels as in traditional spectrum sensing algorithms, a modulation classifier can distinguish between several modulation formats. This information can be used by the cognitive node, for example, to obtain more suitable statistics, to make different decisions in function of the detected signal or to distinguish its network from other transmissions.

The two main solutions to carry out this task are: likelihood based classification and feature based classification [55]. With likelihood based classification, the decision is taken through a function which is calculated under the entire possible hypothesis, choosing the one which maximizes the function [56]. Depending on how data are treated, a likelihood-based classifier can be Average Likelihood Ratio Test (ALRT), Generalized Likelihood Ratio Test (GLRT) and Hybrid Likelihood Ratio Test (HLRT) [57]. With the feature based classification, the receptor extracts several characteristics of the signal, which are then analyzed by a classifier in order to establish the modulation format. Examples of features are: signal statistics [58], signal wavelet transform [59],

cummulants [60] or cyclostationary characteristics [61]; while classifiers can be implemented using Neural Networks, Support Vector Machines, k-Nearest Neighbor, Naïve Bayes, Linear Discriminant Analysis or Neuro-Fuzzy algorithms [61].

2.2.2 Cognitive-based MAC

The MAC layer is in charge of coordinating nodes when accessing to the shared medium. In traditional wireless networks, a MAC protocol has to deal with network start-up, collisions and node joining, among others. Hidden node, which occurs when a node is visible from a wireless access point but no from other nodes, may lead to difficulties in MAC layer, so it must also be taken into account. However, in CR networks the MAC layer must ensure the DSA method in order to exploit the spectrum holes in the band; therefore, some functions are added to traditional MAC protocols. These functions are designed to access the spectrum whenever PUs are not using it, and to evacuate it when any PU appears. Spectrum sensing, spectrum sharing, spectrum allocation, spectrum access and spectrum mobility are the main functions [62, 63].

2.2.2.1 Spectrum sensing

Jointly with the signal processing algorithm explained above, the MAC layer has to manage the spectrum sensing task.

The design of the MAC depends of the architecture of the network and the available hardware resources. If the nodes have multiple Radio Frequency (RF) stages, the spectrum sensing task can be done at the same time as data transmission. One of the RF stages is used to transmit data while the other is used to sense the others channels. The main problem in this kind of networks is to determine the scheduling of the sensing time of the second RF stage to sense as many channels as possible [64].

However, if only one RF stage is used, sensing and transmission have to be done sequentially. The MAC protocol has to cope with two problems:

1. Determine the spectrum sensing period.
2. Determine when the spectrum sensing task has to be carried out.

To determine when sensing has to be carry out, periodic schemes have been proposed [65, 66]. Regarding the spectrum sensing period, the longer it is, the better the performance; however, a long period leads to an inefficient spectrum utilization. Thus, length and frequency of the spectrum sensing period must be fixed to optimize the tradeoff between spectrum sensing precision and spectrum utilization. In [67], an adaptive spectrum sensing period is proposed where the length of the sensing period depends on the accuracy of the previous spectrum sensing results. Using only one RF stage, the accuracy of spectrum sensing is lower than using two; however, single antenna systems lead to cheaper cognitive radio nodes.

A cooperative sensing scheme can be used in order to increase the spectrum sensing accuracy. Moreover, cooperative spectrum sensing utilizes spatial diversity, so some problems such as hidden node problem can be solved. The cooperative organization depends on the architecture, available hardware resources and the possibility of a control channel. In cooperative sensing, all nodes send the sensing information to the coordinator of the network, which is in charge of combining all the

data to achieve more accurate decisions. Cooperative spectrum sensing has been designed for centralized networks [68] and for distributed networks [69]. Furthermore, the diffusion of the information depends on the availability of a Common Control Channel (CCC). The spectrum sensing data are transmitted through the CCC if it exists [70], or some bandwidth must be reserved to transmit this information [71].

Either centralized or distributed cooperative sensing can be adopted [72]. In centralized cooperative sensing the information is reported to a central unit which examines it and broadcasts the decision. Under distributed cooperative sensing, information is shared among nodes but each node takes its own decisions. In cooperative spectrum sensing, data fusion is the task which combines all the information and makes a global decision. Different possibilities are available; soft combining, quantified soft combining or hard combining [73]. Under soft combining, each CR user sends all samples. If quantified soft combining is used, nodes quantify the sensing results locally and report the quantified data. Finally, hard combining means that users make decisions locally and report it. Obviously, soft combining leads to a larger required bandwidth, but it may achieve a better detection performance [73].

2.2.2.2 Spectrum access

The MAC layer has to ensure that nodes access the spectrum in a coordinated way in order to avoid collisions with each other. Collisions with PU should be avoided as well. Different spectrum access modes can be used:

- Contention-based MAC: a mechanism similar to CSMA/CA in 802.11 is used. The nodes determine whether the channel is busy or not, if the spectrum band is free, the user transmits after a backoff period to avoid simultaneous transmissions. Some CSMA cognitive radio MACs have been proposed [74] or implemented in real hardware [75]. The performance of these MACs for different PU traffic is shown in [76].
- Time slot-based MAC: this mode tries to avoid collisions between nodes. Time is divided into slots, and every node has a dedicated slot where only this node can transmit. Synchronization is a fundamental requirement for these MACs. Time slot-based MACs are proposed in [77, 78].
- Hybrid MAC: contention-based MACs and time slot-based MACs have their strengths and their weaknesses. Contention-based MACs are more flexible. However they lead to collisions between nodes when the network grows. On the other hand, time slot-base MACs are not as flexible but collisions are avoided, hence, a better performance is obtained [63]. Hybrid MACs have been proposed to combine both modes. They achieve a tradeoff between the flexibility of contention-based MACs and the bigger spectrum efficiency of time slot-based MACs [79].

2.2.2.3 Spectrum allocation

Spectrum allocation is the process of allocating free channels to CR nodes. Non-cooperative and cooperative approaches are possible.

A non-cooperative spectrum allocation scheme is simpler and leads to lower computational complexity. The goal is to maximize local parameters such as throughput, and decisions are taken in function of local information [80].

Cooperative spectrum allocation tries to optimize the global network. Some approaches have been proposed:

- Stochastic algorithms: a Markov chain process is used in order to model the channel. The statistics of the historical access and the spectrum sensing results are used to take decisions. Periodically, nodes sense the channels and update the model with the results [81].
- Game theory-based algorithms: in these algorithms, the interaction between CR users is considered as a game. Game theory is used in order to take decisions to pursue a certain goal. Every node has to take decisions based on a strategy which tries to optimize a utility function; depending on which different goals can be set. Many utility functions have been proposed to optimize different parameters, such as bandwidth utilization [82], transmission rate [83], throughput [84] or to reduce interference to PU [85].
- Bio-inspired algorithms: in this case, spectrum allocation is carried out by an algorithm inspired by biological behavior. This task can be modeled by interesting characteristics of collaborative individuals of biological systems. Genetic algorithms, neural networks or insect colonies are some of the possibilities [86]. Genetic algorithms mimic the natural selection, and they are generally used to optimization and search problems. A genetic algorithm searches a solution which maximizes a function by evolving a population of many solutions. An approach using genetic algorithms to optimize the use of spectrum resources is proposed in [87] or multiple objectives are considered in [88]. In neural networks a number of neurons are interconnected and exchange messages between each other. Connections between neurons have numeric weights that are set in function of experience. This gives adaptability to the neural network, which can be used for radio parameter adaptation in CR and to set different optimization goals, such as maximizing the throughput [89].

2.2.2.4 Spectrum sharing

Different paradigms to access the spectrum band can be used in CR. The way CR users access the medium can be classified into two categories [63]:

- Spectrum underlay: CR users are allowed to transmit if their transmission power is constrained below an interference temperature defined for the PUs. Hence, CR nodes can transmit simultaneously with the PU, and no spectrum sensing algorithm is needed.
- Spectrum overlay: CR users use the spectrum holes to carry out their transmission. After a PU is detected in the channel, the CR transmission must be stopped, so spectrum sensing is required.

2.2.2.5 Spectrum mobility

CR nodes must vacate the channel if a PU appears. This is known as spectrum mobility or spectrum handoff. Minimizing delay and losses during the handoff period is an important issue of these algorithms. Two strategies to vacate the band may be used [90]:

- Reactive handoff: the decision on the backup channel is done when a handoff triggering event happens. Spectrum sensing is carried out after this event in order to select the backup channel. Nevertheless, since CR users sense the spectrum once the handoff triggering event occurs, the delay of handoff process is due mostly to the spectrum sensing algorithm.
- Proactive handoff: in proactive handoff the spectrum sensing algorithms looks for a backup channel before a handoff event happens. CR nodes use the PU traffic statistics to decide the backup channel and the handoff actions. Latency is lower because everything is planned before the handoff happens. However, the backup channel selected can be obsolete when the handoff happens.

Various techniques have been proposed in order to model the behavior of PU, such as queuing theory, ON/OFF random processes, hidden Markov models or Bernoulli random processes [91, 92].

2.2.2.6 Common Control Channel

Some of the tasks detailed below need to share information in order to ensure a correct functioning; sensing, mobility and allocations required data to be shared between all nodes. To do this, some CR networks use a CCC; nevertheless, the use of a CCC has its limitations [93]. The major limitation is that CCC has to be a dedicated channel in order to avoid interference from a PU, but this is difficult to ensure in CR paradigm. Furthermore, finding a channel common to all nodes may not be possible. Therefore, the confidence in CCC may compromise the performance of the CR network. As a consequence, CR networks without a dedicated CCC are investigated.

Some approaches have tried to ensure a interference-free channel, being frequency hopping or underlay CCC some of the possibilities [70]. These solutions do not use a dedicated channel; however, they do not avoid interference from a PU. Control information may be transmitted in a dedicated period inside the data frame [94], during which all nodes transmit control information to the coordinator. In [95] a mechanism to select a group of CCCs is proposed and various CCCs are used because it takes into account that there is not a channel available to access by all nodes. Another option chosen rather than a CCC is *rendezvous* process, especially in the configuration phase. In the *rendezvous* process, nodes look for each other in the available channels. I.e., a node tries every channel until it comes across the destination node [96]. The order in which nodes access the channels has been investigated, and different sequences have been proposed in order to ensure the *rendezvous* as quickly as possible [96-98].

2.2.3 Cognitive radio for mission-critical and time-critical wireless sensor and actuator networks

Normally, WSAN networks work in ISM bands. Therefore, transmissions from other networks may interfere and compromise the performance of the network. Frequency hopping spread spectrum can be used in order to reduce interference from other sources. It uses a pseudorandom sequence to do channel hopping in order to take advantage of frequency diversity. Nevertheless, it does not consider quality of channels [9]. CR may be a more useful tool for this purpose.

2.2.3.1 Common Control Channel-based MACs

Some CR-based MACs with CCC have been proposed to be used in mission-critical and time-critical WSAN applications. In [99] a MAC known as CH-MAC which ensures that every data arrive at destination is proposed. It uses a CCC to share spectrum sensing information and to carry out the *rendezvous* process. During this process the allocation is done taking into account the available channels for both nodes. Then, both nodes reconfigure their radios to the data channel to start the communication, as shown in Figure 22. If a packet is lost both nodes hop to the next channel from the list to go on with the communication. A similar MAC is proposed in [100], but in this case nodes have two antennas. One of the antennas operates in a dedicated CCC and is accessed through CSMA/CA, and the other is used to transmit data and is dynamically reconfigurable. Therefore, increasing the nodes in the networks leads to increasing collisions in the CCC. Due to the CSMA/CA method used to control the access in the CCC, this MAC is not capable of ensuring a time bound as is needed in time-critical applications.

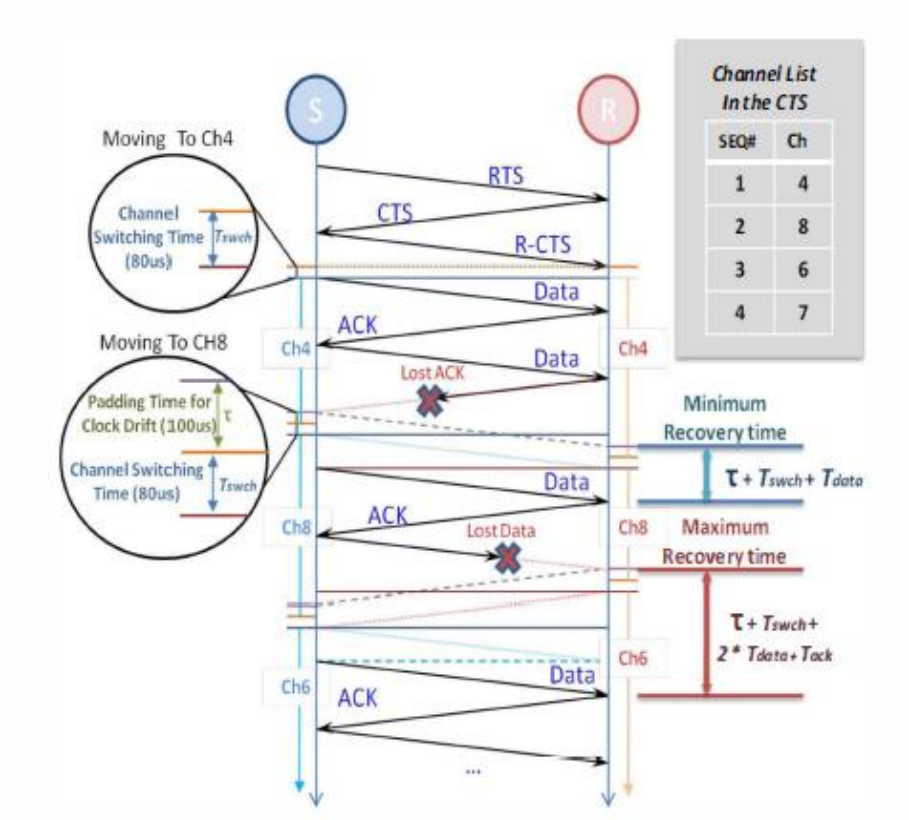

Figure 22. Packet exchanging on CH-MAC [99].

A TDMA approach for the CCC is used in [101], where each node exchanges information about packets waiting to be sent. Taking into account this data, nodes create a queue with the packets of the whole network; if any channel is free the node with the first packet in the queue takes this channel. Early Deadline First (EDF) schedule is used in order to create the global queue; however, other schedulers can be used. In addition to TDMA access, Frequency Division Multiple Access (FDMA) may be used jointly [102]. Using frequency diversity more than one node can transmit at the same time. A base station is in charge of assigning the temporal slot and the frequency channel to the different nodes of the network.

All of these MACs have the disadvantages of the CR systems which depend on a CCC. A CCC would be necessary to ensure the correct working of the networks. Without the CCC, it may be interfered and the performance could be compromised. Moreover, under these approaches all nodes share information for the whole network in the same channel, but there may not be a common channel to all the networks or it is impossible to connect a node with all the others. Consequently, WSAN applications demand a reliable non CCC-based MAC.

2.2.3.2 MACs with no CCC

In order to avoid the problems which lie behind a CCC, several MACs have been proposed. One of these MACs is DRMAC, where a specific period is reserved to transmit coordination data which usually is shared in CCC in [94]. The frame in this DRMAC is divided into 4 different periods: sense, control, feedback and data, as shown in Figure 23. During the sensing time, all nodes carry out spectrum sensing. Then,

spectrum sensing results and packets in queue information are transmitted to the coordinator in the control period. Afterwards, the coordinator configures the TDMA structure and sends it in the feedback period. Finally, nodes access the medium according to the TDMA frame generated by the coordinator. A similar approach is DynMAC [9], which is based on GinMAC. DynMAC added cognitive characteristics to GinMAC: monitoring of environment conditions, decision on best channel, sharing information and mobility.

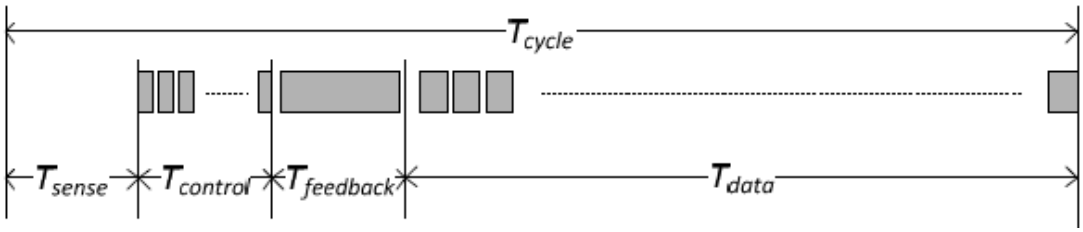

Figure 23. Frame structure of DRMAC [94].

A *rendezvous* sequence may be used to obtain correct transmission of data in QB2IC [103]. The proposed sequence has been designed in order to ensure that two nodes come across with each other in at least one channel over the sequence duration. Therefore, if there is an available channel between sender and receiver, the *rendezvous* scheme ensures the correct reception. This MAC does not need a CCC because no coordination information is exchanged. However, time bound ensured by this MAC is determined by the length of the sequence, which is much higher than in other CCC-based approaches.

The sequence is different for the transmitter and the receiver. The transmitter chooses n channels, as shown in the example in Figure 24. The receiver generates a random sequence with all the available channels where every channel has a length of n time slots. The number of available channels is called m. A receiver sequence is also shown in Figure 24 for an available channel set of {1, 2, 3}, and it can be seen how the *rendezvous* is possible if an available channel exists in common. This sequence could be repeated more than once, resulting in a length S of the sequence.

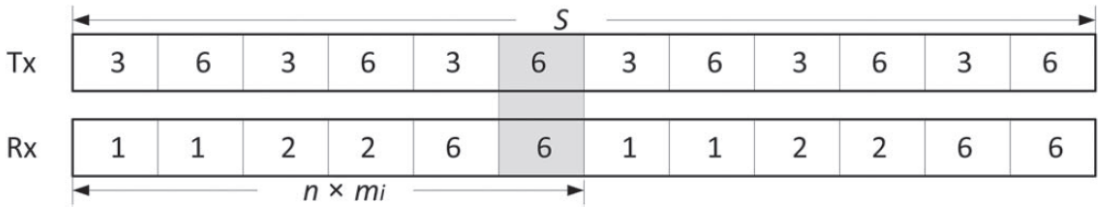

Figure 24. Example of rendezvous sequence with QB2IC [103].

2.3 Summary

This chapter has presented the requirements and challenges of mission-critical and time-critical IWSAN. The existing standards for IWSAN have also been detailed.

The inability of these standards to ensure the IWSAN requirements has led to new proposals, which have been delved in this chapter. However, these solutions are not capable of working under interference, which is a requirement in industrial applications. CR may be the answer to this problem, therefore, this technology is explained in this chapter. CR algorithms have been delved. Furthermore, several MACs for time-critical and mission-critical IWSAN applications, both CR-based and non-CR-based, have been detailed.

Chapter 3

EVALUATION OF MACS FOR IWSAN

From the related work described in Chapter 2, several MACs have been chosen and their application for IWSAN has been analyzed. Different CR-based and non-CR-based MACs have been selected in order to establish the benefits of CR for mission-critical and time-critical applications in WSAN. A theoretical analysis using Network Calculus (NC) has been developed to establish the maximum delay that every MAC ensures. Furthermore, simulations in OPNET have been done in order to contrast the results obtained by NC. Several industrial environments have been simulated, including log-normal shadowing, Rayleigh fading and interference. Moreover, some simulations for non-CR-bases MACs and Frequency Hopping (FH) have been carried out to compare FH and CR.

3.1 Selected MACs and simulated scenarios

Below, the chosen MACs and the simulated environments are described.

3.1.1 MAC selection

Six MACs from the state of the art have been chosen, and the main characteristics of all of them are detailed in Table 2. Three of them are not CR-based (GinMAC, PriorityMAC and IsoMAC) and three are CR-based (QB2IC, DRMAC and

DynMAC). All of them have been introduced in Sections 2.1.4 and 2.2.3. These MACs have been evaluated on top of an 802.15.4 IEEE physical layer. The performance has been measured through OPNET simulations under different industrial environments, which are described in Section 3.1.2. PER and delay have been measured to compare between the different MACs. To measure the PER, an error is considered if the packet is not correctly delivered after all the possible retransmissions. If a packet is received two times, the delay is calculated only for the first reception, discarding the second packet.

MAC	Topology	Single/multi hop	Priorities	CR
GinMAC [37]	Tree	Multi-hop	No	No
PriorityMAC [32]	Any	Multi-hop	Yes	No
IsoMAC [38]	Any	Single-hop	No	No
QB2IC [103]	Any	Multi-hop	No	Yes
DRMAC [94]	Any	Single-hop	Yes	Yes
DynMAC [9]	Tree	Multi-hop	No	Yes

Table 2. Main characteristics of considered MAC schemes.

3.1.2 Description of simulated scenarios

Since both multi-hop and single-hop topologies are common in WSAN, the selected MACs have been evaluated for both scenarios. Some of the selected MACs are valid for multi-hop networks Therefore, these MACs have been evaluated for both multi-hop and single-hop scenarios. However, single-hop MACs are not valid for multi-hop networks, so they have been only evaluated for the single-hop network. A tree-topology network (Figure 25) is simulated for the multi-hop case, and a star-topology network (Figure 26) for the single-hop case. The network is made up of a number of sensors which gather data from the environment and transmit it to the root, which is the coordinator of the network and takes some decisions according to the gathered information. These decisions are transmitted to the actuators, which are in charge of carrying out the actions determined by the coordinator.

In simulations, the nodes generate packets randomly. The nodes have been randomly placed in a 100m x 100m square, where both x and y coordinates of each node follow a uniform distribution between 0 and 100 meters. Pathloss, and therefore SNR, are calculated in function of the random distance between nodes. The pathloss is calculated as in Equation (1) defined in Section 2.1.2.1 for an index $n = 2$. The SNR, calculated in function of the pathloss, follows a log-normal distribution due to the random deployment of the nodes. The simulated Probability Density Function (PDF) of the SNR is represented in Figure 27, as well as the theoretical distribution. The Signal to Noise Ratio (SNR) for every link has a mean of 14.23 dB and it is always higher than 6 dB.

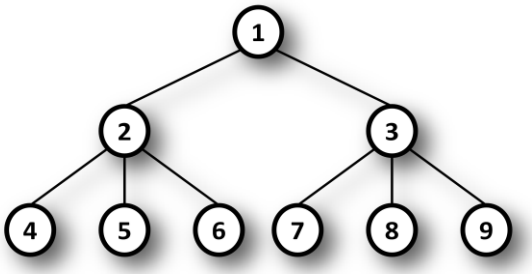

Figure 25. Tree-topology network.

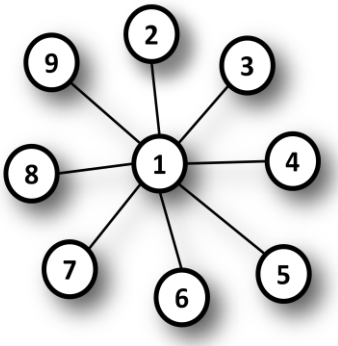

Figure 26. Start-topology network.

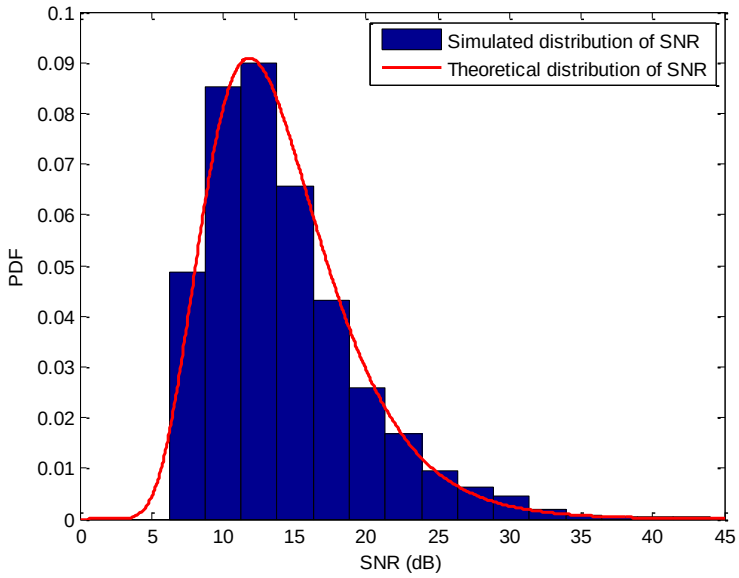

Figure 27. PDF for simulated and theoretical distribution of SNR for nodes placed randomly.

Shadowing and fast fading are also common in industrial environments and has been considered in this work. Shadowing depends on the space, and as static nodes are considered, it is calculated at the beginning of the simulation and remains constant afterwards. Shadowing is modeled by a log-normal distribution, whose σ value has been chosen according to industrial channels measurements [13, 14] ($\sigma = 1.9$). Fast fading is modeled by a Rayleigh distribution, whose gain is calculated for every packet and remains constant during the transmission of this packet. Thus, flat fading is considered.

Furthermore, the performance of the different MACs has also been analyzed under interference. Wi-Fi users coexist with the system under consideration, interfering each other. Different simulations have been done for different occupation of the channel. Wi-Fi users take up the channel during a certain percentage of the time, which can range from 0% to 25% of the time depending of the traffic load. This traffic is generated accordingly to a Poisson distribution, with an arrival time of λ [104]. The

packet inter-arrival time is distributed exponentially according to the distribution function:

$$F(t) = 1 - e^{-\lambda \cdot t}. \tag{28}$$

3.1.3 MACs parameters

The parameters of the selected MACs have been defined to work correctly in the networks shown in Figure 25 and Figure 26. The GinMAC frame used for the single-hop network is shown in Figure 28a, and in Figure 28b for the multi-hop network. The GinMAC has been configured to use 2 additional slots. Therefore, packets are transmitted 3 times before being discard.

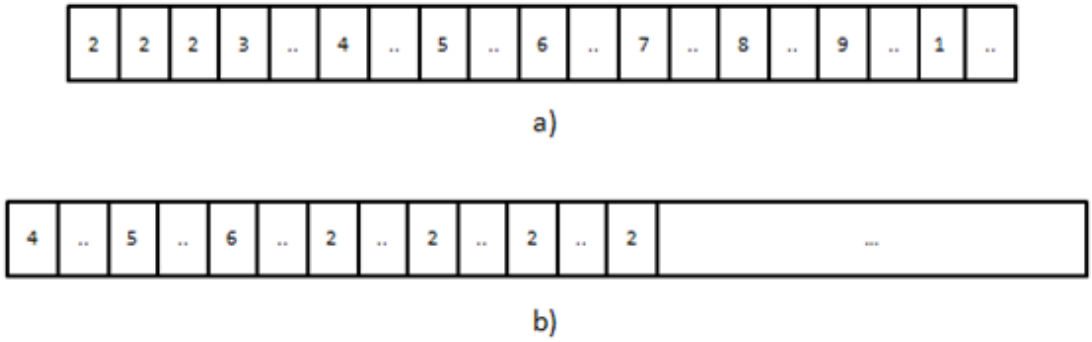

Figure 28. GinMAC frame with two additional slots for: a) single-hop network b) multi-hop network.

In PriorityMAC, the frame has been set to have 10 slots, and, as well as GinMAC, the packets are discarded after 3 erroneous transmissions. In IsoMAC, the frame has 20 slots, and nodes generate periodic traffic with a period of 2.5 times the frame time. In this MAC every packet is only transmitted once. IsoMAC has been designed for periodic traffic, and it considers that a packet is not valid if it is sent after the fixed slot.

QB2IC, explained in Section 2.2.3.2, has been configured for $n = 2$ and $m = 6$, and the generated sequence for the receiver is repeated 3 times. The sequence is repeated 3 times to ensure that 2 nodes come across at least 3 times. Therefore, the *rendezvous* sequence has a length of 36 slots.

For DRMAC, the frame depicted in Figure 23 has been configured for 9 nodes. Hence, the control period has 9 slots. Also, the data period has been configured to allocate 10 transmissions. The times for all periods in function of the length of the frame are shown below:

$$T_{SENSE} = 0.2857\ frames. \tag{29}$$

$$T_{CONTROL} = 0.2575\ frames. \tag{30}$$

$$T_{FEEDBACK} = 0.1711\ frames. \tag{31}$$

$$T_{DATA} = 0.2857\ frames. \tag{32}$$

$$t_{slot} = 0.0286\ frames. \tag{33}$$

Finally, DynMAC has been configured as GinMAC, but an extra slot for spectrum sensing has been added at the beginning of the frame. This spectrum sensing slot has a length equal to 2 data slots.

3.2 Theoretical analysis

A theoretical analysis has been carried out to study the validity of the MACs described in Section 3.1. In this Section the tool used to carry out the analysis is explained, and the results of the analysis are delved.

3.2.1 Network Calculus

NC [105] is a mathematical tool which allows calculating the theoretical bounds in time that a network is capable of ensuring. This mathematical tool characterizes a flow by a wide-sense increasing and left-continuous cumulative function R, where $R(t)$ is the amount of bits generated in the interval $[0, t]$. 0 bits are considered in the initial state ($R(0) = 0$). A flow $R(t)$ is α constrained if:

$$\forall t, s \geq 0, s \leq t, R(t) - R(s) \leq \alpha(t - s), \tag{34}$$

where the function α is the arrival curve for the data flow defined by the cumulative function R.

Considering $R(t)$ and $R^*(t)$ as input and output flow through a node, the node offers to the flow a service curve β if and only if β is wide sense and:

$$R^*(t) \geq \inf_{0 \leq s \leq t} \big(R(s) + \beta(t - s)\big), \tag{35}$$

which is called in [105] as min-plus convolution:

$$R^*(t) \geq R(s) \otimes \beta. \tag{36}$$

The output flow in this node is at least β, as Figure 29 shows.

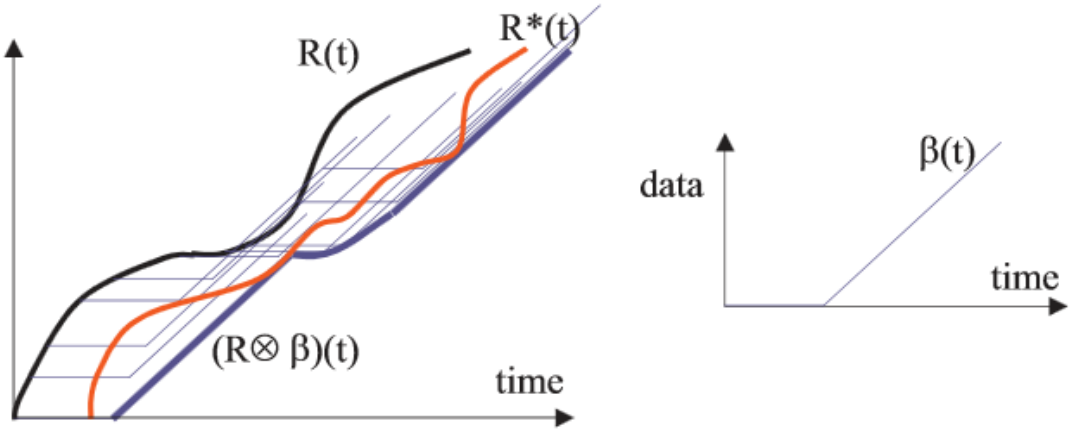

Figure 29. Definition of service curve. The output R* must be above R(s)⊗β [105].

Using the arrival and the service curves two bounds can be determined, backlog bound and delay bound. In a network characterized by the arrival curve α and by the service curve β, the backlog $R(t) - R^*(t)$ is bounded by:

$$R(t) - R^*(t) \leq \sup_{s \geq 0}(\alpha(s) - \beta(s)), \tag{37}$$

while delay is bounded by:

$$\delta(s) \leq \sup_{s \geq 0}(inf\{\tau \geq 0 : \alpha(s) \leq \beta(s + \tau)\}). \tag{38}$$

These two bounds are more intuitively defined as the maximum vertical distance between α and β, $v(\alpha, \beta)$, for the backlog bound, and the maximum horizontal distance, $h(\alpha, \beta)$, for the delay bound.

For the word carried out in this thesis, the analysis is only focused on delay bounds. This allows knowing whether the time requirements can be guaranteed or not. On the other hand, no requirements in backlog are imposed by IWSAN applications, so its analysis will be withdrawn.

Below, the analysis for every MAC is presented. In order to introduce NC, an example for a TDMA MAC for a single-hop network is also delved.

3.2.2 TDMA

In order to carry out the theoretical analysis, the arrival curve (α) and the service curve (β) defined in Equations (34) and (35) have to be defined. The arrival curve α for a periodic traffic is defined as:

$$\alpha(t) = L\left\lceil \frac{t}{T} \right\rceil, \tag{39}$$

where T is the period of the flow and L the length of the packet. This arrival curve is also valid for sporadic traffic whose minimal interarrival time between packets is T.

Assuming a TDMA whose frame has one slot for each node, and every slot has the same duration, the length of the frame is:

$$c = \sum_{k=1}^{M} t_{slot} + t_{sync}, \tag{40}$$

where M is the number of nodes in the network, t_{slot} is the length of the slot and t_{sync} is the timer required to carry out synchronization. A node may not have access to the medium during at maximum $c - t_{slot}$, i.e., it may have to wait during the entire frame until its dedicated slot. Consequently, the service curve is defined as:

$$\beta(t) = B \cdot max\left(\left\lfloor \frac{t}{c} \right\rfloor t_{slot}, t - \left\lceil \frac{t}{c} \right\rceil (c - t_{slot})\right) \forall t \geq 0, \tag{41}$$

where B is the transmission capacity.

The service and the arrival curve for a TDMA and a traffic flow whose minimal interarrival time is identical to the frame duration are shown in Figure 30. It can be seen how it is possible to establish a maximum delay, which correspond to the horizontal distance between α and β ($D_{max} = h(\alpha, \beta) = c$).

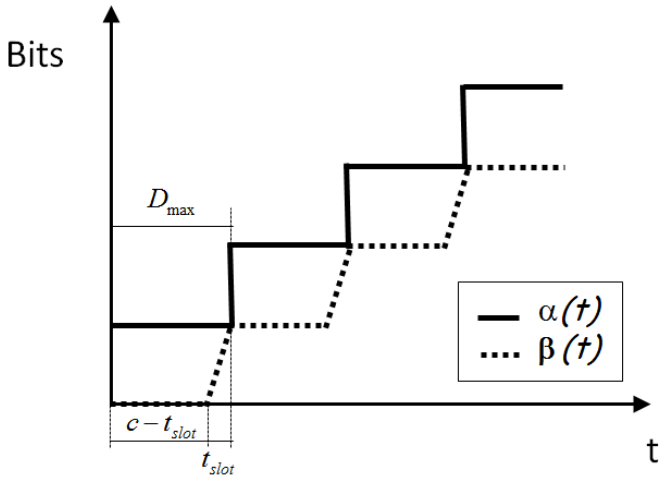

Figure 30. Arrival curve and service curve for a TDMA MAC.

3.2.3 GinMAC

From Figure 28 a), the service curve, β, for GinMAC can be obtained. It can be determined the maximum time which a node has to wait to access de medium, which is $c - 3 \cdot t_{slot}$. Once the node accesses the medium, it has three opportunities to send the packet; thus, the service curve for this MAC is:

$$\beta(t) = B \cdot max\left(\left\lfloor \frac{t}{c} \right\rfloor t_{slot}, t - \left\lceil \frac{t}{c} \right\rceil c\right) \forall t \geq 0, \tag{42}$$

and it is represented in Figure 31, jointly with the arrival curve defined in Section 3.2.2. The traffic is generated in a way that the minimal inter packet time is the frame length. Therefore, in this case, the maximum delay is:

$$D_{max} = c + t_{slot}. \tag{43}$$

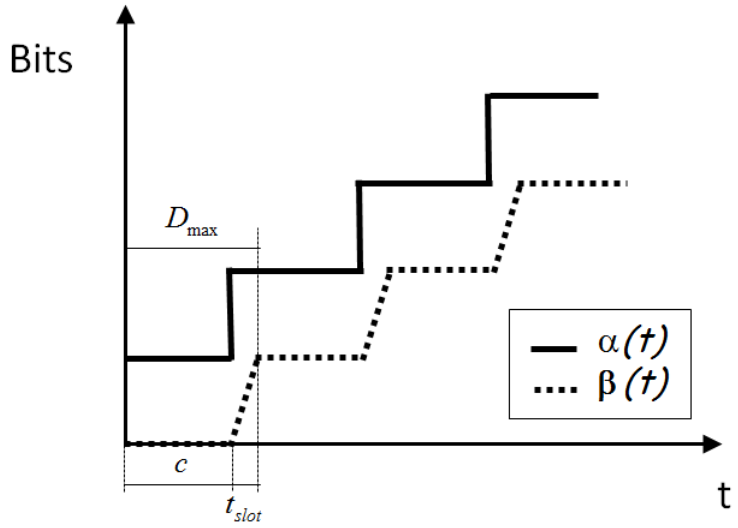

Figure 31. Arrival curve and service curve in GinMAC for the single-hop network.

In the multi-hop case, a node has to wait the same maximum time than in the single-hop case, $c - 3 \cdot t_{slot}$. However, the maximum time since the source node transmits the packet and the destiny node receives is $21 \cdot t_{slot}$ because it has to go through two hops. This can be seen in the frame for the multi-hop network (Figure 28 b), if the node 4 transmits a packet to the node 2 in its first slot, it may not arrive at the node 1until the last slot of the node 2. Therefore, the service curve for the multi-hop network is:

$$\beta(t) = B \cdot max\left(\left\lfloor\frac{t}{c}\right\rfloor t_{slot}, t - \left\lceil\frac{t}{c}\right\rceil (c + 20 \cdot t_{slot})\right) \forall t \geq 0, \tag{44}$$

and the maximum delay is:

$$D_{max} = c + 21 \cdot t_{slot}. \tag{45}$$

3.2.4 PriorityMAC

In PriorityMAC the three different priorities have different access mechanisms. For the highest priority, the nodes can defer other transmissions. The maximum time a highest priority packet has to wait to access the medium is t_{slot}. Therefore, the service curve for this priority is:

$$\beta(t) = B \cdot max\left(\left\lfloor\frac{t}{t_{slot}}\right\rfloor t_{slot}, t - \left\lceil\frac{t}{t_{slot}}\right\rceil (c - t_{slot})\right) \forall t \geq 0, \tag{46}$$

and the maximum delay for the single-hop network is:

$$D_{max} = 2 \cdot t_{slot}. \tag{47}$$

The access mechanism for priority 2 packets is based on a CSMA scheme, so delay for priority 2 is not bounded due to the access mechanism used for this priority. Finally, the access mechanism for priority 3 packets depends on the higher priority

packets, so it is not possible establish a delay bound because it is not possible to establish it for priority 2.

In the multihop network a packet has to hop two nodes to get its destination. Consequently, the maximum delay for priority 1 packets is two times the maximum delay obtained for the single-hop network:

$$D_{max} = 4 \cdot t_{slot}. \tag{48}$$

As well as in the single-hop network, delay for priority 2 and 3 packets can not be guaranteed.

3.2.5 IsoMAC

This MAC has been designed for periodic traffic, ensuring a delay limited to the period of every flow. The scheduler is in charge of allocating the slots for the different flows in the network. If it is possible to obtain a schedule which ensures the requirements of a flow, some slots are assigned to guarantee a maximum delay:

$$D_{max} = T, \tag{49}$$

where *T* is the period of the flow. Otherwise, if it is not possible ensure the requirements of this flow, the scheduler transmits an error, and no slots are allocated in the frame for this traffic.

3.2.6 QB2IC

This MAC is based on a *rendezvous* sequence, as it has been stated in Section 2.2.3.2. The proposed sequence allows two nodes to come across on the same channel. The *rendezvous* sequence ensures a Maximum Time To Rendezvous (MTTR) equal to the sequence length. Therefore, the service curve is:

$$\beta(t) = B \cdot max\left(\left\lfloor\frac{t}{S}\right\rfloor t_{slot}, t - \left\lceil\frac{t}{S}\right\rceil (S - t_{slot})\right) \; \forall t \geq 0, \tag{50}$$

where S is the sequence length and t_{slot} is the slot length. Therefore, the maximum delay in the single-hop case for this MAC is the sequence length. For the multi-hop case the service curve is:

$$\beta(t) = B \cdot max\left(\left\lfloor\frac{t-S}{S}\right\rfloor t_{slot}, (t-S) - \left\lceil\frac{t-S}{S}\right\rceil (S - t_{slot})\right) \; \forall t \geq 0, \tag{51}$$

which leads to doubled the maximum delay obtained in the single-hop case, i.e., the delay is bounded by $2 \cdot S$ in the multi-hop network.

However, as every node in the network is trying to access the channel, collisions may happen. Therefore, Equation (51) is only valid if there is only one node trying to transmit. Consequently, this MAC does not ensure successful transmissions, especially as the network size increases. The sequence is repeated 3 times in order to maximize the probability of transmitting a packet correctly. This is comparable to using two retransmissions, since in every sequence two nodes come across once. Therefore, the maximum delays are bounded by:

$$D_{max} = 3 \cdot S, \tag{52}$$

$$D_{max} = 6 \cdot S, \tag{53}$$

for single-hop and multi-hop network repectively.

3.2.7 DRMAC

This MAC is capable of adapting the frame to the traffic available. DRMAC allocates as many slots as packets to transmit as long as the packets to transmit are less than the maximum assignable slots. Furthermore, the maximum waiting time depends on the priority of the packet, since higher priority packets are allocated before. The service curves for the different priorities when there are enough slots for all the packets are:

$$\beta_1(t) = B \cdot max\left(\left\lfloor\frac{t}{c}\right\rfloor \alpha_1(t1), t - \left\lceil\frac{t}{c}\right\rceil \alpha_1(t1)\right). \tag{54}$$

$$\beta_2(t) = B \cdot max\left(\left\lfloor\frac{t}{c}\right\rfloor \alpha_2(t1), t - \left\lceil\frac{t}{c}\right\rceil \alpha_2(t1)\right). \tag{55}$$

$$\beta_3(t) = B \cdot max\left(\left\lfloor\frac{t}{c}\right\rfloor \alpha_3(t1), t - \left\lceil\frac{t}{c}\right\rceil \alpha_3(t1)\right). \tag{56}$$

Where $\alpha_1(t_1)$, $\alpha_2(t_1)$ and $\alpha_3(t_1)$ are the maximum values allowed for the arrival curves for every priority at the beginning of the $T_{CONTROL}$ period, in the frame for DRMAC shown in Figure 23. Assuming $\alpha_1(t_1) = \alpha_2(t_1) = \alpha_3(t_1) = \alpha(t_1)$, the arrival curve and the service curves are shown in Figure 32. The arrival curve has been fixed in order not to overcome the number of available slots in a frame. Consequently, the maximum delay can be stated for each priority:

$$D_{max,1} = c + \alpha(t_1) \cdot t_{slot}. \tag{57}$$

$$D_{max,2} = c + 2 \cdot \alpha(t_1) \cdot t_{slot}. \tag{58}$$

$$D_{max,3} = c + 3 \cdot \alpha(t_1) \cdot t_{slot}. \tag{59}$$

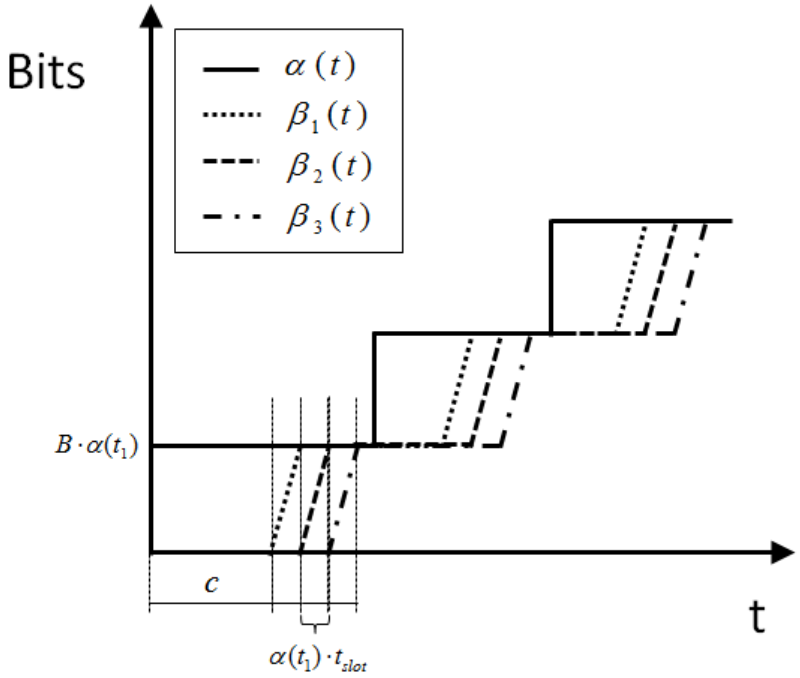

Figure 32. Arrival curve and service curve for DRMAC.

However, these results do not consider retransmissions. The NC analysis with retransmissions has been carried out in [106], where it is stated that increasing the number of transmission of the same message is equivalent to increasing the quantity of generated traffic, i.e. the arrival curve. However, in DRMAC, increasing the arrival curve leads to increasing the service curve. Under this principle, the same message would be transmitted n times in the same frame, n being the number of retransmissions. Nevertheless, in DRMAC a message is sent once in a frame, and if an error happens it is sent again in the next frame. Therefore, retransmissions require to be considered differently in DRMAC. A different way of handling retransmissions is proposed below.

Instead of modifying the arrival curve to consider retransmissions, as in [106], in this thesis modifying the service curve is proposed. In the worst case, a packet is transmitted the maximum number of retransmissions in consecutive frames. As a result, the service curve is delayed according to the number of transmissions. For example, the service curve for priority 1 is shown in Figure 33 for 3 maximum transmissions. In this example, the arrival curve has been fixed in such a way that one packet is generated every frame period in order to make the analysis simple. To obtain the priorities 2 and 3, it must be taken into account that, in every frame, three priority 1 packets are transmitted due to retransmissions. Therefore, priority 2 packets are allocated after these packets. The same happens for priority 3 packets, which are allocated after the priority 2 packets. The service curves for all priorities are shown in Figure 34, and the maximum delay for DRMAC with retransmissions is obtained straightforward:

$$D_{max,1} = 3 \cdot c + t_{slot}. \quad (60)$$

$$D_{max,2} = 3 \cdot c + 4 \cdot t_{slot}. \quad (61)$$

$$D_{max,3} = 3 \cdot c + 7 \cdot t_{slot}. \quad (62)$$

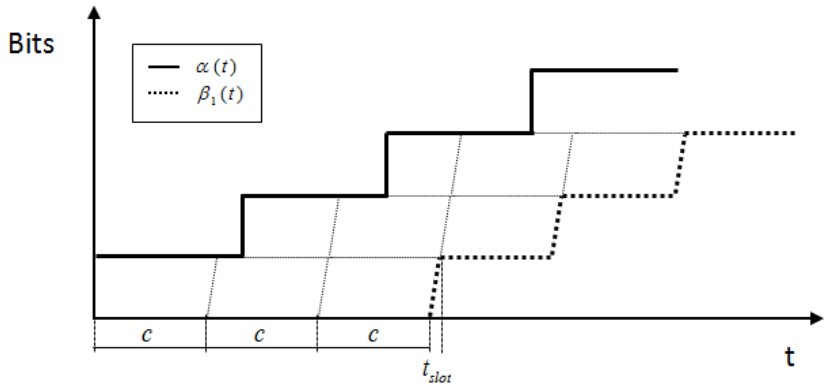

Figure 33. Arrival curve and service curve for priority 1 in DRMAC with retransmissions.

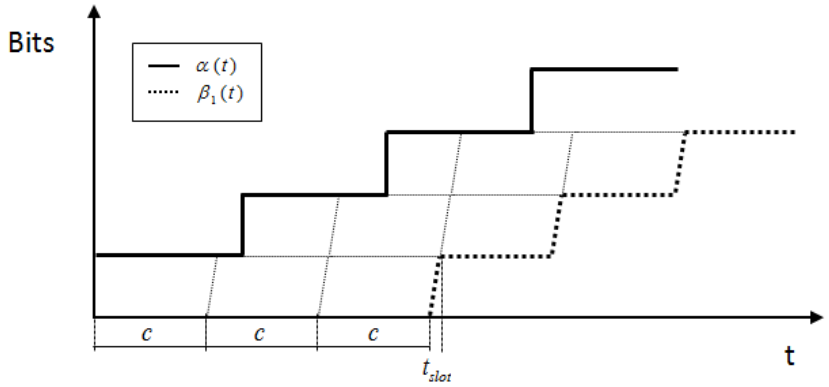

Figure 34. Arrival curve and service curve for DRMAC with retransmissions.

3.2.8 DynMAC

This MAC is a GinMAC-based solution which adds CR to GinMAC. Therefore, the maximum delay is the same as for GinMAC, and expressed in Equation (43) and Equation (45) for single-hop and multi-hop network respectively. However, it must be taken into account that the frame length (c) is longer in DynMAC than in GinMAC due to the time taken for the CR algorithms. As it has been stated in Section 3.1.3, the frame for DynMAC is 2 slots longer than the frame for GinMAC because 2 slots have been added to carry out spectrum sensing.

3.3 Simulations results

In order to confirm the results obtained by NC, simulations have been carried out in OPNET considering the scenarios described in Section 3.1. Firstly, the results for

a multi-hop tree-topology network are shown. Afterwards, a single-hop star topology network is studied. Finally, some results using FH are presented to compare FH and CR.

3.3.1 Multi-hop network

The Cumulative Distribution Functions (CDF) of the delays for every MAC under log-normal shadowing channel are shown in Figure 35. All CDFs are normalized to the frame time, except for QB2IC, based on a *rendezvous* sequence, which is normalized to the sequence length. In the PriorityMAC case, the three CDFs correspond to the three priorities the MAC is capable of handling. DRMAC and IsoMAC are not presented because, as it has been stated in Section 3.1.2, both of them may only be used in single-hop networks.

Looking at Figure 35, it can be seen how the lowest delay is achieved by PriorityMAC. This is due to the access mechanism which it uses for priority 1 and 2 packets, and which may defer priority 3 transmissions. On the other hand, this way of working leads to the highest delay for priority 3 transmissions. GinMAC and DynMAC obtain similar results since DynMAC is based on GinMAC; however, the delay in GinMAC is lower because DynMAC has a period of time used for sensing the spectrum. Finally, with QB2IC delay is constrained by 6 times the sequence length because a node discards a packet after 3 sequence length, which for a 2 hop transmission the maximum time is 6 time the sequence length. This MAC, as it is not based on a TDMA scheme, suffers collisions between the nodes in the network.

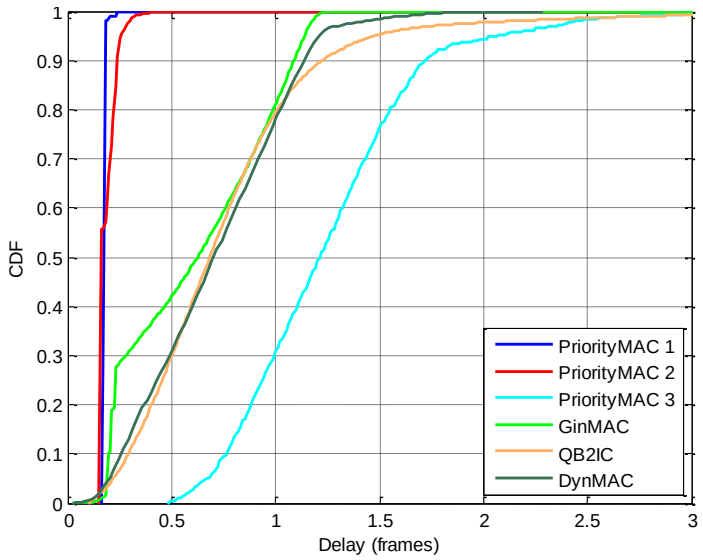

Figure 35. Delay in multi-hop network under log-normal shadowing channel.

The results under a Rayleigh channel are shown in Figure 36. In this case similar results are obtained. However, it must be taken into account that the delay increases with regard to the shadowing channel because this channel is more dispersive. Two of the selected MACs, GinMAC and DynMAC, achieve the same delay results in both environments, shadowing and Rayleigh channels. These results for GinMAC and DynMAC are due to their design, which pursue a constant delay. In QB2IC the delay has increased regarding the delay obtained in the shadowing channel. This is due to the fact that in this channel there are more retransmissions which compromise the delay of future packets. These packets have to spend more time waiting in the queue because of

the retransmissions of the previous packets. Moreover, the higher number of retransmissions, the higher number of collisions, which leads to an increasing in the delay.

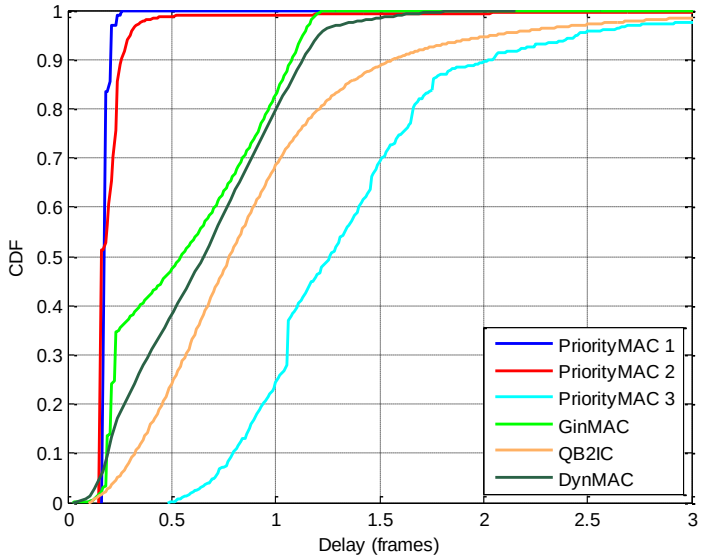

Figure 36. Delay in multi-hop network under Rayleigh channel.

In Table 3 the PER is shown for shadowing and Rayleigh channels. To obtain PER values, a packet is considered an error if it is not delivered after all the possible retransmissions. The Rayleigh channel, as well as provoking an increment in delay, also leads to higher PER. Only priority 1 in PriorityMAC preserves the same PER in Rayleigh as in the shadowing channel, and this is because this transmissions are emergency messages and they are retransmitted until final destination is reached. However, no delay bound is guaranteed by this MAC. The CDF of the delay for priority 1 is represented in Figure 37 to show the increase in a Rayleigh channel. PriorityMAC2, due to it is based on CSMA, achieves a high increase in PER because of collisions between different priority 2 packets. The results for GinMAC and DynMAC show how the PER increase less in Rayleigh channels if CR is used. The PER for QB2IC is the same in shadowing channel and in Rayleigh channel; however, it is much higher than the achieved by other MACs due to collisions between the nodes. This PER makes this MAC a non-feasible solution for IWSAN applications.

	PriorityMAC 1	PriorityMAC 2	PriorityMAC 3	GinMAC	QB2IC	DynMAC
Shadowing	0	2.5e-3	0.6e-3	0.8e-3	56e-3	3.3e-3
Rayleigh	0	36e-3	30e-3	20e-3	57e-3	5.3e-3

Table 3. PER in multi-hop network under shadowing and Rayleigh channels.

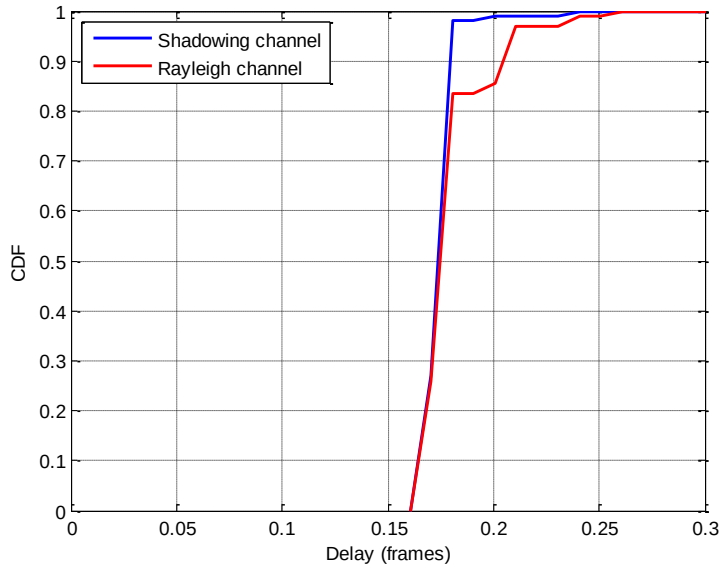

Figure 37. Delay in multi-hop network for PriorityMAC1 in shadowing channel and Rayleigh channel.

The same tree-topology network has been simulated with all the MACs in an environment under interference, as explained in Section 3.1.2. Results are shown in Figure 38 and Table 4 for delay and PER respectively. These results show how the use of CR leads to maintain the results obtained in shadowing channel, for both delay and PER, under interference. While the performance of PriorityMAC and GinMAC decrease, for QB2IC and DynMAC the performance obtained in the shadowing channel is maintained.

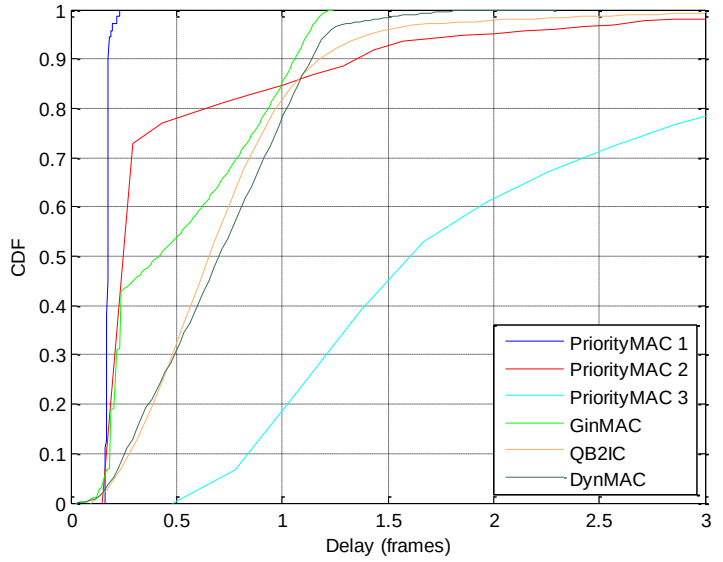

Figure 38. Delay in multi-hop network under interference.

Furthermore, the results for PriorityMAC show how, by using different access mechanisms, the increase in delay and PER is lower for higher priorities at the price of worsening the others. However, delay increases for every priority under interference.

Therefore, it is not possible ensure a correct working for IWSANs in industrial environments by PriorityMAC or GinMAC because the performance is compromised under interference. On the other hand, CR-based solutions are capable of maintaining their performance against interference.

	0%	5%	10%	15%	20%	25%
PriorityMAC 1	0	0	0	0	0	0
PriorityMAC 2	2.5e-3	3.1e-3	3.7e-3	5.9e-3	6.6e-3	9e-3
PriorityMAC 3	0.6e-3	0.6e-3	0.6e-3	0.8e-3	1.2e-3	0.9e-3
GinMAC	0.8e-3	2.4e-3	6.6e-3	20.8e-3	51.7e-3	123.8e-3
QB2IC	56e-3	57.5e-3	63.8e-3	63.8e-3	67.6e-3	63.8e-3
DynMAC	3.3e-3	7.9e-3	8.1e-3	8.1e-3	8.2e-3	8.5e-3

Table 4. PER in multi-hop network under interference.

3.3.2 Single-hop network

A single-hop network has also been studied. A star topology, as shown in Figure 26, is considered for simulations. For such networks, DRMAC and IsoMAC can also be simulated. The CDF under log-normal shadowing is shown in Figure 39. For DRMAC 3 CDF curves are represented corresponding to the three priorities, as well as in the PriorityMAC case. However, the delays for the different priorities in DRMAC are similar because DRMAC does not use a mechanism to defer lower priorities. Priorities are handled by DRMAC by allocating higher priorities before in the TDMA frame. Delay in IsoMAC is lower than the obtained by the other MACs because traffic periodic is only considered, and the MAC adapts the frame to the period of the traffic. Non-periodic traffic has been simulated because this MAC does not ensure delay bounds for non-periodic traffic. Delays for IsoMAC are lower than the achieved by other MACs, but it must be taken into account that results for IsoMAC are only for period traffic.

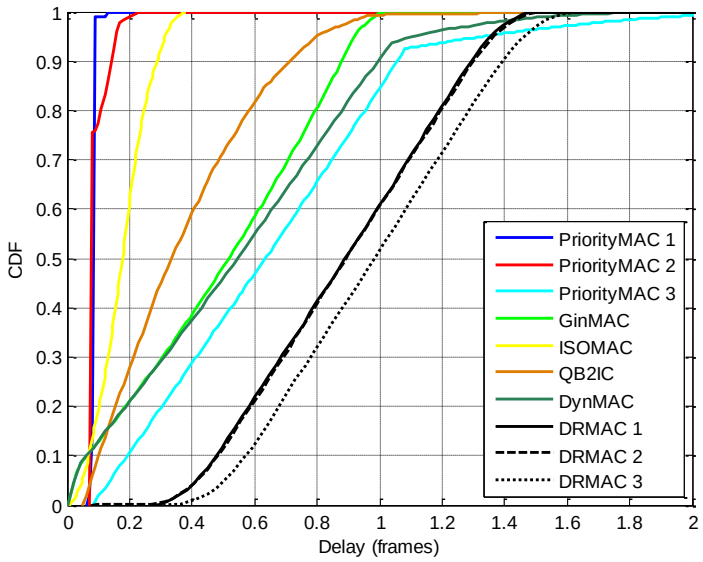

Figure 39. Delay in single-hop network under log-normal shadowing channel.

Rayleigh channel has also been simulated and the results are shown in Figure 40. In this case, as well as for the multi-hop network, the results are similar for both log-normal and Rayleigh channels. The Rayleigh channel leads to a higher delay in almost all MACs. Delays for GinMAC, IsoMAC and DynMAC have not increased with regard to the log-normal shadowing channel, but the PER is higher, as shown in Table 5. For IsoMAC, the increase in PER is higher than for the other MACs due to not using retransmissions.

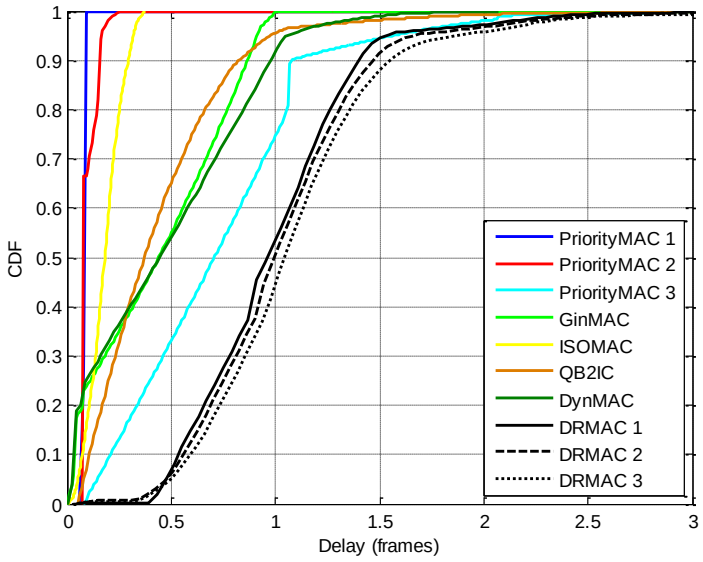

Figure 40. Delay in single-hop network under Rayleigh channel.

	PriorityMAC 1	PriorityMAC 2	PriorityMAC 3	IsoMAC	GinMAC
Shadowing	0	2.98e-3	0.91e-3	23.6e-3	0.11e-3
Rayleigh	0	3.24e-3	14.5e-3	164.4e-3	12.2e-3
	QB2IC	DynMAC	DRMAC 1	DRMAC 2	DRMAC 3
Shadowing	2.2e-3	0.19e-3	0.99e-3	0.88e-3	4.52e-3
Rayleigh	3.4e-3	16.3e-3	22.3e-3	28.7e-3	73.2e-3

Table 5. PER in single-hop network under shadowing and Rayleigh channels.

Finally, results of all MACs under interference are shown, the CDF of the delay is presented in Figure 41 when interference occupies the 25 % of the channel. In Table 6 PER for the different MACs under different occupations of the channel is expressed. Looking at Figure 41 and Table 6, the same conclusions as in the multi-hop network simulations can be obtained for PriorityMAC, GinMAC, QB2IC and DynMAC. For IsoMAC, the delay is always the same due to the fact that the packets are not retransmitted if they fail. This leads to a higher increase in PER than other MACs. Differently, DRMAC keeps the PER, but not the delay. This means that this MAC is capable of avoiding interference but it does not do it in a bounded time.

Therefore, it has been proved how CR could be used to add robustness and reliability in industrial environments. However, although delay and PER increase less for CR-based MACs, the studied MAC are not capable of maintain delay and PER at the same time under interference. Moreover, the solutions which are available for WSAN in industrial environments are based on a CCC. Therefore, a CR-based MAC which does not rely on a CCC and is capable of maintaining its performance under interference is required. A MAC with these requirements is presented in Section 4.2. This MAC is based on DRMAC, and a handoff process which ensures a deterministic behavior in interfered environments is used.

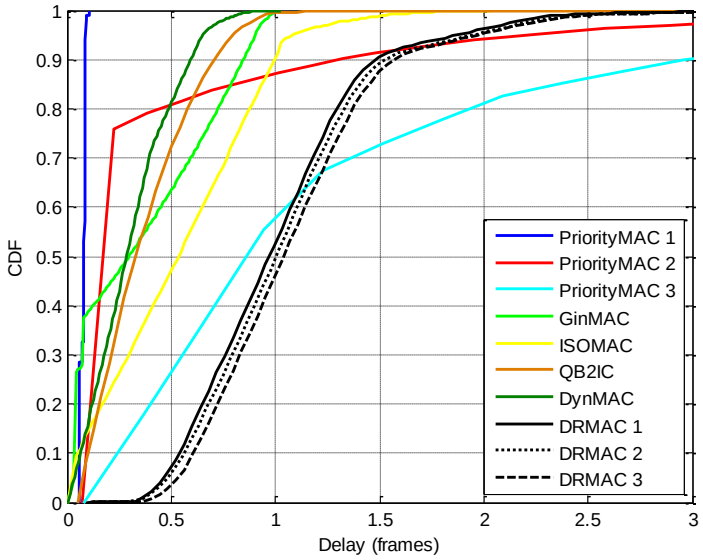

Figure 41. Delay in single-hop network under interference.

3.3.3 Frequency hopping

Finally, the non-CR-based MACs have been checked for a star-topology single-hop network under interference using FH. As FH has been proposed to avoid interference, it has been simulated for the non-CR-based MAC to know if FH is capable of ensuring robustness and reliability in IWSAN applications. A random FH sequence has been used by the network to avoid interference, and the performance under interference for single-hop networks has been simulated. FH and CR are compared to establish which of them the best option is.

Comparing the results using FH with not using FH (Figure 42 and Figure 41 respectively), FH allows PriorityMAC to reduce delay times, as well as the PER, as it can be seen comparing Table 7 and with Table 6. For GinMAC and IsoMAC, the improvement is reflected only in PER. However, the results show that CR is a more interesting tool to cope with interference.

	0%	5%	10%	15%	20%	25%
PriorityMAC 1	0	0	0	0	0	0
PriorityMAC 2	2.9e-3	3.6e-3	4.6e-3	7.2e-3	10.4e-3	14.5e-3
PriorityMAC 3	0.9e-3	0.8e-3	0.8e-3	0.8e-3	0.9e-3	0.8e-3
GinMAC	0.1e-3	5.6e-3	5.6e-3	28.1e-3	55.7e-3	92.5e-3
IsoMAC	24e-3	86e-3	132e-3	179e-3	226e-3	275e-3
QB2IC	2.2e-3	2.5e-3	2e-3	2e-3	2e-3	2e-3
DynMAC	0.2e-3	1.2e-3	1.2e-3	1.4e-3	1.8e-3	2.4e-3
DRMAC 1	0.9e-3	1e-3	0.9e-3	0.9e-3	1e-3	0.9e-3
DRMAC 2	0.8e-3	0.8e-3	0.8e-3	0.8e-3	0.8e-3	0.9e-3
DRMAC 3	4.5e-3	4.5e-3	4.5e-3	4.5e-3	4.6e-3	4.5e-3

Table 6. PER in single-hop network under interference.

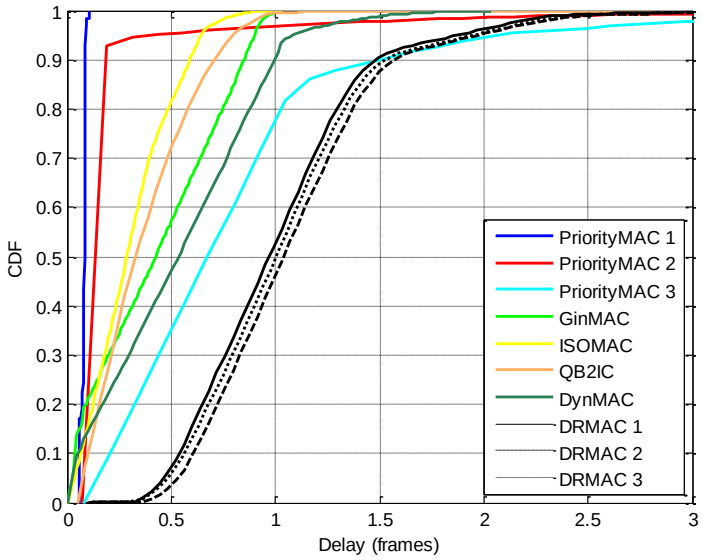

Figure 42. Delay in single-hop network under interference using frecuency hopping.

	0%	5%	10%	15%	20%	25%
PriorityMAC 1	0	0	0	0	0	0
PriorityMAC 2	3e-3	3e-3	3.7e-3	4.2e-3	5e-3	5.8e-3
PriorityMAC 3	0.8e-3	0.8e-3	0.9e-3	0.9e-3	1e-3	1e-3
GinMAC	0.2e-3	0.9e-3	2.1e-3	5.1e-3	12.5e-3	21.7e-3
IsoMAC	24e-3	40e-3	52e-3	64e-3	75e-3	87e-3
QB2IC	2.2e-3	2.5e-3	2e-3	2e-3	2e-3	2e-3
DynMAC	0.2e-3	1.2e-3	1.2e-3	1.4e-3	1.8e-3	2.4e-3
DRMAC 1	0.9e-3	1e-3	0.9e-3	0.9e-3	1e-3	9.9e-3
DRMAC 2	0.8e-3	0.8e-3	0.8e-3	0.8e-3	0.8e-3	0.9e-3
DRMAC 3	4.5e-3	4.5e-3	4.5e-3	4.5e-3	4.6e-3	4.5e-3

Table 7. PER in single-hop network under interference using FH.

3.4 Comparison between simulations and theoretical analysis

A comparison between the results obtained in simulation and the theoretical bounds has been carried out. Results are presented for log-normal shadowing channel and for interference environments.

3.4.1 Log-normal shadowing channel

All the results are shown in Table 8-13 for GinMAC, PriorityMAC, IsoMAC, QB2IC, DRMAC and DynMAC respectively. The priority 1 is only shown for PriorityMAC because it is the only priority which has a theoretical bound, as it has been explained in Section 3.2. According to al the tables, for every MAC the theoretical bounds match with simulation results for a log-normal shadowing channel.

	Theoretical bound	Maximum simulated time
Single-hop	1.03 frames	1.0022 frames
Multi-hop	1.4375 frames	1.2304 frames

Table 8. Theoretical bound and maximum simulated time for GinMAC in single-hop and multi-hop network.

	Theoretical bound	Maximum simulated time
Single-hop	0.2 frames	0.1275 frames
Multi-hop	0.4 frames	0.1797 frames

Table 9. Theoretical bound and maximum simulated time for PriorityMAC in single-hop and multi-hop networks.

	Theoretical bound	Maximum simulated time
Single-hop	1 T	0.75 T

Table 10. Theoretical bound and maximum simulated time for IsoMAC in single-hop network.

	Theoretical bound	Maximum simulated time
Single-hop	3 S	1.2851 S
Multi-hop	6 S	3.6683 S

Table 11. Theoretical bound and maximum simulated time for QB2IC in single-hop and multi-hop networks.

	Theoretical bound	Maximum simulated time
Priority 1	3.0286 frames	2.93 frames
Priority 2	3.1143 frames	3.002 frames
Priority 3	3.2 frames	3.096 frames

Table 12. Theoretical bound and maximum simulated time for DRMAC in single-hop network.

	Theoretical bound	Maximum simulated time
Single-hop	1.0328 frames	1.003 frames
Multi-hop	1.433 frames	1.228 frames

Table 13. Theoretical bound and maximum simulated time for DynMAC in single-hop and multi-hop network.

3.4.2 Interference environment

The comparison for an interference environment is shown in Table 14-19 for GinMAC, PriorityMAC, IsoMAC, QB2IC, DRMAC and DynMAC respectively. In this case, the maximum delay obtained in simulations does not comply with the theoretical

bound in some MACs because these MACs are not capable of ensuring time requirements against interference. GinMAC, QB2IC, IsoMAC and DynMAC achieve the same maximum delay in interference environment and in log-normal shadowing channel, however, the PER is higher under interference. Thus, despite better results are obtained against interference if CR is used, none of the evaluated MACs ensure both robustness and time requirements at the same time. The evaluated CR-based MACs avoid interference, but not in a bounded time, which is an import requirement in IWSAN applications.

	Theoretical bound	Maximum simulated time
Single-hop	1.03 frames	1.0022 frames
Multi-hop	1.4375 frames	1.2304 frames

Table 14. Theoretical bound and maximum simulated time for GinMAC in single-hop and multi-hop network.

	Theoretical bound	Maximum simulated time
Single-hop	0.2 frames	0.275 frames
Multi-hop	0.4 frames	0.5310 frames

Table 15. Theoretical bound and maximum simulated time for PriorityMAC in single-hop and multi-hop networks.

	Theoretical bound	Maximum simulated time
Single-hop	1 T	0.79 T

Table 16. Theoretical bound and maximum simulated time for IsoMAC in single-hop network.

	Theoretical bound	Maximum simulated time
Single-hop	3 S	2.2851 S
Multi-hop	6 S	3.9683 S

Table 17. Theoretical bound and maximum simulated time for QB2IC in single-hop and multi-hop networks.

	Theoretical bound	Maximum simulated time
Priority 1	3.0286 frames	5.3698 frames
Priority 2	3.1143 frames	6.1295 frames
Priority 3	3.2 frames	8.9574 frames

Table 18. Theoretical bound and maximum simulated time for DRMAC in single-hop network.

	Theoretical bound	Maximum simulated time
Single-hop	1.0328 frames	1.003 frames
Multi-hop	1.433 frames	1.228 frames

Table 19. Theoretical bound and maximum simulated time for DynMAC in single-hop and multi-hop network.

3.5 Summary

The evaluation of cognitive radio for mission-critical and time-critical IWSAN has been presented in this chapter. Different existing MACs, both CR-based and non-CR-based, have been selected and evaluated for IWSAN. Firstly, a theoretical analysis using NC has been carried out in order to establish the maximum delay for every MAC. Furthermore, these MACs have been simulated through OPNET in different industrial environments. Shadowing channels, fading channel (Rayleigh and Rice) and interfered environments have been considered. Finally, simulation and theoretical results have been compared in order to contrast both of them.

The results presented in this chapter show how it is possible to achieve a deterministic behavior in non-industrial channels by some of the studied MACs. However, in fading channels or against interference, none of the MACs evaluated are capable of ensuring robustness and reliability. Delay and PER are compromised in these channels. Despite no deterministic behavior is achieved by any approach, it has been shown how the CR paradigm may be the tool for avoiding interference and ensuring the time-critical and mission-critical requirements in IWSANs. CR-based MACs have achieved a better performance in dispersive channels and under interference. Thus, in the next chapter CR is explored for IWSANs. DynMAC and DRMAC are the MACs which achieve better performance in industrial environments. However, none of them are capable of ensuring both PER and delay. While DynMAC does not ensure a constant PER, DRMAC does not maintain the delay against interference because, although it is capable of avoiding interference, it does not achieve it in a bounded time.

In the next chapter a handoff algorithm is proposed to be used jointly with DRMAC and avoid interference in a deterministic way. Furthermore some spectrum algorithms to obtain information about the environment are explored in the next chapter.

The proposed scheme uses these algorithms to characterize the channels and decide the best channel to use.

Chapter 4

CR-BASED SYSTEM FOR IWSAN

In this chapter, a CR-based MAC is proposed to be used in mission-critical and time-critical IWSAN. The MAC is based on DRMAC and it includes a novel deterministic handoff algorithm which allows a successful transmission in a bounded time, even when interference arises. The handoff algorithm is capable of detecting interference while the system is transmitting. The proposed algorithm provides DRMAC with the capability of detecting interference in a bounded time. Therefore, the MAC is capable of ensuring the requirements for IWSAN applications in industrial environments. The handoff scheme is explained in this chapter, and its performance is shown, as well as the performance of DRMAC. A theoretical analysis by NC is presented, as well as results from simulations through OPNET. Comparing both results for DRMAC with and without the proposed handoff, it is possible to see how DRMAC is not capable of ensuring a reliable behavior unless the proposed handoff is used. The MAC makes use of an ED [107] in order to obtain information about the environment. This spectrum sensing algorithm is described in this chapter, and results from simulations are presented.

Furthermore, a cyclostationary Modulation Classifier (MC) has been designed. It is capable of distinguishing between OFDM, QPSK and GFSK modulations. The classifier has been simplified as much as possible in order to obtain an algorithm which can be implemented on an FPGA, which is the first implementation of this kind of algorithms which is capable of distinguishing between 3 modulations. Also, its performance under some impairment effects (frequency offset, DC offset and I/Q

imbalance) in the receiver has been measured. This study has been carried out in order to figure out potential problems of a real implementation.

4.1 Spectrum sensing algorithms

As explained in Section 2.2.1.1, the objective of spectrum sensing is to distinguish between busy and free channels. An ED [107] has been selected to carry out this task. As it has been stated, a cyclostationary MC has also been designed which provides information about the received signal, determining its modulation. OFDM, QPSK and GFSK signals can be detected. These algorithms are used by the system in order to avoid interference.

4.1.1 Energy detector

ED is widely used to find the available channels because of its simplicity, allowing the system to choose one of these channels for transmission. In order to decide between the two possible hypotheses (H_0 for an available channel and H_1 for a channel which is occupied by another signal), an ED analyzes the energy of the received signal, as it has been defined in Equation (16). Below, the detector proposed in [107] is explained and evaluated.

The ED is based on two stages. In the first stage, every time a new sample is obtained, the energy of the last N samples of the signal is measured. If the energy level is higher than a defined threshold, the detector stops operation saying that the channel is busy. The threshold in the first stage has been fixed to achieve $P_{F_A} = 1\%$, while in the second stage the threshold has been fixed to achieve $P_{F_A} = 10\%$. After a number of samples (N) are obtained, if the detector has not stopped operation, the second stage is executed. In this stage the energy is compared with two thresholds which define three regions (H_0, H_1 and undetermined). The channel is considered free under the hypothesis H_0. If the channel is busy (H_1), or the result is in the undetermined zone, the system must keep searching for a free channel. A flow chart of the ED detector is shown in Figure 43.

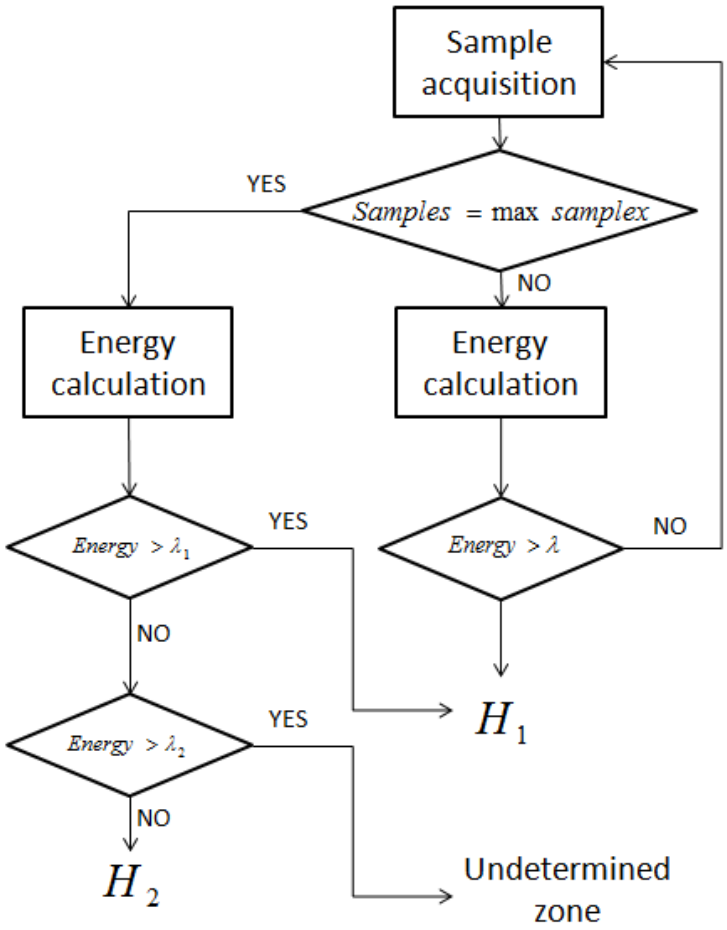

Figure 43. Two-stage ED flow chart.

The ED has been evaluated in MATLAB for an OFDM signal, and the results are shown in Figure 44. The number of maximum samples (N) has been fixed to 70, which obtains a correct detection in an assumable time. This detector is capable of detecting signals if the SNR is greater than 0dB.

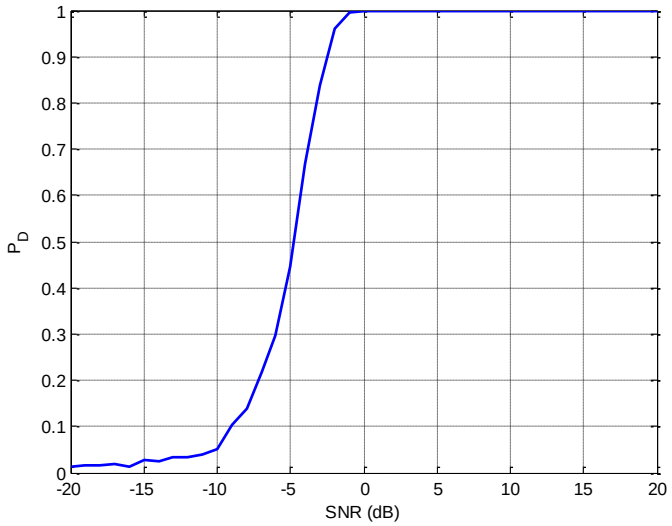

Figure 44. Probability of detection of the ED vs SNR.

4.1.2 Cyclostationary modulation classifier

This detector has been designed in order to provide more information than a traditional spectrum sensing algorithm. The aim is not only to decide between whether the channel is free or not, but to establish the modulation format of the received signal. Some cyclostationary characteristics of the received signal are analyzed, and results allow distinguishing between the main modulations typically used in the 2.4 GHz ISM band by IEEE 802.11, IEEE 802.15.4 or Bluetooth (i.e. OFDM, QPSK and GFSK). The amount of computed cyclostationary characteristics, which will be described later, is limited in order to ensure that the classifier can be implemented on an FPGA device. The implementation of the MC is explained in Section 5.2.2.

4.1.2.1 Cyclostationary modulation classifier description

The classifier extracts some cyclostationary characteristics of the received signals using Equation (20), expressed in Section 2.2.1.4. In particular, three characteristics are computed, for three pairs of α and d ($R_x^{\alpha}[d] = R_x^0[2], R_x^0[4], R_x^{32}[0]$. These three characteristics allow distinguishing OFDM, QPSK and GFSK signals for a received signal length of $N = 200$ and a sampling frequency of 40 MHz. The classifier has been designed to distinguish among QPSK, GFSK and OFDM signals with the parameters shown in Table 20.

	Bandwidth	FFT size	Cyclic Prefix	Modulation
QPSK	6.4MHz	-	-	-
GFSK	6.4MHz	-	-	-
OFDM	20MHz	64	16	16-QAM

Table 20. Parameters of the signals detected by the MC.

4.1.2.1.1 Cyclostationary characteristics

The higher bandwidth in the OFDM signal leads to a narrower autocorrelation, as shown in Figure 45. Therefore, $R_x^0[2]$ allows distinguishing between OFDM and QPSK or GFSK signals. Likewise, the GFSK signal can be distinguished from the QPSK because its narrower autocorrelation, using $R_x^0[4]$ to compute this distinction. However, $R_x^0[4]$ is not sufficient and another characteristic, $R_x^{32}[0]$, is used because it becomes zero for GFSK signals, as shown in Figure 46.

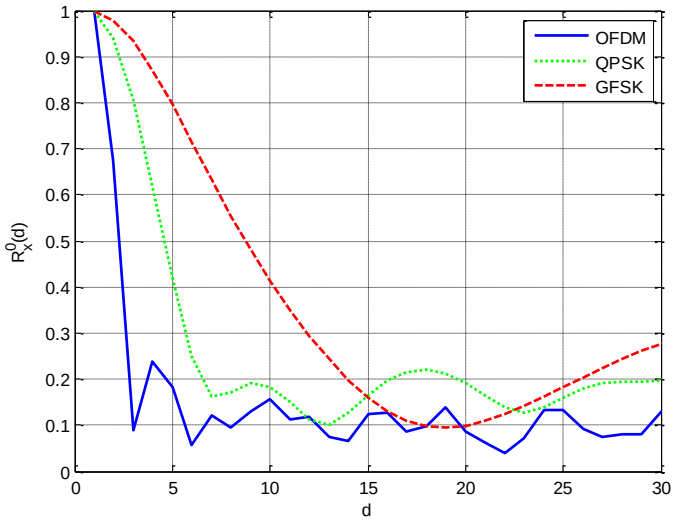

Figure 45. Autocorrelation of OFDM, QPSK and GFSK signals.

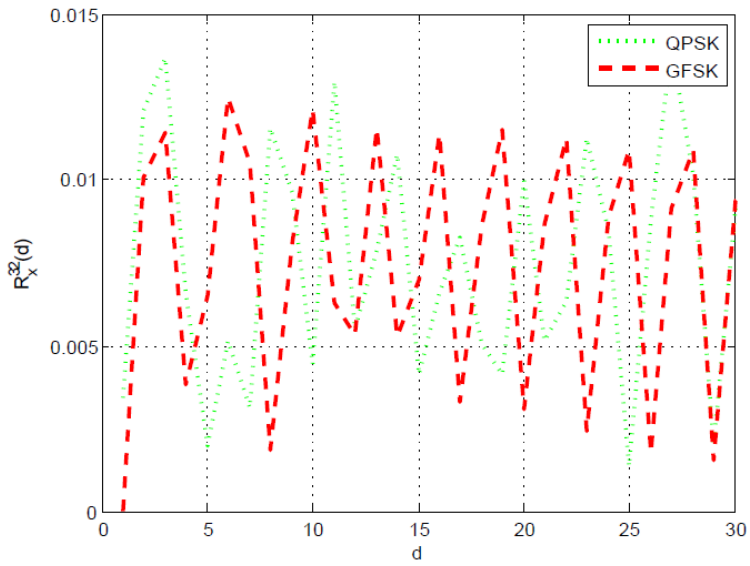

Figure 46. $R_x^{32}[0]$ for OFDM, QQPSK and GFSK signals.

To show how distinctive these characteristics are for different modulations, their values are represented for several OFDM, QPSK and GFSK signals in Figure 47 and Figure 48. These results also show, as stated before, that OFDM signals can be identified using $R_x^0[2]$, while QPSK and GFSK signals can be distinguished using $R_x^0[4]$ and $R_x^{32}[0]$.

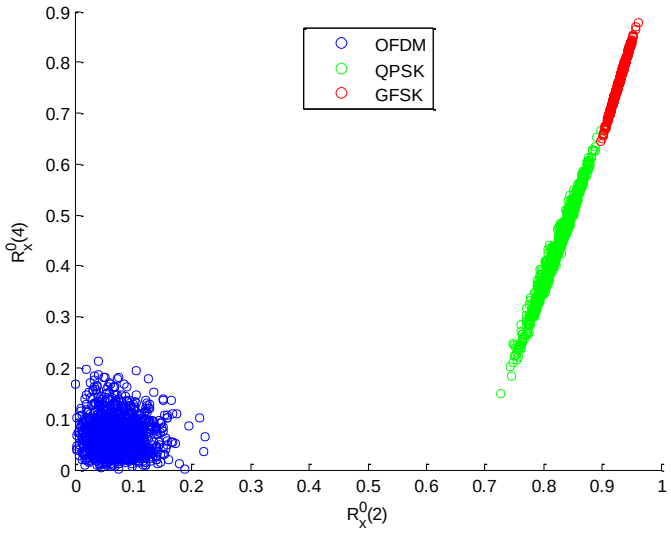

Figure 47. Cyclostationary characteristics $R_x^0[2]$ and $R_x^0[4]$ for OFDM, QPSK and GFSK signals.

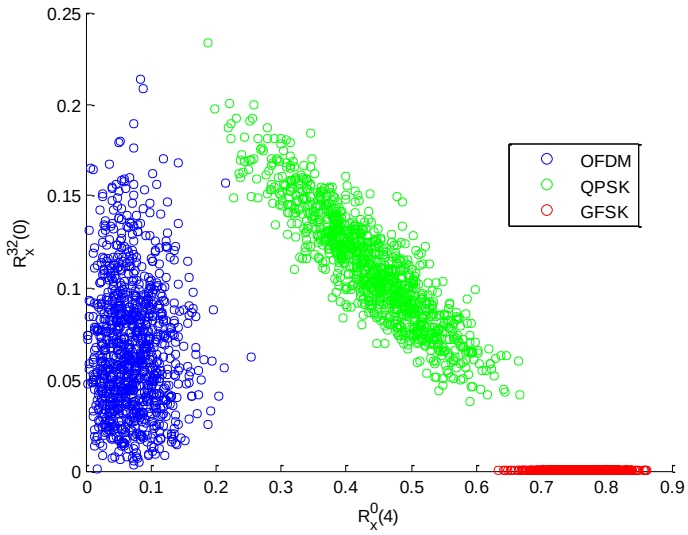

Figure 48. Cyclostationary characteristics $R_x^0[4]$ and $R_x^{32}[0]$ for OFDM, QPSK and GFSK signals.

4.1.2.1.2 Classifier

A Naïve Bayes classifier has been used in order to determine the modulation of the received signal. This classifier applies the Bayes theorem to take decisions, which means that it decides the more probable hypothesis.

The detector obtains $R_x^0[2]$, $R_x^0[4]$ and $R_x^{32}[0]$, and compares these values with two thresholds. These thresholds have been defined in function of the PDF of every modulation and cyclostationary characteristic, to create different regions where the Bayes theorem is applied. The PDF function of $R_x^0[2]$ for every modulation is shown in Figure 49, it represents the characteristics when the signals are not corrupted by noise. It can be seen how the three signals can be distinguished using this characteristic. However, due to the dependence of this characteristic on the noise for QPSK and GFSK signals, they cannot be distinguished using this characteristic. The dependency of this characteristic on the noise can be seen comparing Figure 49 with Figure 50 (in Figure 50, $R_x^0[2]$ is shown for more realistic situation (SNR = 15dB). The threshold λ_1, which is represented in Figure 49 and Figure 50, has been set to 0.3 to distinguish OFDM from the other two signals.

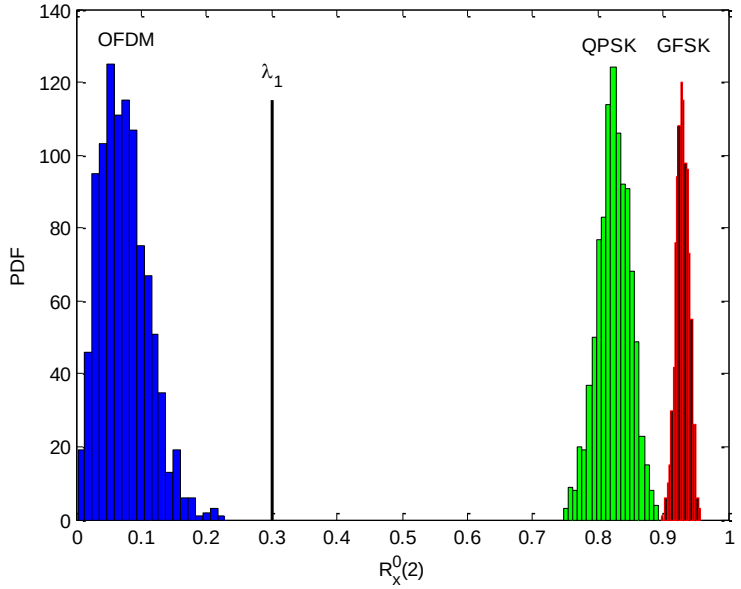

Figure 49. PDF of $R_x^0[2]$ without noise.

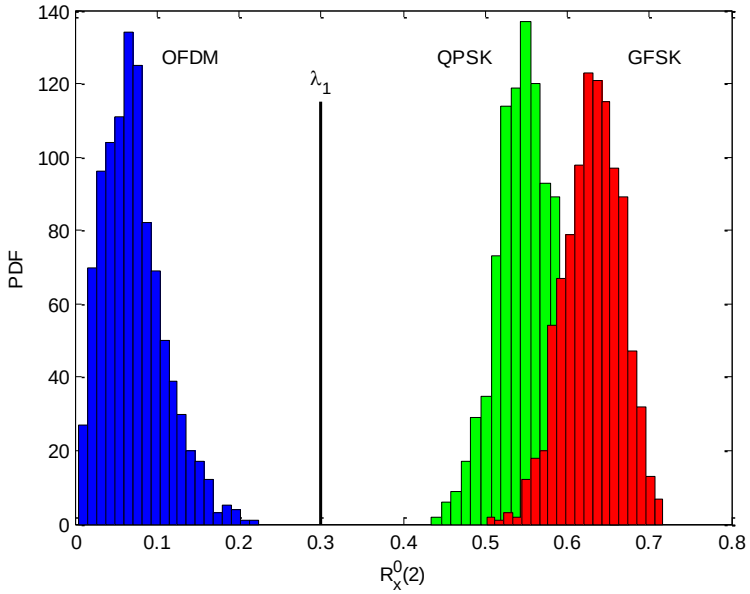

Figure 50. PDF of $R_x^0[2]$ for SNR = 15 dB.

In order to distinguish between QPSK and GFSK signals, a linear combination of $R_x^0[4]$ and $R_x^{32}[0]$ is used:

$$a \cdot R_x^0[4] + b \cdot R_x^{32}[0], \tag{63}$$

where $a = 0.0227$, and $b = -1$. The PDF function for this linear combination is shown in Figure 51 (without noise) and Figure 52 (for SNR = 15 dB). Taking into account this PDF function, a threshold λ_2 has been fixed in order to distinguish between both signals.

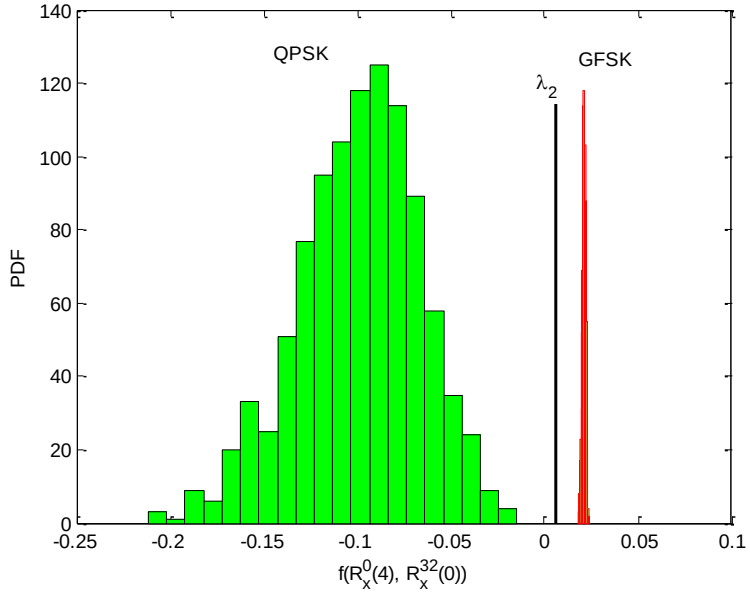

Figure 51. PDF of the linear combination of $R_x^0[4]$ and $R_x^{32}[0]$ without noise.

These three cyclostationary characteristics allow the classifier to distinguish between OFDM, QPSK and GFSK signals. However, they do not allow distinguishing between these signals and noise. Thus, an energy detector has been added to know if there is a signal in the channel. Once a signal is detected, the classifier determines the kind of modulation. The steps followed by the classifier are shown in Figure 53.

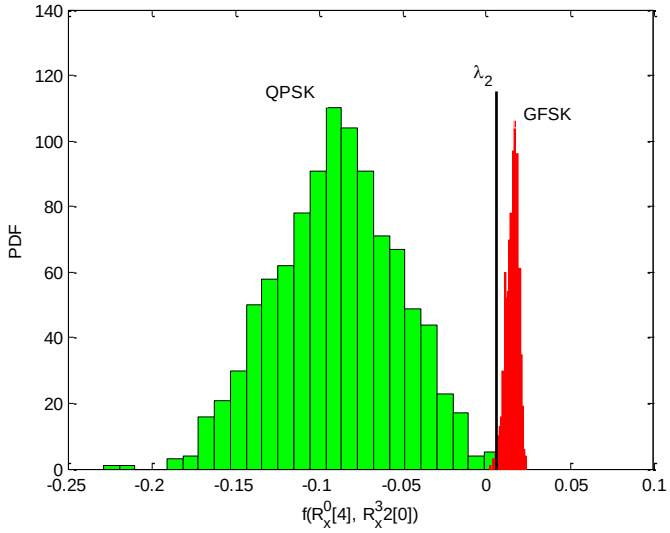

Figure 52. PDF of the linear combination of $R_x^0[4]$ and $R_x^{32}[0]$ for SNR = 15 dB.

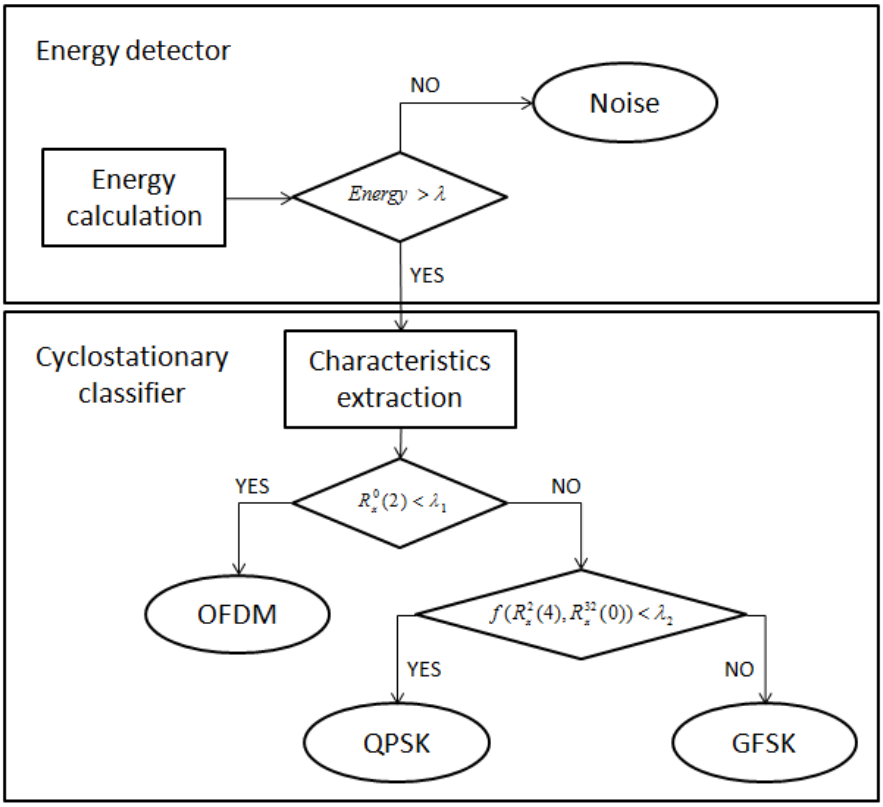

Figure 53. Flow diagram for the modulation classifier.

4.1.2.2 Results

To evaluate the performance of the proposed modulation classifier, Monte Carlo simulations have been carried out in MATLAB. The algorithm gets N samples (N = 200) of the signal to classify and decide among the four possible options (QPSK, GFSK, OFDM or only noise). The performance of the classifier has been evaluated under white Gaussian noise and under some receiver impairments such as frequency offset, DC offset and I/Q imbalance. The joint performance of the modulation classifier and the energy detector is shown in Figure 54 under white Gaussian noise. As it can be seen, the algorithm classifies correctly all the modulations for a SNR of 17 dB. However, the correct classification depends on the kind of modulation; OFDM signals are well classified for SNRs greater than 0 dB, while for a correct classification of QPSK signals SNR must be greater than 7 dB.

The classifier presents a lower performance than some proposed cyclostationary detectors, such as the proposed in [108, 109]. Both of them achieve a good performance for SNR = 10 dB with WiFi or DVB-T signals. However, these solutions only detect the presence of a determined signal. The lower performance of the classifier is due to the fact that it faces a more complex task, distinguishing different types of modulation techniques, and because it has been designed to require a reduced implementation complexity.

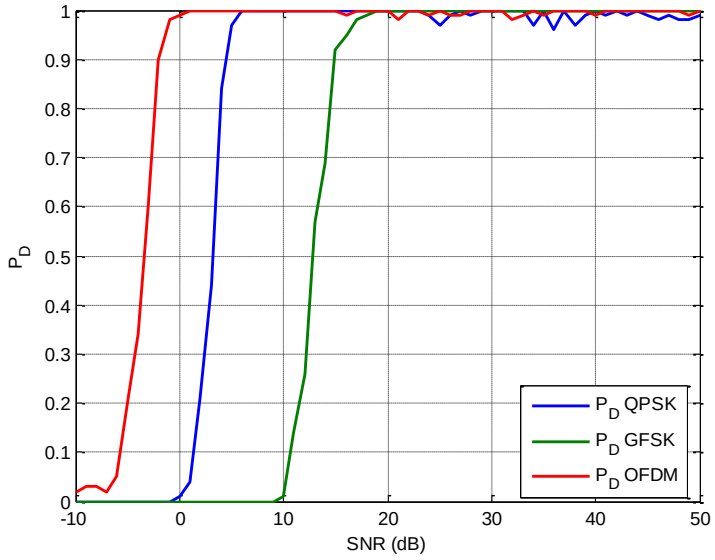

Figure 54. Probability of detection of the cyclostationary classifier vs SNR.

In addition to P_D, it is important to analyze the behavior of the algorithm when modulations are improperly classified. Table 21 and Table 22 show the percentage of mismatched modulations. Due to the behavior of cyclostationary characteristics, GFSK signals may be classified as QPSK for SNR below 17 dB, as shown in Table 21 for 13 dB. For lower SNRs, the mismatches may be due to two different possibilities (Table 22, for 3 dB). If modulations are mistaken for one another, the mismatch is due to the behavior of cyclostationary features. On the other hand, if any signal is classified as noise, the miss detection is due to the energy detector.

	Classified as QPSK	Classified as GFSK	Classified as OFDM	Classified as Noise
QPSK signal	100%	0%	0%	0%
GFSK signal	43%	57%	0%	0%
OFDM signal	0%	0%	100%	0%

Table 21. Performance of the classifier for SNR = 13 dB.

	Classified as QPSK	Classified as GFSK	Classified as OFDM	Classified as Noise
QPSK signal	48%	0%	37%	15%
GFSK signal	61%	0%	23%	16%
OFDM signal	0%	0%	100%	0%

Table 22. Performance of the classifier for SNR = 3 dB.

Figure 55-58 show the results for the classifier under the following receiver impairments: frequency offset, I/Q imbalance and DC offset. The results when no impairments are added to the signal are also shown in order to compare both results. Frequency offset and I/Q imbalance do not affect the performance of the system. However, the performance is reduced under DC offset, as it can be seen in Figure 58.

Therefore, frequency offset and I/Q imbalance do not need to be taken into account in a real implementation because they do not disturb the performance of the algorithm. On the other hand, DC offset level must be considered in the design due to its effect in the performance of the classifier.

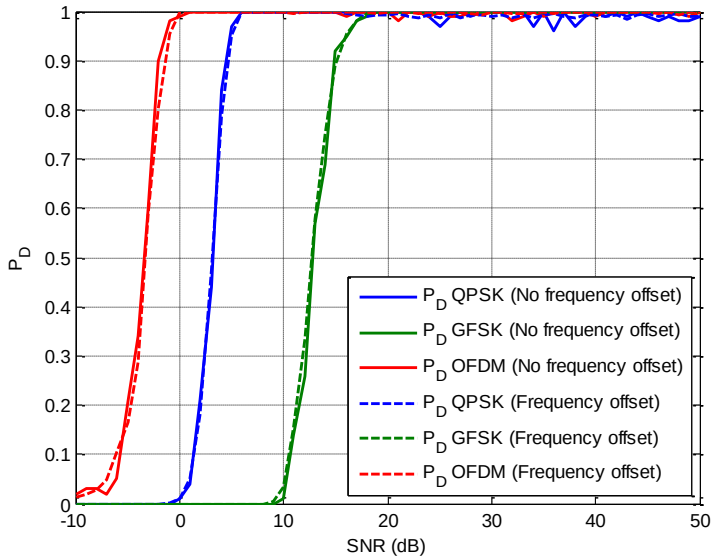

Figure 55. Probability of detection of the cyclostationary classifier under frequency offset (10 kHz) vs SNR.

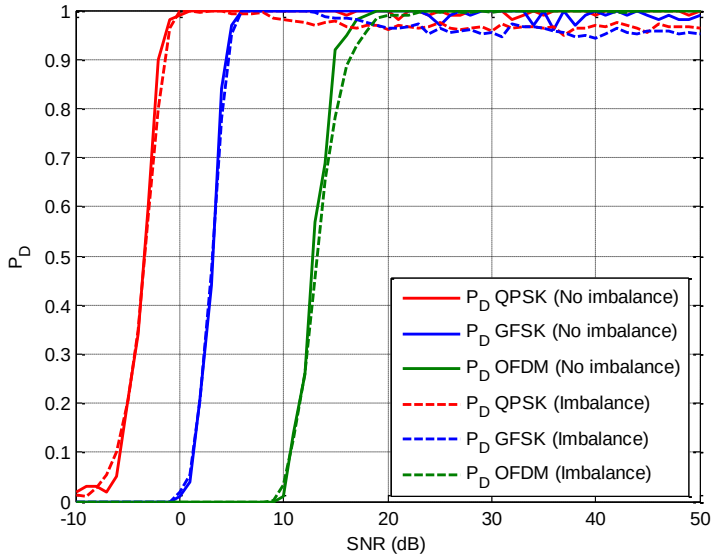

Figure 56. Probability of detection of the cyclostationary classifier under amplitude I/Q imbalance (30 dB) vs SNR.

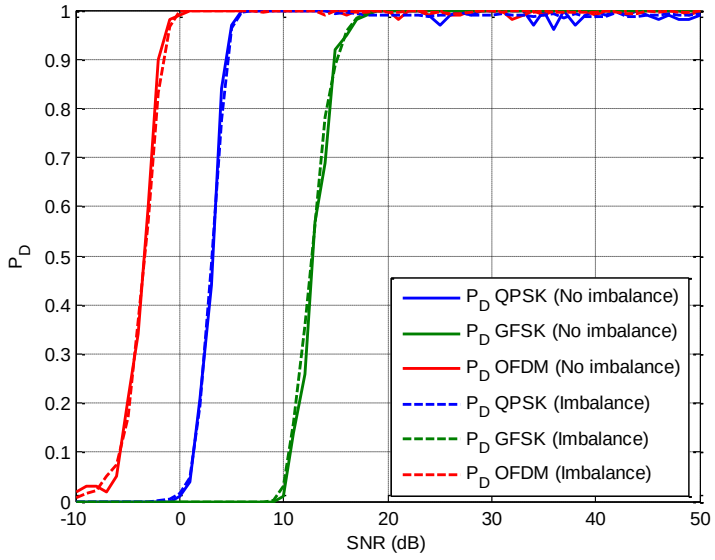

Figure 57. Probability of detection of the cyclostationary classifier under phase I/Q imbalance (45º) vs SNR.

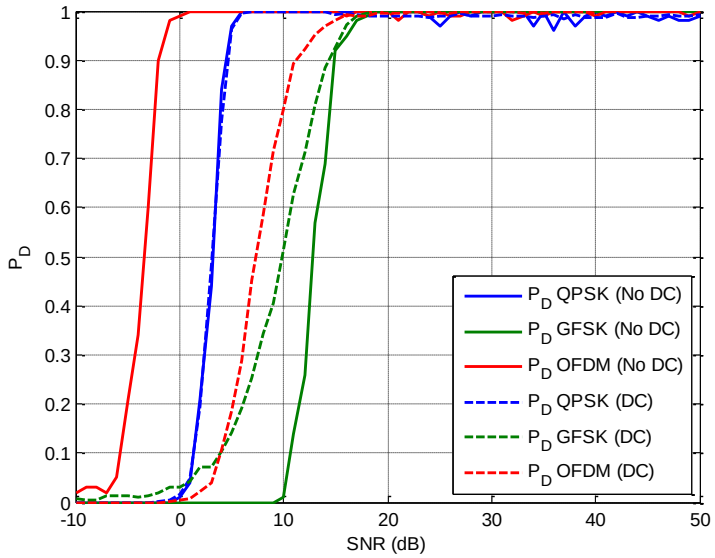

Figure 58. Probability of detection of the cyclostationary classifier under DC offset vs SNR.

4.2 Spectrum Handoff and Medium Access Control

DRMAC has been chosen as the basis to achieve a MAC for mission-critical and time-critical IWSAN. DRMAC is based on CR, making interference avoidance possible, and on TDMA, which can satisfy IWSAN requirements. From the study delved in Chapter 3, it has been stated that DRMAC is the MAC which is capable of ensuring a better performance against interference. However, although DRMAC can cope with interference, it does not achieve a deterministic behavior in these environments. In order to enhance DRMAC with the possibility of avoiding interference in a deterministic way, a handoff algorithm has been implemented. The proposed mechanism is capable of detecting interference and recovering communication in another channel in a bounded time. Therefore, DRMAC can be used in IWSAN in if the proposed handoff algorithm is used. Below, the handoff mechanism is described and evaluated.

4.2.1 MAC description

DRMAC was proposed for a single-hop network, and a central node is in charge of coordinating the entire network. The frame structure is divided into four different periods, as shown in Figure 23. At the beginning of the frame, each node senses the spectrum during the period T_{SENSE}. Then, during the control period, the spectrum sensing results obtained by every node are broadcast, as well as information about the packets available to transmit. Nodes access the medium in a TDMA way during the control phase. All the information which has been sent during the control phase is used by the coordinator to set up the TDMA for data. Three priorities are allowed, assigning firstly in the frame the higher priority packets. In the feedback period this configuration

is sent to all the nodes. Finally, nodes transmit data according to this TDMA configured by the coordinator.

The spectrum sensing task is carried out by all the nodes in the network. The ED has been chosen for this task due to its simplicity. Each node senses a different channel, which is defined by the coordinator. In this way, as many channels as nodes are in the network can be sensed during a frame. Furthermore, the channel which a node senses changes from one frame to the next, thus allowing the network to explode the spatial diversity of all nodes for spectrum sensing. Once the results of the spectrum sensing are known by the coordinator, it can decide the channel to use, which is transmitted to the entire network in the feedback interval. Furthermore, a Markov Process has been added in order to obtain statistics about the occupation of all the channels [110] and to choose a channel accordingly. However, despite the network is capable of hopping to the best channel in terms of occupancy, interference may jam the network in the middle of a transmission, making the network lose connectivity. The proposed handoff addresses this problem, since it is capable of detecting interference and recovering the network operation in other available channels. Furthermore, the recovery of the transmission is achieved in a deterministic manner.

4.2.2 Spectrum handoff algorithm

The handoff algorithm takes advantage of the way DRMAC operates. In a traditional TDMA a reserved slot may be used or not, depending on whether there are or not packets to transmit during the reserved slot. However, in DRMAC a node always accesses the medium if the slot has been reserved. This is due to the fact that a slot is only reserved for a node if it has packets to transmit. Every slot in the control phase and on the data phase is always used. Hence, if the coordinator does not receive any packet in one of these slots an error is considered. In the same way, an error happens if a node in the network does not receive anything during the feedback period. As ACKs are transmitted by the coordinator, they are also used by the nodes to detect activity in the slot. A node does not take into account transmission by other nodes because they may not be visible between each other.

Therefore, errors are detected in the MAC layer. The lack of activity during a slot can be counted as an error, and burst losses due to interference can be detected. After a certain number of consecutive errors it is considered that the channel is jammed by interference and the network must hop to another channel. An example of the interference detection process is shown in Figure 59 for a network consisting of two nodes and one coordinator. In this example all nodes look for three consecutive errors to hop to another channel. It must be taken into account that some errors may not only be due to interference, since some errors may have happened because of the signal propagations in a dispersive channel. This is what happens in the slot 2 which is considered as an error by Node 1. Errors due to the channel may lead some nodes to detect the interference before others. In this case, Node 2 considers the slot 4 as an error and makes it hop before the others. This way of operating allows the system to detect interference in a deterministic time, without the need to carry out spectrum sensing.

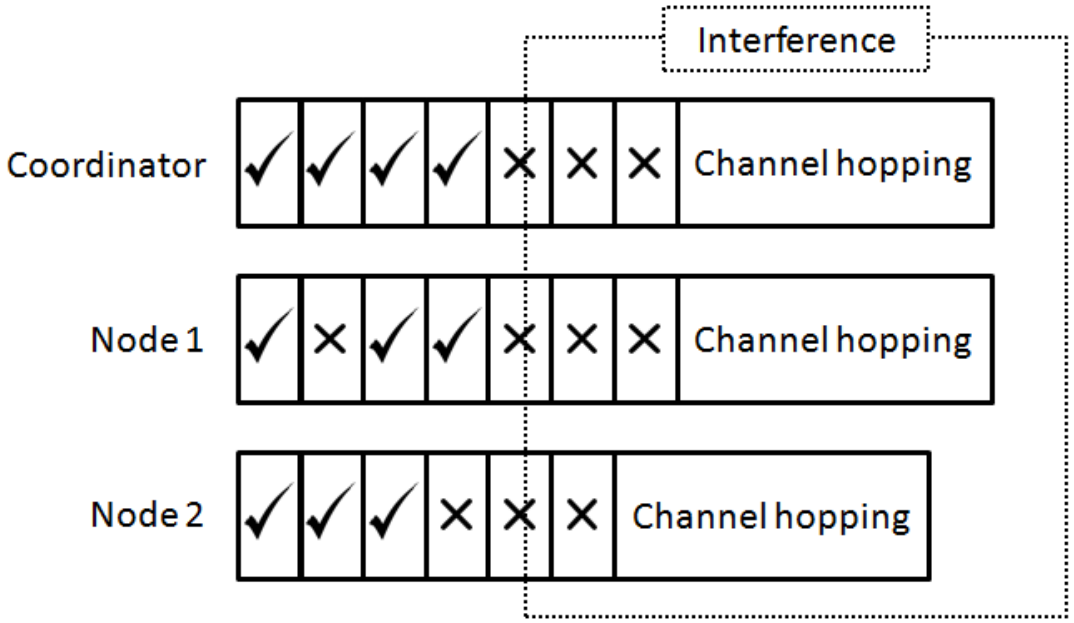

Figure 59. Example of interference detection.

When interference is detected, all nodes hop to the same channel. In order to do this the coordinator generates a list of channels organized according to their occupation, which has been estimated by the Markov Process from the spectrum sensing results. This list is known by all nodes because it is transmitted in the feedback period. Therefore, in the hopping process all nodes hop to the next channel in the list. Once the coordinator has been tuned up to the new channel, it waits a time to allow all the nodes to hop to it. Finally, the coordinator recovers the communication sending a feedback message with the configuration of the TDMA, according to which the nodes transmit their data.

In the following sections, the performance of this proposal is assessed and compared with DRMAC without the proposed handoff mechanism. For both with and without handoff, the same frame as the one described in Section 3.1.3 for DRMAC is used. The proposed algorithm has been configured to reestablish the connectivity in a period of time equal to the frame length. This time has been set targeting the best compromise between speed and robustness. Firstly, the theoretical analysis, based on NC, is explained. The results from simulation are then presented and compared to the theoretical ones.

4.2.3 Network calculus

The analysis adding the handoff process to DRMAC is detailed in order to establish the maximum delay that it is possible to ensure. The handoff process allows the system to avoid interference, but adds certain time to the maximum delay. This time, which is used to detect interference and recover the communication in another channel, has been set to the duration of a frame, as stated in the previous section. The system has been analyzed for the same arrival curve and the number of retransmissions as in Section 3.2. The arrival and the service curves for every priority are shown in Figure 60. To accomplish these service curves, the time to carry out the handoff has been added to

the service curves of DRMAC, expressed in Section 3.2.7. The worst case is considered, which is when two packets are in the queue when the handoff is triggered due to the detection of interference. Therefore, delays are now bounded by:

$$D_{max,1} = 3 \cdot c + T_{sense} + T_{control} + 2 \cdot t_{slot}. \quad (64)$$

$$D_{max,2} = 3 \cdot c + T_{sense} + T_{control} + 5 \cdot t_{slot}. \quad (65)$$

$$D_{max,3} = 3 \cdot c + T_{sense} + T_{control} + 8 \cdot t_{slot}. \quad (66)$$

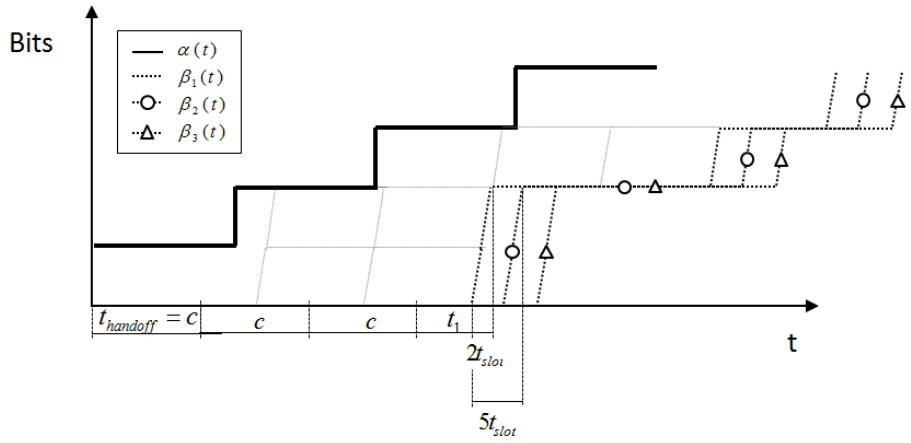

Figure 60. Arrival curve and service curve for DRMAC with handoff.

These bounds are higher than the ones obtained for DRMAC (Section 3.2.7), but in this case they are also valid under interfered environments. To prove that these bounds are correct, some simulations have been carried out.

4.2.4 Simulation results

The performance of the proposed handoff algorithm has been measured through OPNET simulations for the environments described in Section 3.1.2. Here, the results are shown. The performance for DRMAC is also shown to compare both solutions.

In Figure 61 and Figure 62 the CDF of the delay for DRMAC with and without handoff under log-normal shadowing and Rayleigh channels are shown, respectively. Furthermore, in Table 23 the PER under these channels is shown. The delay under log-normal shadowing channel, in Figure 61, is similar in both cases, with and without handoff. Also, PER is similar in this channel, as it can be seen in Table 23. However, the behavior with handoff under Rayleigh channel (Figure 62) differs from the behavior of the MAC without handoff, since the performance of DRMAC without handoff decreases while DRMAC with handoff maintains its performance. This can also be seen in Table 23, where PER increases for DRMAC without handoff but it does not when the proposed handoff is used. Therefore, the performance of the MAC has not decreased due to the handoff process when no interference are present in the channel, but it adds robustness in dispersive channels.

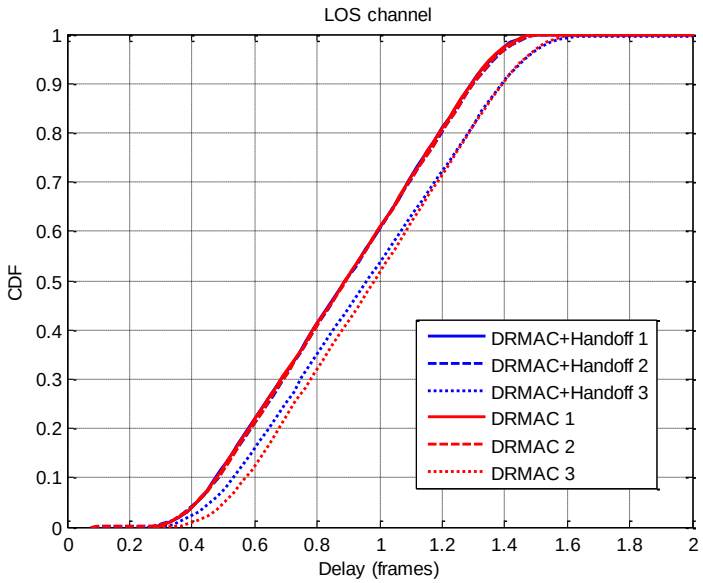

Figure 61. Delay for DRMAC under log-normal shadowing channel.

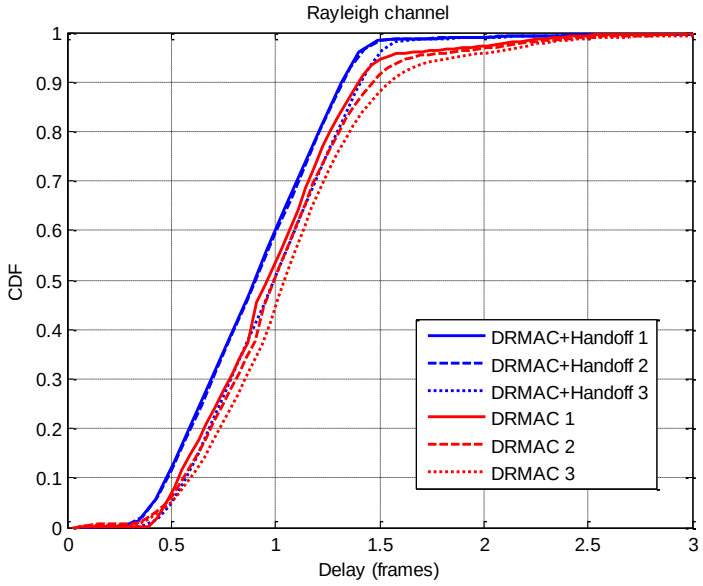

Figure 62. Delay for DRMAC under Rayleigh channel.

	DRMAC 1 + HANDOFF	DRMAC 2 + HANDOFF	DRMAC 3 + HANDOFF	DRMAC 1	DRMAC 2	DRMAC 3
Shadowing	0.4e-3	0.5e-3	1e-3	1e-3	0.9e-3	4.5e-3
Rayleigh	1.7e-3	3.7e-3	7.3e-3	22.3e-3	28.7e-3	73.2e-3

Table 23. PER for DRMAC under shadowing and Rayleigh channels.

The comparison has been also carried out in an environment under interference, as detailed in Section 3.1.2. The CDF of the delay when the interference occupies the 25% of the channel is shown in Figure 63, and the PER for the different levels of occupation in Table 24. Both Figure 63 and Table 24 show the differences between using the proposed algorithm and not using it. While not using the handoff increases the delay, using it leads to a system which is capable of avoiding interference and ensuring delay values as in an interfere-free environment. In addition, the resistance to interference is shown in PER values (Table 24). The PER is similar for all the levels of interference if the proposed mechanism is incorporated into DRMAC. Thus, the handoff guarantees an interference-free environment which allows the system to ensure bounds in time and reliability for IWSAN.

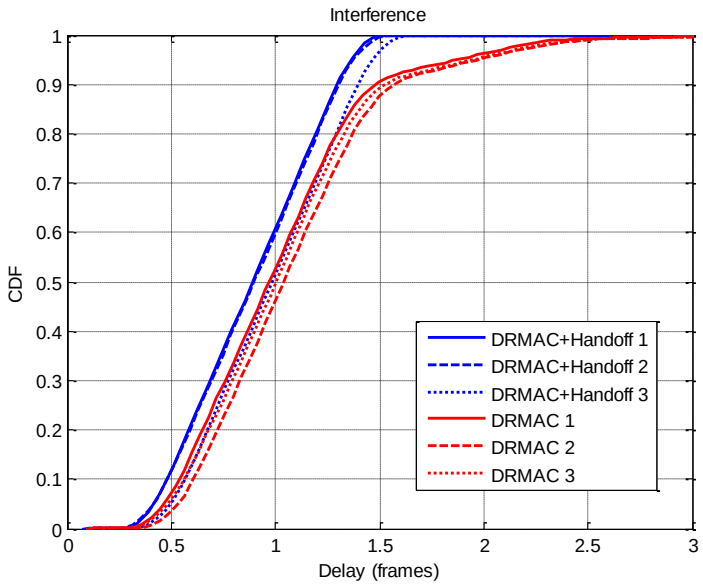

Figure 63. Delay for DRMAC under interference.

	0%	5%	10%	15%	20%	25%
DRMAC 1 + HANDOFF	1e-3	4.2e-3	4e-3	3.9e-3	4.3e-3	4.7e-3
DRMAC 2 + HANDOFF	0.9e-3	1.3e-3	1.2e-3	1.3e-3	1.4e-3	1.5e-3
DRMAC 3 + HANDOFF	4.5e-3	6.2e-3	6.4e-3	6.5e-3	7e-3	7.2e-3
DRMAC 1	0.4e-3	0.3e-3	0.8e-3	0.9e-3	0.6e-3	1.1e-3
DRMAC 2	0.5e-3	0.3e-3	0.3e-3	0.3e-3	0.2e-3	0.4e-3
DRMAC 3	1e-3	0.9e-3	1e-3	1.2e-3	1.1e-3	1.9e-3

Table 24. PER for DRMAC under interference.

4.2.5 Comparison between theoretical analysis and simulations

A comparison between the theoretical bound and simulation results has been carried out. In Table 25 and Table 26 all the results are shown for the log-normal shadowing channel and against interference. The results presented in Section 3.4 for DRMAC without handoff are also shown to compare both options and to show the advantages that the proposed algorithm provides. In log-normal shadowing channel, both theoretical bounds and simulated delays are higher for the MAC with handoff than without handoff. This time is due to the time required to carry out the handoff. However, despite the higher delay in non interfered environments, the handoff is capable of ensuring these times against interference, as it is shown in Table 26. Thus, the proposed handoff scheme allows the system to achieve a deterministic behavior in interfered environments, enabling its use for WSAN applications in industrial environments.

	DRMAC		DRMAC + handoff	
	Theoretical bound	Maximum simulated time	Theoretical bound	Maximum simulated time
Priority 1	3.0286 frames	2.93 frames	3.7714 frames	3.5306 frames
Priority 2	3.1143 frames	3.002 frames	3.8571 frames	3.6091 frames
Priority 3	3.2 frames	3.096 frames	3.9429 frames	3.7494 frames

Table 25. Theoretical bound and maximum simulated time for DRMAC in log-normal shadowing channel.

	DRMAC		DRMAC + handoff	
	Theoretical bound	Maximum simulated time	Theoretical bound	Maximum simulated time
Priority 1	3.0286 frames	5.3698 frames	3.7714 frames	3.5228 frames
Priority 2	3.1143 frames	6.1295 frames	3.8571 frames	3.6447 frames
Priority 3	3.2 frames	8.9574 frames	3.9429 frames	3.7381 frames

Table 26. Theoretical bound and maximum simulated time for DRMAC against interference.

4.3 Summary

In this chapter, a novel CR-based system for IWSAN applications has been delved. A novel handoff algorithm has been proposed which makes the system capable of ensuring robustness and reliability against interference, ensuring IWSAN requirements.

Two spectrum sensing algorithms, an energy detector and a cyclostationary modulation classifier, have been proposed, described and evaluated in MATLAB. The energy detector [107] has been chosen to be used in the CR-based system because of its simplicity. Its description and its performance have been described. A simplified Modulation Classifier (MC) has also been explained and evaluated. The simple structure of the algorithm allows implementing it on real hardware at a limited cost, as it is shown in Section 5.2.2. The MC distinguishes between OFDM, QPSK and GFSK signals. It performance has been measured for different receiver impairments such as frequency offset, DC offset and I/Q imbalance.

The proposed handoff algorithm avoids interference in a bounded time, allowing a deterministic behavior in industrial environments. This algorithm has been designed to be used jointly with DRMAC, which is capable of avoiding interference in a non-deterministic way. The proposed handoff mechanism detects interference while the system is transmitting, ensuring that the detection of the interference and the hop to another channel are done in a bounded time. The performance of the handoff scheme has been analyzed using NC, and validated through OPNET simulations, and results have been presented jointly with the results of DRMAC. Both theoretical and simulation results have been compared to show the benefits that the handoff process adds. The results show how it is only possible to ensure time and reliability requirements with DRMAC if the proposed algorithm is used.

Chapter 5

COGNITIVE PLATFORM

In this Section a cognitive platform designed in collaboration with a working group which is composed by researches from IK4-IKERLAN and Mondragon Unibertsitatea is presented. This platform has been used in order to validate the implementation of some of the algorithms detailed in Chapter 4.

A XC6VLX240T Xilinx Virtex 6 FPGA is the basis of the platform, on which the ED and the MC spectrum sensing algorithms have been implemented and evaluate. The results presented in this chapter allow validating the results obtained in simulation in a real implementation.

Furthermore, an example of application is presented that consists of an Ethernet-to-RF (and RF to Ethernet) bridge which captures the Ethernet frames, transmits them wirelessly and reconstructs them at the receiver side. The aim of these RF-Ethernet bridges is to replace a wired Ethernet links by wireless ones for IWSAN applications. The bridges use the mentioned spectrum sensing algorithms in order to ensure a reliable communication link under interference.

5.1 Platform description

The platform is composed of a Xilinx Virtex 6 FPGA in charge of baseband processing, an RF front-end and an antenna, all of which are reconfigurable. The systems works in a half duplex mode and it is able to transmit in two ISM bands (868 MHz and 2.45 GHz) [111]. Furthermore, the platform allows small in-band frequency changes (<100MHz) in the transmission frequency by reconfiguring the digital oscillator that generates the Intermediate Frequency (IF). This allows transmitting in the most suitable frequency in order to avoid interference.

The signal-processing tasks of the platform have been implemented on an FPGA device, thanks to the high performance and flexibility it offers. System Generator for Digital Signal Processor (DSP) [112], Xilinx's rapid prototyping tool, has been used for designing, implementing and testing the baseband data processing algorithms. A MicroBlaze is uses for controlling different parts of the architectures and carries out the following tasks: FPGA dynamic partial reconfiguration, programming of the front-end and control of the antenna.

A picture of the platform is shown in Figure 64, which depicts the FPGA boards, the reconfigurable RF boards and the reconfigurable antennas with their associated electronics.

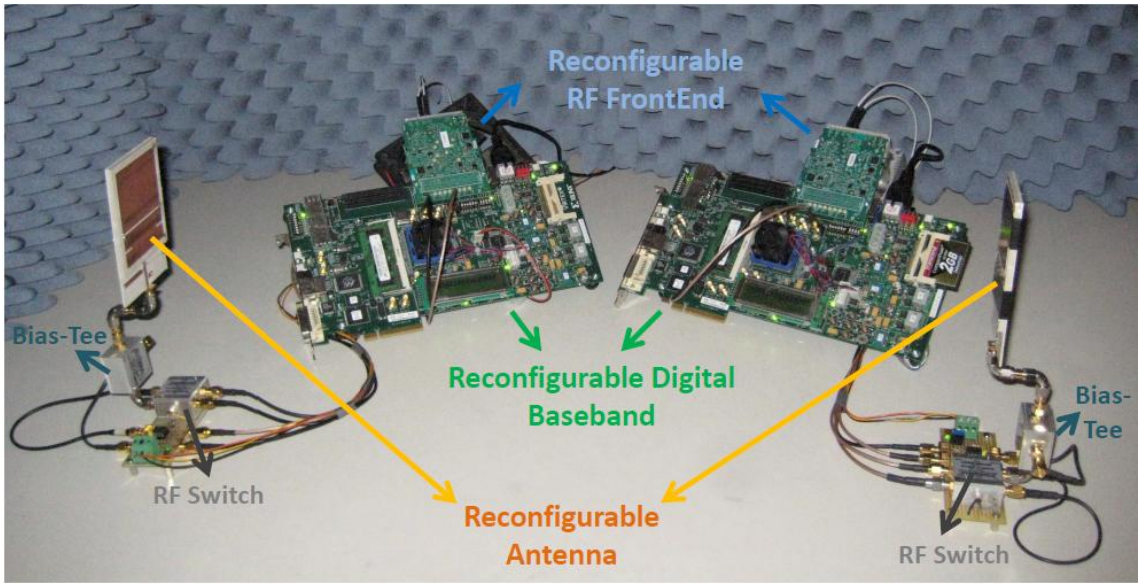

Figure 64. Cognitive platform.

5.2 Spectrum sensing algorithms

Both spectrum sensing algorithms presented in Section 4.1 have been implemented using System Generator on the platform with the help of researches from IK4-Ikerlan and Mondragon Unibertsitatea. To measure the performance of the

algorithms, test signals have been generated using a signal generator, and transmitted to the cognitive platform. The set up used for spectrum sensing validation is shown in Figure 65. The signals have been programmed in the signal generator using MATLAB and have been transmitted wirelessly to the cognitive platform. The results for both spectrum sensing algorithms are presented in this section.

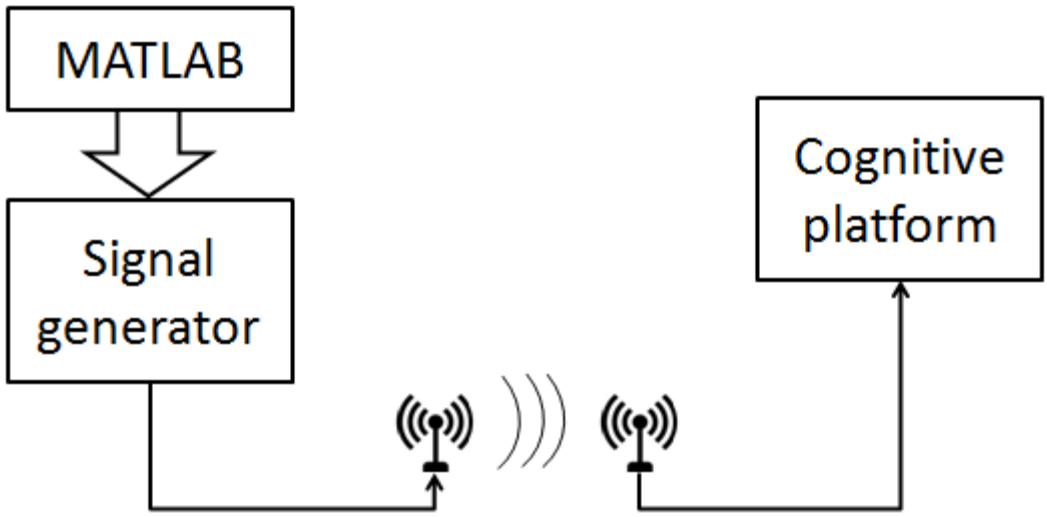

Figure 65. Set up for spectrum sensing validation.

5.2.1 Energy detector

The ED described in the flow chart shown in Figure 43 has been implemented in the platform. The computational complexity of the energy detector is shown in Table 27 in terms of FPGA resource occupation. The complexity of a QPSK modem [113] is also shown in Table 27 in order to contextualize the results. As it can be seen, the simplicity of the ED leads to a complexity of 3% of the whole system (only the signal processing algorithms, without considering uBlaze).

	SLICES	6 in-LUT	FF	LUTRAM (32 bit)	DSP48
Energy detector	303	503	425	64	40
QPSK modem [113]	21953	56249	41478	4192	446
QPSK modem (without uBlaze) [113]	10632	31698	18678	2138	427

Table 27. Computation complexity of the energy detector.

The ED has been evaluated with a real OFDM signal with the parameters detailed in Table 20 using the set up shown in Figure 65. The results for both simulations and the implementation are shown in Figure 66. As it can be seen, the performance of the implementation with real signals matches the performance in simulations.

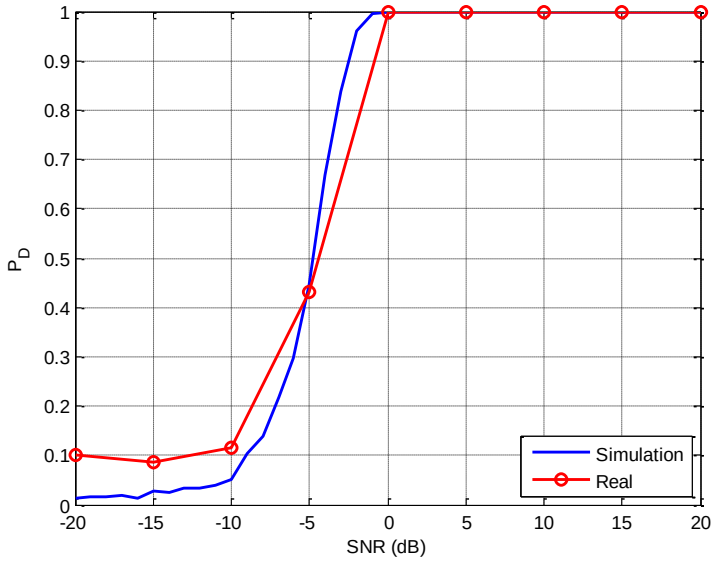

Figure 66. Probability of detection of the implemented energy detector vs SNR.

5.2.2 Cyclostationary modulation classifier

The MC explained in Section 4.1.2 has also been implemented on the cognitive platform. This implementation has allowed measuring the performance of the classifier with real signals. The results from these measurements are presented here.

5.2.2.1 Implementation

As it has been stated in Section 4.1.2, the MC must extract $R_x^{\alpha}[d]$ (Equation (20)) for different pairs of α and d. To do this, the block shown in Figure 67 has been implemented on the FPGA device, proposed for a time-domain cyclostationary detector in [114]. The block consists of a Shift Register Lut (SRL), which delays the signal, and a COordinate Rotation DIgital Computer (CORDIC) block, in charge of generating the complex exponential. This block must be parallelized as many times as cyclostationary characteristics must be extracted (three time in our approach). That is the main reason for limiting the number of characteristic calculated by the MC.

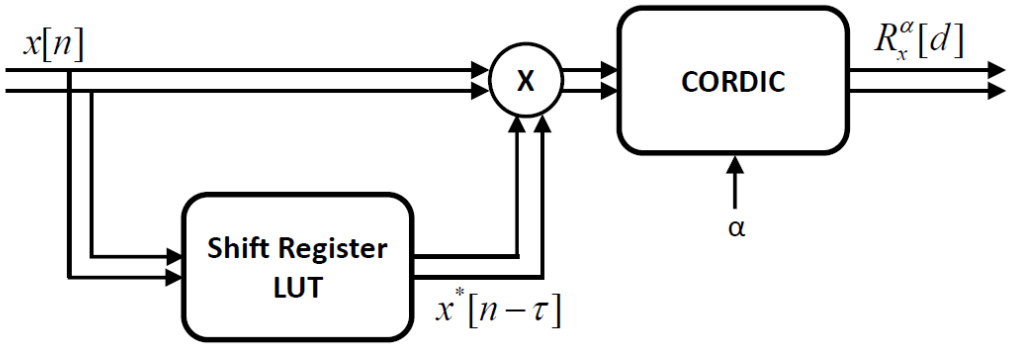

Figure 67. Block diagram of the FPGA implementation of the cyclostationary classifier.

The computational complexity of the classifier has been measured in terms of FPGA resource occupation and it is shown in Table 28, where it is compared to other similar implementations found in the literature. Since the mentioned complexity measurements have been carried out over different FPGA architectures, an estimation (marked with an asterisk*) of the resource utilization that these implementations would achieve in a Xilinx Virtex 6 FPGA has been obtained and used for comparison.

Considering the time-domain cyclostationary detector (CYCTIME) implemented in [114] as the implementation with more similarities (from the algorithmic point of view) to the proposed classifier, our implementation consumes 50% more Look-Up-Tables (LUT) and 3 times more Flip-Flops, but 40 time less embedded memory resources (LUTRAMs), as it is shown in Table 28. These results suggest that FPGA implementation differs from the one used in the detectors implemented in [114]. Our approach, based on streaming processing, results in lower memory requirements. However, evaluating all the resources as a whole, it could be stated that a similar complexity has been achieved. Besides, taking into account that the cyclostationary detector in [114] is only able to determine if an OFDM signal is present or no, it is worth mentioning that the classifier proposed in this thesis is capable of distinguishing between OFDM, QPSK and GFSK modulations. Therefore, the increase in LUT and FF utilization is considered assumable.

In order to contextualize the achieved results, the complexity of a complete wireless transmitter/receiver system, in the form of an QPSK modem [113] is also shown in Table 28. As it can be seen, the complexity of the classifier is equivalent to 10% of the complete modem. Only considering the signal processing algorithms, i.e. without taking into account the resources consumed by the MicroBlaze control microprocessor, the proposed modulation classifier occupies a 25% of the system, which is assumable if the obtained functionalities are considered. These results show how the simplification of the MC algorithm allows its practical FPGA implementation at a limited cost.

	SLICES	6 in-LUT	FF	LUTRAM (32 bit)	DSP48	9b-mult
Cyclostationary classifier (proposal)	2482	8806	3700	268	30	-
CYCFREC [114]	-	11060*	8802	12677*	-	76
CYCTIME [114]	-	5728*	1291	10240*	-	234
SSCC [114]	-	3362*	811	10240*	-	32
ADSSCC [114]	-	630*	198	4096*	-	0
QPSK modem [113]	21953	56249	41478	4192	446	-
QPSK modem (without uBlaze) [113]	10632	31698	18678	2138	427	-

Table 28. Computation complexity of the cyclostationary modulation classifier.

5.2.2.2 Measurements

The proposed MC has been evaluated with real OFDM, QPSK and GFSK signals using the set up shown in Figure 65. The signals used to validate the implementation have been generated with the same parameters as in simulations (Table 20). The results are shown in Figure 68, for both real implementation and simulation. Frequency offset and DC offset have been added to the simulations in order to obtain the same distortions as in the real receiver. The behavior with real signals performs close to the simulations. Therefore, the classifier is capable of detecting correctly every modulation for SNRs greater than 20 dB.

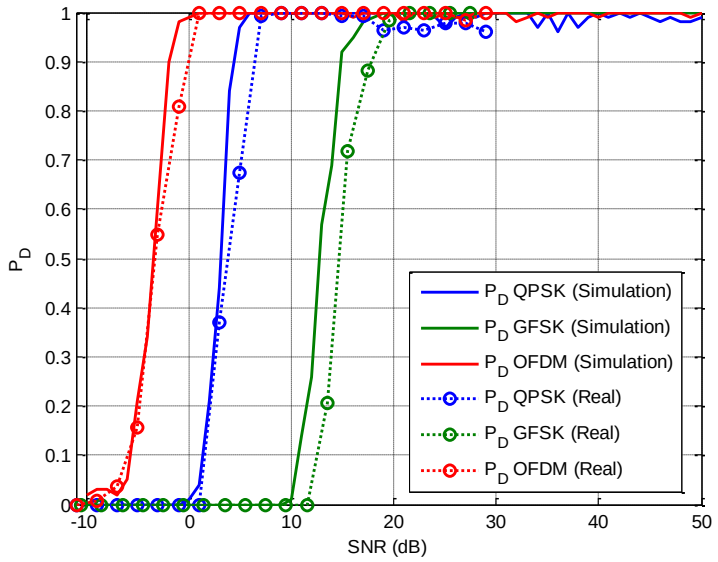

Figure 68. Probability of detection of the implemented cyclostationary classifier vs SNR.

Moreover, the performance of the MC with real signals has been evaluated under I/Q, considering both amplitude and phase imbalance. The results are shown in Figure 69 and Figure 70 respectively, where it can be seen that I/Q imbalance does not affect the performance of the classifier, as already seen in simulations. The performance of the implementation is lower than in simulation because the real signals generated by the signal generator are slightly different from the simulated signals.

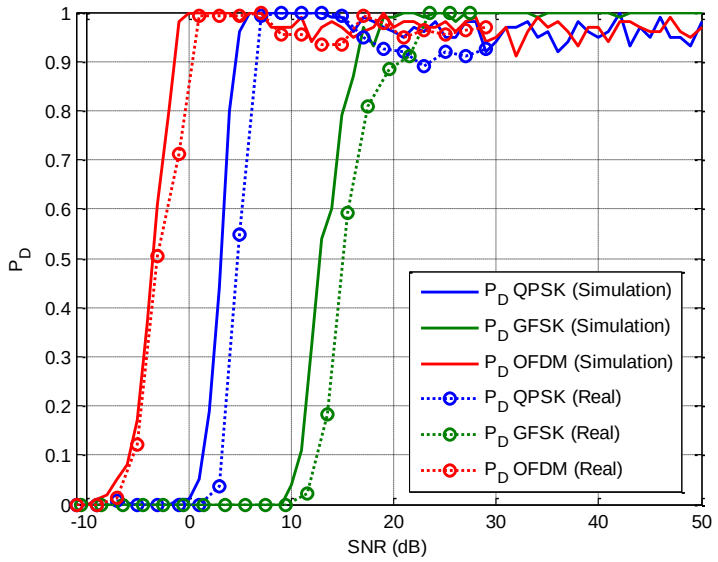

Figure 69. Probability of detection of the implemented cyclostationary classifier under amplitude I/Q imbalance vs SNR.

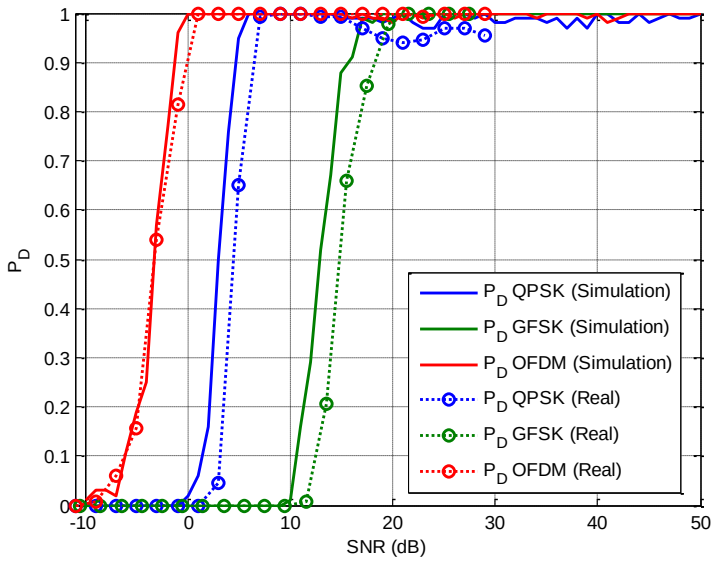

Figure 70. Probability of detection of the implemented cyclostationary classifier under phase I/Q imbalance vs SNR.

5.3 RF-Ethernet bridge

The designed cognitive RF-Ethernet bridge consists of two FPGA-based nodes, being each of them able to carry out both the Ethernet-to-RF and RF-to-Ethernet conversion. The system works in a half duplex mode. This means that each time one of the nodes will act as an Ethernet-to-RF bridge, while the other one will act as an RF-to-Ethernet bridge. In order to achieve the reliability needed in communications for IWSAN applications, the system implements two spectrum sensing algorithms to avoid interference. Taking advantage of the system for transmitting in two ISM bands (868 MHz and 2.45 GHz), and using the spectrum sensing techniques, the most suitable frequency in order to avoid interference is selected. The Ethernet-to-RF bridge implements three functions: an Ethernet processing core, a QPSK modulator and the ED. Similarly, the RF-to-Ethernet bridge carries out the inverse operation, implementing the MC, a QPSK demodulator and an Ethernet frame processing. An overview of the system is shown in Figure 71.

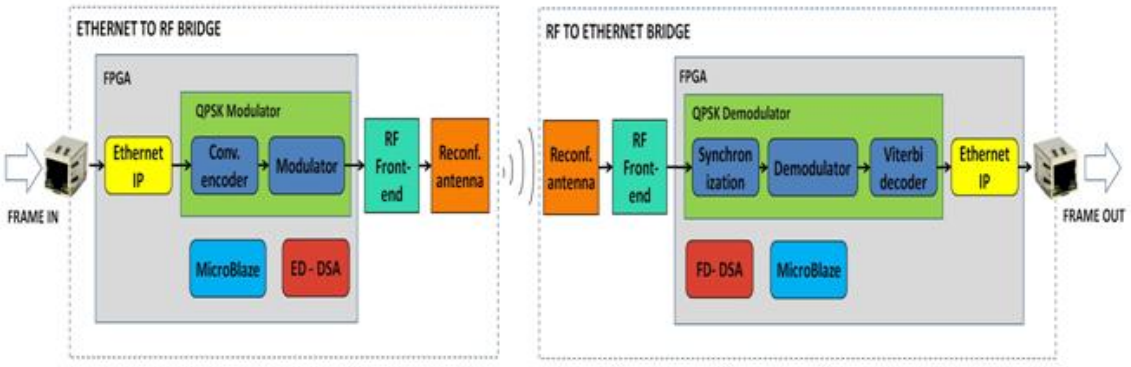

Figure 71. Cognitive wireless RF-Ethernet bridge.

Different spectrum sensing algorithms are used because the Ethernet-to-RF and the RF-to-Ethernet bridges carry out different tasks. The ED is used by the Ethernet-to-RF bridge in order to find a free channel in order to transmit the information. However, the MC is used by the RF-to-Ethernet bridge to look for the Ethernet-to-RF bridge in all the channels. The MC allows distinguishing between different modulations, so it is possible to differentiate between the signal from the Ethernet-to-RF and other signals transmitted by other communication systems.

In Figure 72 the results of the spectrum sensing algorithms are shown for both the desired signal (QPSK) and another signal transmitted by a Wi-Fi user (OFDM). The response of both algorithms is shown when there is no RF signal in the channel (Noise). As it can be seen in Figure 72, the ED detects every signal, while the MC has been configured to detect only the QPSK signal.

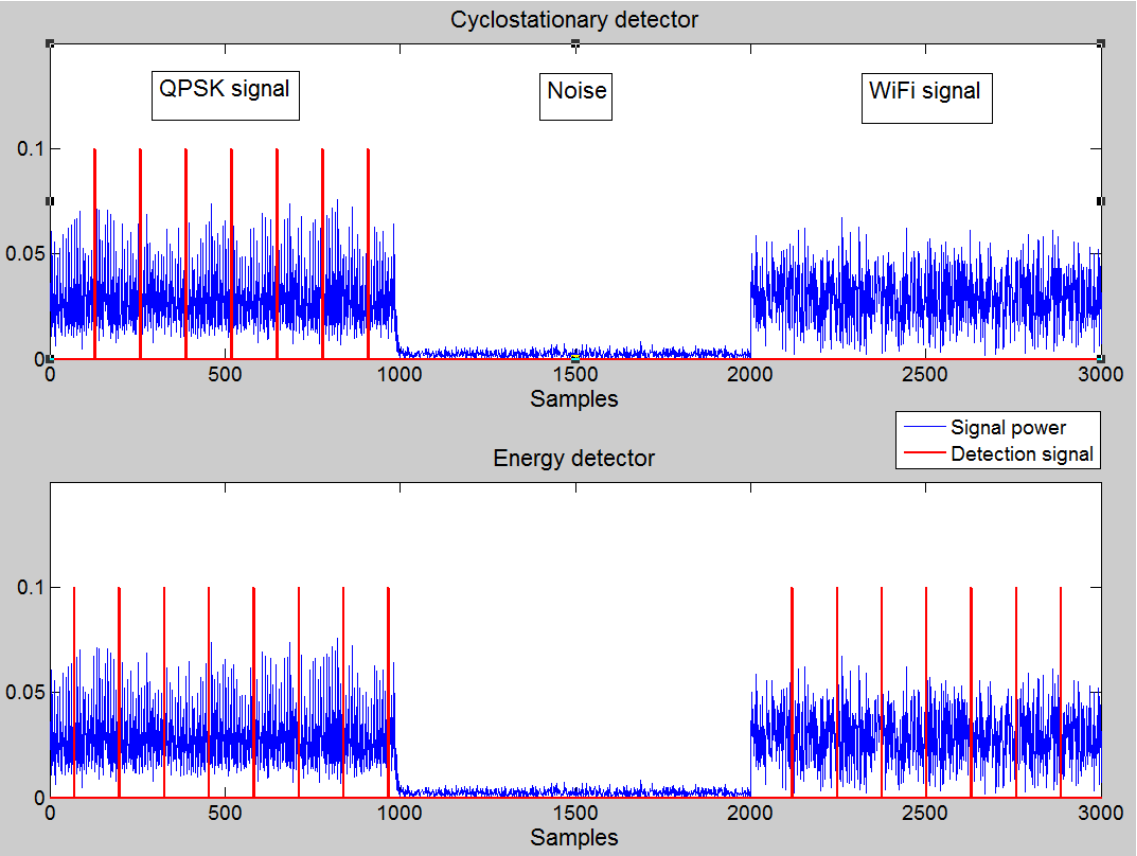

Figure 72. Spectrum sensing algorithms results in the RF-Ethernet bridge.

5.4 Summary

A cognitive platform has been presented in this chapter. This platform has been developed by a working group composed of researches from IK4-Ikerlan and Mondragon Unibertsitatea. A XC6VLX240T Xilinx Virtex 6 FPGA has been used to build the platform, and its working has been explained in this chapter.

This platform has been used in order to prove the spectrum sensing algorithms presented in Section 4.1. Both spectrum sensing algorithms have been implemented on the platform, and the resource utilization has been shown. The computational complexity of the Modulation Classifier (MC) shows how the simplification allows a real implementation at a limited cost. The implemented algorithms have been tested on hardware and with real signals, and the results have been compared with the simulated ones.

Furthermore, this platform has been used as a cognitive RF-Ethernet bridge. The aim of this bridge is to replace an Ethernet wired link by a wireless link. The spectrum sensing algorithms allow the system to achieve robustness against interference, thus it can be used for control applications. Both algorithms have been used because Ethernet-to-RF and RF-to-Ethernet do not carry out the same task. The Ethernet-to-RF is in charge of finding a free channel where the information is transmitted. To achieve this

objective the ED is used. On the other hand, the RF-to-Ethernet bridge has to distinguish between the signal transmitted by the Ethernet-to-RF bridge and other signals. The RF-to-Ethernet bridge uses the MC in order to find out whether the channel is occupied by the transmitter, by other communication systems or whether there is no signal. However, since this system is not based on a TDMA access, no time-critical requirements can be satisfied despite its improvement in robustness against interference.

Chapter 6

CONCLUSION AND FUTURE WORK

6.1 Conclusion

This thesis evaluates the application of CR to mission-critical and time-critical IWSAN applications. These applications demand strict requirements in terms of time and robustness to ensure a correct working of the network. Otherwise, some losses in machinery damage or person injuries can be caused. Moreover, IWSAN applications work in an industrial environment (for example factories or transport scenarios such as aeronautics or railway) where channels are considered highly dispersive due to metal surfaces, which provoke multipath fading and shadowing. Besides, other communication systems or industrial machinery may cause interference to the network. To ensure the requirements demanded by IWSAN and to overcome the problems wrought by industrial environments, the CR paradigm has been studied in this thesis. Although CR was first designed to overcome the low use of some licensed bands, its adaptability can be used to ensure reliability in industrial channels.

To know what CR techniques are suitable to IWSAN applications, a comparison between different non-CR-based MACs and CR-based MACs has been carried out. Several existing MACs have been selected and their performance has been measured theoretically using Network Calculus. Results have been then validated through OPNET simulations. Considering both theoretical and simulation results, the advantages of CR

have been stated. CR-based systems are capable of avoiding interference and ensuring robustness in industrial environments. However, the way in which the evaluated MACs avoid interference is not deterministic. Therefore, none of these MACs can be used for IWSAN applications because time requirements are not accomplished.

Therefore, in this thesis, a CR-based MAC which is capable of ensuring robustness and time requirements against interference has been proposed. Hence, this MAC is suitable for IWSAN applications. To ensure a deterministic behavior against interference, a novel handoff algorithm, which detects interference and hops to another channel, has been proposed. This algorithm has been designed to be used jointly with one of the evaluated MACs (DRMAC), and it detects interference while the system is transmitting allowing detection in a bounded time. Network Calculus and OPNET have been used to determine the performance of the handoff algorithm, and the results have been compared with the system when the proposed process is not used. This comparison shows how it is only possible to ensure time and reliability requirements if the proposed algorithm is used.

Furthermore, the spectrum sensing algorithm used by the CR-based system to obtain information about the environment has been studied. An energy detector has been chosen due to its simplicity and a Modulation Classifier has also been proposed, which distinguishes between OFDM, QPSK and GFSK signals. The performance of the algorithm has been measured for different signals and for different receiver impairments such as frequency offset, DC offset and I/Q imbalance.

Finally, the implementation of the spectrum sensing algorithms in a cognitive platform has been shown. Consequently, the results obtained through simulations have been validated. Moreover, an example of application of the spectrum sensing algorithms has been presented. The example is an Ethernet-to-RF bridge which captures the Ethernet frames and transmits them wirelessly to a reciprocal RF-to-Ethernet bridge, which reconstructs the Ethernet frames. The RF-Ethernet bridge has been designed to replace a wired Ethernet link by a wireless one for IWSAN applications and uses both spectrum sensing algorithms in order to ensure a reliable communication link against interference

6.2 Contributions

To summarize, the main contributions of this thesis are:

- Proposal of a novel handoff algorithm for CR which is capable of ensuring IWSAN requirements.
- Comparison between several MACs, both CR-based and non-CR-based, for IWSAN applications.
- Proposal of a simplified Modulation Classifier which distinguishes between OFDM, QPSK and GFSK signals.
- Validation of the spectrum sensing algorithms in a cognitive platform.

Some of these contributions have been published in Journals, in Conferences and in a Book Chapter:

Journals

- P. M. Rodriguez, A. Lizeaga, M. Mendicute and I. Val. "Spectrum handoff strategy for cognitive radio-based MAC for time-critical and mission-critical industrial wireless sensor and actuator networks". IEEE/ACM Transactions on Networking. (Submitted).
- P. M. Rodriguez, Z. Fernandez, R. Torrego, A. Lizeaga, M. Mendicute and I. Val. "A sub-optimal implementation on FPGA of cyclostationary modulation classifier for cognitive radios". AEÜ - International Journal of Electronics and Communications. (Submitted).
- P.M. Rodriguez, R. Torrego, F. Casado, Z. Fernandez, M. Mendicute, A. Arriola and I. Val "Dynamic spectrum access integrated in a wideband cognitive RF-Ethernet bridge for industrial control applications". Journal of Signal Processing Systems, 83(1), 19-28 (2016).
- F. Casado, R. Torrego, P. Rodríguez, A. Arriola and I. Val. "Reconfigurable Antenna and Dynamic Spectrum Access Algorithm: Integration in a Cognitive Radio Platform for Reliable Communications". Journal of Signal Processing Systems, 78(3), 267-274 (2015).

Conference Papers

- P. M. Rodriguez, I. Val, A. Lizeaga and M Mendicute. "Evaluation of cognitive radio for mission-critical and time-critical WSAN in industrial environments under interference". Factory Communication Systems (WFCS), 2015 IEEE World Conference on (pp. 1-4).
- P. Rodriguez, R. Torrego, F. Casado, Z. Fernandez, M. Mendikute, A. Arriola and I. Val. "Wideband cognitive wireless communication system: implementation of an RF-Ethernet bridge for control applications". SDR-WInnComm-Europe 2014 Conference.

Book Chapters

- A. Arriola, P. M. Rodríguez, R. Torrego, F. Casado, Z. Fernandez, M. Mendicute, E. Muxika, J. I. Sancho, and I. Val, "FPGA-based Cognitive Radio Platform with Reconfigurable Front-End and Antenna," in Computing Platforms for Software-Defined Radio, ed: Springer, 2016.

6.3 Future work

In this section, some new lines of research and future work are described:

- Further use of the proposed Modulation Classifier (MC): Instead of the energy detector used to gather information about the environment, the MC can be used to find out more information about the sensed channel. The MC can additionally extract the modulation of the signal which is

occupying the channel. According to this information, the system can take different decisions in function of the kind of user which is using the medium.

- Implementation of the proposed MAC (DRMAC with handoff) on the real platform: The existing platform provides robustness against interference, but time requirements are not met because it is not based on a TDMA scheme. The implementation of the proposed novel MAC in this platform adds the capability of ensuring robustness and time requirements at the same time.
- Decentralized spectrum sensing decisions: In the proposed MAC, the spectrum sensing information is sent to a coordinator which is in charge of taking decisions, that is, a centralized spectrum sensing scheme is used. However, a centralized solution is vulnerable, since the coordinator can stop working or be attacked by an external user compromising the network. Therefore, a decentralized spectrum sensing scheme may be researched to add more robustness to the network.
- Multi-hop networks: As the proposed solution is only valid for single-hop networks, an extension for multi-hop network can be investigated.
- Jammer detection: Radio frequency jamming is a common technique to block a band which may compromise the system. A jammer is considered as an external attack, and its effect is different from interference from other communication systems. The proposed modulation classifier may be configured in order to detect a possible jammer. The study of a cognitive system for ensuring security may be an interesting future line.

REFERENCES

[1] F. Xia, *et al.*, "Wireless sensor/actuator network design for mobile control applications," *Sensors*, vol. 7, pp. 2157-2173, 2007.

[2] H. Kopetz, *Real-time systems: design principles for distributed embedded applications*: Springer Science \& Business Media, 2011.

[3] G. P. Hancke, "Industrial wireless sensor networks: a selection of challenging applications," in *Antennas and Propagation (EUCAP), 2012 6th European Conference on*, 2012, pp. 64-68.

[4] W. Ikram and N. F. Thornhill, "Wireless communication in process automation: a survey of opportunities, requirements, concerns and challenges," *Requirements, Concerns and Challenges, Control*, 2010.

[5] J. Mitola III and G. Q. Maguire Jr, "Cognitive radio: making software radios more personal," *Personal Communications, IEEE*, vol. 6, pp. 13-18, 1999.

[6] B. Wang and K. J. R. Liu, "Advances in cognitive radio networks: A survey," *IEEE Journal on Selected Topics in Signal Processing 5 (1) , art. no. 5639025 , pp. 5-23*, 2011.

[7] *IEEE 802.22 WG, IEEE Project homepage*. Available: http://www.ieee802.org/22/

[8] I. F. Akyildiz, *et al.*, "CRAHNs: Cognitive radio ad hoc networks," *Ad Hoc Networks*, vol. 7, pp. 810-836, 2009.

[9] L. H. A. Correia, *et al.*, "DynMAC: A resistant MAC protocol to coexistence in wireless sensor networks," *Computer Networks*, vol. 76, pp. 1-16, 2015.

[10] A. A. Kumar S., *et al.*, "An industrial perspective on wireless sensor networks-a survey of requirements, protocols, and challenges," *IEEE Communications Surveys and Tutorials*, vol. 16, pp. 1391-1412, 2014.

[11] P. Suriyachai, *et al.*, "A survey of MAC protocols for mission-critical applications in wireless sensor networks," *IEEE Communications Surveys and Tutorials*, vol. 14, pp. 240-264, 2012.
[12] J. F. Coll, *et al.*, "Simulation and measurement of electromagnetic radiation absorption in a finished-product warehouse," in *Electromagnetic Compatibility (EMC), 2010 IEEE International Symposium on*, 2010, pp. 881-884.
[13] Z. Irahhauten, *et al.*, "UWB channel measurements and results for office and industrial environments," in *IEEE 2006 International Conference on Ultra-Wideband*, 2006, pp. 225-230.
[14] S. Luo, *et al.*, "RF channel modeling of a WSN testbed for industrial environment," in *IEEE Radio and Wireless Symposium (RWS)*, 2011, pp. 375-378.
[15] J. F. Coll, *et al.*, "Industrial environment characterization for future M2M applications," in *IEEE International Symposium on Electromagnetic Compatibility*, 2011, pp. 960-963.
[16] H. MacLeod, *et al.*, "Experimental studies of the 2.4-GHz ISM wireless indoor channel," in *Proceedings of the 3rd Annual Communication Networks and Services Research Conference*, 2005, pp. 63-68.
[17] S. Wyne, *et al.*, "Channel measurements of an indoor office scenario for wireless sensor applications," in *IEEE Global Telecommunications Conference (GLOBECOM)*, 2007, pp. 3831-3836.
[18] S. Wyne, *et al.*, "A statistical model for indoor office wireless sensor channels," *Wireless Communications, IEEE Transactions on*, vol. 8, pp. 4154-4164, 2009.
[19] M. Patzold, *Mobile fading channels*: John Wiley \& Sons, Inc., 2003.
[20] B. Azimi-Sadjadi, *et al.*, "Interference effect on IEEE 802.15. 4 performance," in *Proceedings of 3rd international conference on networked sensing systems (INNS), Chicago, IL*, 2006.
[21] W. Guo, *et al.*, "Impacts of 2.4-GHz ISM band interference on IEEE 802.15. 4 wireless sensor network reliability in buildings," *Instrumentation and Measurement, IEEE Transactions on*, vol. 61, pp. 2533-2544, 2012.
[22] V. C. Gungor, *et al.*, "Opportunities and challenges of wireless sensor networks in smart grid," *Industrial Electronics, IEEE Transactions on*, vol. 57, pp. 3557-3564, 2010.
[23] R. Steigmann and J. Endresen, "Introduction to WISA," *Whitepaper, ABB*, 2006.
[24] D. Christin, *et al.*, "Survey on wireless sensor network technologies for industrial automation: The security and quality of service perspectives," *Future Internet*, vol. 2, pp. 96-125, 2010.
[25] *HART Communication Foundation. WirelessHART homepage*. Available: http://en.hartcomm.org/main_article/wirelesshart.html
[26] *Internet Society of Automation. ISA100, Wireless Systems for Automation homepage*. Available: https://www.isa.org/isa100/
[27] M. Nixon and T. Round Rock, "A Comparison of WirelessHART™ and ISA100. 11a," *Whitepaper, Emerson Process Management*, 2012.
[28] *ZigBee Alliance. The ZigBee Alliance | Control your World homepage*. Available: http://www.zigbee.org/
[29] P. Huang, *et al.*, "The evolution of MAC protocols in wireless sensor networks: A survey," *IEEE Communications Surveys and Tutorials*, vol. 15, pp. 101-120, 2013.

[30] T. Zhong, *et al.*, "Real-time communication in WIA-PA industrial wireless networks," in *IEEE International Conference on Computer Science and Information Technology (ICCSIT)*, 2010, pp. 600-605.

[31] *Survey and Experiments of WIA-PA Specification of Industrial Wireless Network.* Available: http://english.sia.cas.cn/rh/rp/201307/t20130705_105662.html

[32] W. Shen, *et al.*, "PriorityMAC: A priority-enhanced MAC protocol for critical traffic in industrial wireless sensor and actuator networks," *IEEE Transactions on Industrial Informatics*, vol. 10, pp. 824-835, 2014.

[33] S. Munir, *et al.*, "Addressing burstiness for reliable communication and latency bound generation in wireless sensor networks," in *Proceedings of the 9th ACM/IEEE International Conference on Information Processing in Sensor Networks*, 2010, pp. 303-314.

[34] J. Akerberg, *et al.*, "Deterministic downlink transmission in wirelesshart networks enabling wireless control applications," in *Annual Conference of the IEEE Industrial Electronics Society (IECON)*, 2010, pp. 2120-2125.

[35] Z. Iqbal, *et al.*, "Deterministic and event triggered MAC protocol for industrial wireless networks," in *IEEE International Conference on Industrial Technology (ICIT)*, 2013, pp. 1252-1259.

[36] P. Suriyachai, *et al.*, "Implementation of a MAC protocol for QoS support in wireless sensor networks," in *IEEE International Conference on Pervasive Computing and Communications (PerCom)*, 2009, pp. 1-6.

[37] P. Suriyachai, *et al.*, "Time-critical data delivery in wireless sensor networks," in *Distributed Computing in Sensor Systems*, 2010, pp. 216-229.

[38] H. Trsek, *et al.*, "A flexible approach for real-time wireless communications in adaptable industrial automation systems," in *IEEE Conference on Emerging Technologies \& Factory Automation (ETFA)*, 2011, pp. 1-4.

[39] E. Toscano, *et al.*, "A traffic scheduler for real-time wireless communication in adaptable industrial automation systems," in *IEEE Conference on Emerging Technologies and Factory Automation (ETFA)*, 2010, pp. 1-8.

[40] S. Shobana, *et al.*, "Matched filter based spectrum sensing on cognitive radio for OFDM WLANs," *International Journal of Engineering and Technology*, vol. 5, pp. 142-146, 2013.

[41] M. H. Mohamad, *et al.*, "Matched filter detection technique for GSM band," in *International Symposium on Telecommunication Technologies (ISTT)*, 2012, pp. 271-274.

[42] D. M. M. i. Plata, nez and t. Re\'a, \'A,ngel Gabriel Andrade, "Evaluation of energy detection for spectrum sensing based on the dynamic selection of detection-threshold," *Procedia Engineering*, vol. 35, pp. 135-143, 2012.

[43] T. T. Nguyen, *et al.*, "A real-time FPGA implementation of spectrum sensing applying for DVB-T primary signal," in *Advanced Technologies for Communications (ATC), 2013 International Conference on*, 2013, pp. 164-169.

[44] K. Xin and Z. S. He, "Narrowband Signal Localization Based on Enhanced LAD Method," *Journal of Communications and Networks 13 (1) , pp. 6-11*, 2011.

[45] J. Lehtomaki, *et al.*, "Analysis of the LAD Methods," *IEEE Signal Processing Letters 15 , pp. 237-240*, 2008.

[46] D. Panaitopol, *et al.*, "Fast and reliable sensing using a background process for noise estimation," in *Conference on Cognitive Radio Oriented Wireless Networks and Communications (CROWNCOM)*, 2011, pp. 221-225.

[47] C. H. Lim, "Adaptive energy detection for spectrum sensing in unknown white Gaussian noise," *IET Communications*, vol. 6, pp. 1884-1889, 2012.

[48] L. Le, *et al.*, "Energy-efficient detection system in time-varying signal and noise power," in *ICASSP, IEEE International Conference on Acoustics, Speech and Signal Processing - Proceedings*, 2013, pp. 2736-2740.

[49] J. F. Adlard, "Frequency shift filtering for cyclostationary signals," University of York, 2000.

[50] R. Datta, *et al.*, "Cyclostationary detection of 5G GFDM waveform in cognitive radio transmission," in *IEEE International Conference on Ultra-WideBand (ICUWB)*, 2014, pp. 108-112.

[51] R. Zhang, *et al.*, "Multi-antenna based spectrum sensing for cognitive radios: A GLRT approach," *IEEE Transactions on Communications*, vol. 58, pp. 84-88, 2010.

[52] A. Kortun, *et al.*, "Throughput analysis using eigenvalue based spectrum sensing under noise uncertainty," in *International Wireless Communications and Mobile Computing Conference (IWCMC)*, 2012, pp. 395-400.

[53] M. Z. Shakir, *et al.*, "Generalized Mean Detector for Collaborative Spectrum Sensing," *IEEE Transactions on Communications*, 2013.

[54] B. Nadler, *et al.*, "Performance of eigenvalue-based signal detectors with known and unknown noise level," in *IEEE International Conference on Communications*, 2011.

[55] O. A. Dobre, "Signal identification for emerging intelligent radios: Classical problems and new challenges," *IEEE Instrumentation and Measurement Magazine*, vol. 18, pp. 11-18, 2015.

[56] J. L. Xu, *et al.*, "Likelihood-ratio approaches to automatic modulation classification," *Systems, Man, and Cybernetics, Part C: Applications and Reviews, IEEE Transactions on*, vol. 41, pp. 455-469, 2011.

[57] O. A. Dobre, *et al.*, "Survey of automatic modulation classification techniques: Classical approaches and new trends," *IET Communications*, vol. 1, pp. 137-156, 2007.

[58] W. Su, "Modulation classification of single-input multiple-output signals using asynchronous sensors," *IEEE Sensors Journal*, vol. 15, pp. 346-357, 2015.

[59] M. E. M. Keshk, *et al.*, "Automatic Modulation Recognition in Wireless Multi-carrier Wireless Systems with Cepstral Features," *Wireless Personal Communications*, 2014.

[60] D. Chang and P. Shih, "Cumulants-based modulation classification technique in multipath fading channels," *IET Communications*, vol. 9, pp. 828-835, 2015.

[61] S. A. Ghauri, *et al.*, "Modulation classification using cyclostationary features on fading channels," *Research Journal of Applied Sciences, Engineering and Technology*, vol. 7, pp. 5331-5339, 2014.

[62] I. F. Akyildiz, *et al.*, "NeXt generation/dynamic spectrum access/cognitive radio wireless networks: A survey," *Computer Networks*, vol. 50, pp. 2127-2159, 2006.

[63] N. Nguyen-Thanh, *et al.*, "Medium Access Control Design for Cognitive Radio Networks: A Survey," *IEICE Transactions on Communications*, vol. 97, pp. 359-374, 2014.

[64] W. Hu, *et al.*, "Cognitive radios for dynamic spectrum access-dynamic frequency hopping communities for efficient ieee 802.22 operation," *Communications Magazine, IEEE*, vol. 45, pp. 80-87, 2007.

[65] A. Mariani, *et al.*, "Periodic Spectrum Sensing with Non-Continuous Primary User Transmissions," *IEEE Transactions on Wireless Communications*, vol. 14, pp. 1636-1649, 2015.

[66] S. Eryigit, *et al.*, "Energy-efficient multichannel cooperative sensing scheduling with heterogeneous channel conditions for cognitive radio networks," *IEEE TRANSACTIONS ON VEHICULAR TECHNOLOGY*, vol. 62, pp. 2690-2699, 2013.

[67] H. He, *et al.*, "Adaptive Spectrum Sensing for Time-Varying Channels in Cognitive Radios," *IEEE Wireless Communications Letters*, vol. 2, pp. 1-4, 2013.

[68] N. Pratas, *et al.*, "Cooperative spectrum sensing: State of the art review," in *International Conference on Wireless Communication, Vehicular Technology, Information Theory and Aerospace and Electronic Systems Technology, Wireless VITAE*, 2011.

[69] H. A. Bany Salameh and M. F. El-Attar, "Cooperative OFDM-Based Virtual Clustering Scheme for Distributed Coordination in Cognitive Radio Networks," *IEEE TRANSACTIONS ON VEHICULAR TECHNOLOGY*, vol. 64, pp. 3624-3632, 2015.

[70] B. F. Lo, "A survey of common control channel design in cognitive radio networks," *Physical Communication*, vol. 4, pp. 26-39, 2011.

[71] Y. Zou, *et al.*, "A cooperative spectrum sensing scheme without dedicated reporting channels: Interference impact on primary users," in *GLOBECOM - IEEE Global Telecommunications Conference*, 2011.

[72] T. Yucek and H. Arslan, "A Survey of Spectrum Sensing Algorithms for Cognitive Radio Applications," *IEEE Communications Surveys and Tutorials 11 (1) , pp. 116-130*, 2009.

[73] I. F. Akyildiz, *et al.*, "Cooperative spectrum sensing in cognitive radio networks: A survey," *Physical Communication*, vol. 4, pp. 40-62, 2011.

[74] X. Zhang and H. Su, "CREAM-MAC: Cognitive radio-enabled multi-channel MAC protocol over dynamic spectrum access networks," *IEEE Journal on Selected Topics in Signal Processing*, vol. 5, pp. 110-123, 2011.

[75] A. Puschmann, *et al.*, "A flexible CSMA based MAC protocol for software defined radios," *Frequenz*, vol. 66, pp. 261-268, 2012.

[76] G. A. Shah and O. B. Akan, "Performance analysis of CSMA-based opportunistic medium access protocol in cognitive radio sensor networks," *Ad Hoc Networks*, vol. 15, pp. 4-13, 2014.

[77] S. Agarwal, *et al.*, "DSAT-MAC: Dynamic slot allocation based TDMA MAC protocol for cognitive radio networks," in *International Conference on Wireless and Optical Communications Networks (WOCN)*, 2012, pp. 1-6.

[78] S. Hu, *et al.*, "Cognitive medium access control protocols for secondary users sharing a common channel with time division multiple access primary users," *Wireless Communications and Mobile Computing*, vol. 14, pp. 284-296, 2014.

[79] L. Sitanayah, *et al.*, "A hybrid MAC protocol for emergency response wireless sensor networks," *Ad Hoc Networks*, vol. 20, pp. 77-95, 2014.

[80] M. Timmers, *et al.*, "A distributed multichannel MAC protocol for multihop cognitive radio networks," *IEEE TRANSACTIONS ON VEHICULAR TECHNOLOGY*, vol. 59, pp. 446-459, 2010.

[81] X. Wang, *et al.*, "Partially observable Markov decision process-based MAC-layer sensing optimisation for cognitive radios exploiting rateless-coded spectrum aggregation," *IET Communications*, vol. 6, pp. 828-835, 2012.

[82] S. Pandit and G. Singh, "Spectrum sharing in Cognitive Radio using game theory," in *IEEE International Advance Computing Conference (IACC)*, 2013, pp. 1503-1506.

[83] D. Niyato and Z. Han, "Dynamics of multiple-seller and multiple-buyer spectrum trading in cognitive radio networks: A game-theoretic modeling approach," *IEEE Transactions on Mobile Computing*, vol. 8, pp. 1009-1022, 2009.

[84] F. Wang, *et al.*, "Throughput-oriented MAC for mobile ad hoc networks: A game-theoretic approach," *Ad Hoc Networks*, vol. 7, pp. 98-117, 2009.

[85] J. Li, *et al.*, "Multiuser power and channel allocation algorithm in cognitive radio," in *Proceedings of the International Conference on Parallel Processing*, 2007.

[86] A. He, *et al.*, "A survey of artificial intelligence for cognitive radios," *IEEE TRANSACTIONS ON VEHICULAR TECHNOLOGY*, vol. 59, pp. 1578-1592, 2010.

[87] C. K. Huynh and W. C. Lee, "Optimal Solution for Channel Selection and Power Allocation for TVWS-Based Smart Metering System," *Wireless Personal Communications*, vol. 85, pp. 1653-1668, 2015.

[88] S. Chantaraskul and K. Moessner, "Implementation of a genetic algorithm-based decision making framework for opportunistic radio," *IET Communications*, vol. 4, pp. 495-506, 2010.

[89] A. Adeel, *et al.*, "Performance analysis of random neural networks in LTE-UL of a cognitive radio system," in *International Workshop on Cognitive Cellular Systems (CCS)*, 2014.

[90] P. Maheshwari and A. K. Singh, "A survey on spectrum handoff techniques in cognitive radio networks," in *International Conference Contemporary Computing and Informatics (IC3I)*, 2014, pp. 996-1001.

[91] C. Wang and L. Wang, "Modeling and analysis for proactive-decision spectrum handoff in cognitive radio networks," in *IEEE International Conference on Communications*, 2009.

[92] C. Wang and L. Wang, "Analysis of reactive spectrum handoff in cognitive radio networks," *IEEE Journal on Selected Areas in Communications*, vol. 30, pp. 2016-2028, 2012.

[93] Y. Song and J. Xie, "ProSpect: A proactive spectrum handoff framework for cognitive radio Ad hoc networks without common control channel," *IEEE Transactions on Mobile Computing*, vol. 11, pp. 1127-1139, 2012.

[94] K. Kunert, *et al.*, "Deterministic real-time medium access for cognitive industrial radio networks," in *IEEE International Workshop on Factory Communication Systems - Proceedings, WFCS , art. no. 6242549 , pp. 91-94*, 2012.

[95] S. K. Timalsina, *et al.*, "A concurrent access MAC protocol for cognitive radio ad hoc networks without common control channel," *Eurasip Journal on Advances in Signal Processing*, vol. 2013, 2013.

[96] N. C. Theis, *et al.*, "Rendezvous for cognitive radios," *Mobile Computing, IEEE Transactions on*, vol. 10, pp. 216-227, 2011.

[97] Z. Lin, *et al.*, "Ring-walk algorithms for cognitive radio networks," *Ad-Hoc and Sensor Wireless Networks*, vol. 16, pp. 243-271, 2012.

[98] K. Bian, *et al.*, "Control channel establishment in cognitive radio networks using channel hopping," *IEEE Journal on Selected Areas in Communications*, vol. 29, pp. 689-703, 2011.

[99] A. Mishra, *et al.*, "CH-MAC: A multi-channel MAC protocol for dynamic spectrum access networks," in *International Symposium on Wireless Personal Multimedia Communications, WPMC*, 2013.

[100] J. e. Marinho and E. Monteiro, "Enhanced protection of hidden primary users through filtering based on suspect channels classification," in *IEEE International Conference on Wireless and Mobile Computing, Networking and Communications (WiMob)*, 2012, pp. 419-426.

[101] M. Jonsson and K. Kunert, "MC-EDF: A control-channel based wireless multichannel MAC protocol with real-time support," in *IEEE Conference on Emerging Technologies \& Factory Automation (ETFA)*, 2012, pp. 1-6.

[102] D. Abdeli, *et al.*, "RTH-MAC: A real time hybrid MAC protocol for WSN," in *International Symposium on Programming and Systems (ISPS)*, 2013, pp. 153-162.

[103] Y. Song and J. Xie, "QB (2) IC: A QoS-Based Broadcast Protocol Under Blind Information for Multihop Cognitive Radio Ad Hoc Networks," *IEEE TRANSACTIONS ON VEHICULAR TECHNOLOGY*, vol. 63, pp. 1453-1466, 2014.

[104] S. Andreev, *et al.*, "Practical Traffic Generation Model for Wireless Networks," in *FOURTH ERCIM WORKSHOP ON EMOBILITY*, 2010, p. 61.

[105] J.-Y. Le Boudec and P. Thiran, *Network Calculus: A Theory of Deterministic Queuing Systems for the Internet*. Berlin, Heidelberg: Springer-Verlag, 2001.

[106] D. K. Dang and A. Mifdaoui, "Timing Analysis of TDMA-based Networks using Network Calculus and Integer Linear Programming," in *Modelling, Analysis \& Simulation of Computer and Telecommunication Systems (MASCOTS), 2014 IEEE 22nd International Symposium on*, 2014, pp. 21-30.

[107] A. Bagwari and G. S. Tomar, "Cooperative spectrum sensing in multiple energy detectors based cognitive radio networks using adaptive double-threshold scheme," *International Journal of Electronics*, vol. 101, pp. 1546-1558, 2014.

[108] D. Noguet, *et al.*, "Cyclostationarity detectors for cognitive radio: architectural tradeoffs," *EURASIP Journal on Wireless Communications and Networking*, vol. 2010, p. 5, 2010.

[109] S. L. Sabat, *et al.*, "FPGA realization of spectrum sensing techniques for cognitive radio network," in *Cognitive Radio (IWCR), 2010 International Workshop on*, 2010, pp. 1-5.

[110] Q. Zhao, *et al.*, "Decentralized cognitive MAC for opportunistic spectrum access in ad hoc networks: A POMDP framework," *IEEE Journal on Selected Areas in Communications*, vol. 25, pp. 589-599, 2007.

[111] F. e. Casado, lix, *et al.*, "Reconfigurable Antenna and Dynamic Spectrum Access Algorithm: Integration in a Cognitive Radio Platform for Reliable Communications," *Journal of Signal Processing Systems*, vol. 78, pp. 267-274, 2015.

[112] Xilinx, "System Generator for DSP", http://www.xilinx.com/products/design-tools/vivado/integration/sysgen.html

[113] P. Rodriguez, *et al.*, "Wideband cognitive wireless communication system: implementation of an RF," in *WInnComm-Europe 2014 Conference*, 2014.

[114] M. Kosunen, *et al.*, "Survey and Analysis of Cyclostationary Signal Detector Implementations on FPGA," *IEEE Journal on Emerging and Selected Topics in Circuits and Systems*, vol. 3, pp. 541-551, 2013.